

This dissertation has been 65-9919  
microfilmed exactly as received

OWEN, Tobias Chant, 1936-  
STUDIES OF PLANETARY SPECTRA IN THE  
PHOTOGRAPHIC INFRARED.

University of Arizona, Ph.D., 1965  
Astronomy

University Microfilms, Inc., Ann Arbor, Michigan

STUDIES OF PLANETARY SPECTRA  
IN THE PHOTOGRAPHIC INFRARED

by  
Tobias Chant Owen

---

A Dissertation Submitted to the Faculty of the  
DEPARTMENT OF ASTRONOMY

In Partial Fulfillment of the Requirements  
For the Degree of

DOCTOR OF PHILOSOPHY

In the Graduate College

THE UNIVERSITY OF ARIZONA

1 9 6 5

THE UNIVERSITY OF ARIZONA

GRADUATE COLLEGE

I hereby recommend that this dissertation prepared under my  
direction by Tobias Chant Owen  
entitled Studies of Planetary Spectra in the Photographic  
Infrared  
be accepted as fulfilling the dissertation requirement of the  
degree of Doctor of Philosophy

Robert Kump  
Dissertation Director

Nov. 3 1964  
Date

After inspection of the dissertation, the following members  
of the Final Examination Committee concur in its approval and  
recommend its acceptance:\*

<u>AB Merrill</u>	_____
<u>_____</u>	_____
<u>D. G. Staley</u>	_____
<u>J. E. McDonald</u>	_____
_____	_____

\*This approval and acceptance is contingent on the candidate's  
adequate performance and defense of this dissertation at the  
final oral examination. The inclusion of this sheet bound into  
the library copy of the dissertation is evidence of satisfactory  
performance at the final examination.

# STATEMENT BY AUTHOR

This dissertation has been submitted in partial fulfillment of requirements for an advanced degree at The University of Arizona and is deposited in the University Library to be made available to borrowers under rules of the Library.

Brief quotations from this dissertation are allowable without special permission, provided that accurate acknowledgement of source is made. Requests for permission for extended quotation from or reproduction of this manuscript in whole or in part may be granted by the head of the major department or the Dean of the Graduate College when in his judgment the proposed use of the material is in the interests of scholarship. In all other instances, however, permission must be obtained from the author.

SIGNED: Tobias Chant Owen

## PREFACE

The research program which is described in this dissertation was first conceived in the summer of 1961. The primary stimuli were provided by the papers of G. P. Kuiper and G. Herzberg and their collaborators, describing their work on the identifications and interpretations of planetary spectra. At the Berkeley meeting of the I.A.U. in August of that year, the writer had the opportunity to discuss some of these projected studies with Dr. Herzberg who generously offered the use of a small absorption tube which he had constructed several years earlier and was no longer using. The writer subsequently visited Dr. Herzberg's laboratory in Ottawa where Mr. J. Shoosmith described and illustrated the alignment and use of different forms of the modified White mirror system used in the absorption tube which was to be loaned.

A spectroscopic laboratory was set up at the Lunar and Planetary Laboratory of the University of Arizona under the supervision of Dr. Kuiper who strongly encouraged the initiation of the proposed research program. The Herzberg tube was installed in this laboratory and other equipment was gradually added. The spectra obtained with the absorption tube were used to interpret planetary spectra

generously made available by Dr. Kuiper from his McDonald series as well as some low-dispersion spectra obtained by the writer at the Kitt Peak National Observatory.

Throughout the course of this work, important contributions were made by a number of people which are gratefully acknowledged. The construction of the 72-foot absorption tube and 10-foot spectrograph was greatly aided by the insights and experience of Drs. A. B. Meinel and H. L. Johnson, while Mr. S. Case provided valuable suggestions regarding mechanical details. Helpful assistance with various aspects of the laboratory program was furnished by Messrs. A. Binder, D. Cruikshank, D. Hoxie, J. Marshall, and D. McLean. The observations obtained at the Kitt Peak Observatory were made possible through the courtesy of Drs. N. U. Mayall and A. K. Pierce, while Mr. C. Slaughter provided valuable assistance and instruction with the McMath Solar Telescope. The writer is indebted to the following people for helpful comments and discussions regarding different problems which have arisen in the course of these studies: Drs. A. Abt, J. Chamberlain, G. Herzberg, J. McDonald, A. B. Meinel, H. Spinrad, D. O. Staley, and R. Weymann. Special thanks should go to Dr. Herzberg for the stimulus to this program provided by his example and by the loan of his absorption tube. Finally, it is a pleasure to acknowledge the continuing support and contributions of

Dr. G. P. Kuiper to all aspects of this work and the inspiration and encouragement he has provided throughout the course of the program.

Most of the laboratory studies reported here were supported by the Office of Naval Research under contracts Nonr G-00050-62 and ONR G-00014-64.

## TABLE OF CONTENTS

	Page
LIST OF ILLUSTRATIONS . . . . .	viii
LIST OF TABLES . . . . .	xi
ABSTRACT . . . . .	xii
1. INTRODUCTION . . . . .	1
2. HISTORICAL BACKGROUND . . . . .	7
2.1 Jupiter . . . . .	15
2.2 Mars . . . . .	28
3. INSTRUMENTS . . . . .	34
3.1 A 72-Foot Multiple Path Absorption Tube . .	34
Introduction . . . . .	34
Optical Principles . . . . .	35
The LPL 72-Foot Tube . . . . .	39
Alignment and Adjustment Procedures . .	43
3.2 A 10-Foot Plane Grating Spectrograph . . . .	51
Introduction . . . . .	51
Design Considerations . . . . .	52
A Description of the Instrument . . . . .	60
Discussion of Performance and Results . .	61
4. THE SPECTRUM OF JUPITER - IDENTIFICATIONS AND INTERPRETATIONS . . . . .	66
4.1 A New Ammonia Band in the Jovian Spectrum .	66
Introduction . . . . .	66
Laboratory Analysis . . . . .	67
4.2 The Spectrum of Jupiter from 7750 - 8800 Å . . . . .	75
Introduction . . . . .	75
Experimental Procedure . . . . .	77
Discussion of Results . . . . .	78
Conclusions . . . . .	87



## TABLE OF CONTENTS (Continued)

	Page
4.3 The Spectrum of Jupiter from 9000 - 10100 Å . . . . .	88
Introduction . . . . .	88
Equipment and Experimental Procedure . . . . .	89
Identifications . . . . .	93
Upper Limits . . . . .	99
4.4 The Spectrum of Jupiter from 9700 - 11200 Å . . . . .	105
Introduction . . . . .	105
Observational Material and Experimental Procedure . . . . .	105
Identifications . . . . .	108
Upper Limits . . . . .	118
The 3ν <sub>3</sub> Band of CH <sub>4</sub> and a Determination of Mean Temperature . . . . .	122
Discussion of Results . . . . .	135
5. LOW-DISPERSION INFRARED SPECTRA OF JUPITER, SATURN, IO AND GANYMEDE . . . . .	145
Introduction . . . . .	145
The Observations . . . . .	146
6. A DETERMINATION OF THE MARTIAN CO <sub>2</sub> ABUNDANCE . . . . .	157
Introduction . . . . .	157
Observations and Experimental Procedure . . . . .	158
The Martian CO <sub>2</sub> Abundance . . . . .	160
7. CONCLUSIONS . . . . .	173
APPENDIX A: THE TRANSFER OF RADIATION IN A SCATTERING ATMOSPHERE . . . . .	176
APPENDIX B: ATMOSPHERIC TEMPERATURE AND THE 1.05μ CO <sub>2</sub> BANDS . . . . .	184
APPENDIX C: A CONSIDERATION OF SATURATION EFFECTS IN THE MARTIAN CO <sub>2</sub> LINES . . . . .	189
REFERENCES . . . . .	194

## LIST OF ILLUSTRATIONS

Figure	Page
1. Schematic Representation of White Mirror System (not to scale) . . . . .	36
2. Front View of Mirror A with System Arranged for Eight Traversals ( $n = 3$ ) in the Bernstein-Herzberg Modification . . . . .	38
3. Front View of Mirror A in the LPL 72-foot Tube. Entrance Slit at Right of Mirror . .	41
4. Front View of Mirrors B and C in the LPL 72-foot Tube. Adjustable Mirror (C) at Left . . . . .	42
5a and b. Two Configurations of Camera and Collimating Mirrors for a Plane-Grating Spectrograph. Grating is Omitted Since Only Symmetry of Mirror System is Considered . . . . .	54
6. The Czerny-Turner Design. The Angles Between the Mirrors and the Grating are Exaggerated . . . . .	55
7. The Lunar and Planetary Laboratory 10-foot Spectrograph (not to scale) . . . . .	56
8. The H and K lines of Ca II. $1.6\mu$ Grating, 4th Order, $10\mu$ Slit . . . . .	63
9. The $D_1$ and $D_2$ Lines of Na I. $1.6\mu$ Grating, 4th Order, $10\mu$ Slit . . . . .	64
10. Paschen 6 of H I and Telluric Water Vapor Lines. $2.0\mu$ Grating, 2nd Order, $50\mu$ Slit .	65
11. Laboratory Spectrum of Ammonia in the Region $7535 \text{ \AA}$ to $7803 \text{ \AA}$ . Original Dispersion $20 \text{ \AA/mm}$ , Path Length 80 m, Pressure 350 mm Hg . . . . .	68

## LIST OF ILLUSTRATIONS (Continued)

Figure	Page
12. Spectra of the Sun (A), Jupiter (B), and 313 m atm (NTP) of $\text{CH}_4$ Plus Sunlight (C), 8350 Å to 8500 Å . . . . .	81
13. Spectra of the Sun (A), Jupiter (B), and 313 m atm (NTP) of $\text{CH}_4$ Plus Sunlight (C), 8500 Å to 8685 Å . . . . .	83
14. Spectra of Jupiter and Methane, 9630 Å to 10100 Å . . . . .	94
15. Spectra of Methane, Jupiter, and the Moon, 9300 Å to 9775 Å . . . . .	96
16. Spectra of Ammonia, Jupiter, and the Sun, 9080 Å to 9455 Å . . . . .	98
17. Spectrum of Jupiter with Comparison Spectra of 170 m atm of Methane and 3.4 m atm of Ammonia (NTP), 9700 Å to 10500 Å . . . . .	113
18. Spectrum of Jupiter with Comparison Spectra of Sun and 340 m atm of Methane (NTP), 10900 Å to 11175 Å . . . . .	115
19. Spectrum of Jupiter with Comparison Spectra of Sun and 13.6 m atm of Ammonia (NTP), 10500 Å to 10900 Å . . . . .	117
20. Normal Vibrations of a Tetrahedral Spherical Top Molecule . . . . .	123
21. Normalized Intensities of Rotational Lines of the $3\nu_3$ Band of $\text{CH}_4$ : A Comparison of Theoretical and Laboratory Intensities at $T = 295^\circ\text{K}$ . . . . .	131
22. Normalized Intensities of Rotational Lines of the $3\nu_3$ Band of $\text{CH}_4$ : A Comparison of Laboratory Intensities at $T \sim 210^\circ\text{K}$ with Theoretical Intensities at $T = 200^\circ\text{K}$ . . . .	132

## LIST OF ILLUSTRATIONS (Continued)

Figure	Page
23. Normalized Intensities of Rotational Lines of the $3\nu_3$ Band of $\text{CH}_4$ : A Comparison of Intensities in the Spectrum of Jupiter with Theoretical Intensities at $T = 200^\circ\text{K}$ and $T = 175^\circ\text{K}$ . . . . .	134
24. Spectra of Jupiter and Saturn (three exposures) on I-M Emulsions, 7300 Å to 9900 Å . . . . .	148
25. Spectra of Jupiter and Saturn on I-Z Emulsions, 8800 Å to 11000 Å . . . . .	150
26. Laboratory Spectra for Comparison with Plate II. These are Pairs of Spectra of Sunlight Reflected by a Layer of $\text{MgO}$ (lower, wider spectrum in each case) and an Ice (upper, narrower spectrum) as follows: A) $\text{CO}_2$ Ice Block, B) $\text{H}_2\text{O}$ Ice Crystals, C) $\text{H}_2\text{O}$ Ice Block.	152
27. Spectra of Jupiter and Satellites Io (JI) and Ganymede (JIII) on I-M Emulsions, 8500 Å to 9700 Å. The Lower Spectrum of Jupiter is Deliberately Overexposed to Show Details of 8873 Å Methane Band . . . . .	156
28. Spectra of the Sun Obtained at Two Zenith Angles ( $z$ ) to Show the Presence of Telluric $\text{CO}_2$ Absorptions with a Large Air Mass . . .	161
29. Spectra of Venus, Mars, and a Laboratory Path Length of 223 m atm (NTP) of $\text{CO}_2$ with the Sun as Light Source. The J Numbers of R and P Branch Lines of the $5\nu_3$ Band are Shown at the Bottom . . . . .	165
30. a) Solar Spectrum from the Liege <u>Photometric Atlas</u> , (b) Mt. Wilson Mars Spectrogram, (c) Laboratory Comparison (Sun + $\text{CO}_2$ ). Note Presence of Three Rotational $\text{CO}_2$ Lines in (b) and (c). . . . .	167
31. Laboratory Spectra of $2\nu_1 + 3\nu_3$ and $\nu_1 + 2\nu_2 + 3\nu_3$ of $\text{CO}_2$ at Three Path Lengths (NTP). The Sun was Again Used as Light Source. . .	187

## LIST OF TABLES

Table	Page
1. Jovian Temperature Measurements (a) . . . . .	25
2. Laboratory Lines of the 7654 Å Band of NH <sub>3</sub> . . .	70
3. A Comparison of Jovian and Laboratory Ammonia Wavelengths . . . . .	71
4. The Assignment of Vibrational Frequencies to Bands of CH <sub>4</sub> in the Spectrum of Jupiter . .	86
5. Laboratory Spectra of Gases . . . . .	91
6. Spectra of Jupiter (a) . . . . .	92
7. Upper Limits on the Abundances of Six Gases in the Jovian Atmosphere . . . . .	101
8. Spectra of Jupiter (b) . . . . .	107
9. Identification of Absorption Lines in the Spectrum of Jupiter from 9690 Å to 11206 Å .	109
10. Upper Limits on the Abundances of Eight Gases in the Jovian Atmosphere . . . . .	121
11. Jovian Temperature Measurements (b) . . . . .	139
12. Low Dispersion Spectra Obtained at the Kitt Peak Observatory . . . . .	147
13. CO <sub>2</sub> Bands Near 1.05μ . . . . .	186

## ABSTRACT

The investigation of planetary atmospheres by means of spectroscopy may be said to have begun a little over 100 years ago when Lewis Rutherford discovered two bands in the spectrum of Jupiter which were not present in the spectrum of the sun. Since that time, our knowledge of the physical characteristics of the atmospheres of the planets has depended heavily on studies of planetary spectra.

The interpretation of the spectra of the planets is virtually a hopeless task without the aid of appropriate laboratory investigations. Such studies contribute to all phases of the work from the identification of absorption lines to determinations of atmospheric temperature and pressure. Two instruments were constructed to meet the needs of a useful laboratory program. A 72-foot multiple-path absorption tube was built to facilitate the duplication of atmospheric conditions by allowing long optical paths to be obtained at relatively low pressures. The second instrument was a 10-foot plane grating spectrograph capable of producing the high resolution needed to match observations at the telescope and to permit detailed studies of the fine structure of some of the more complex band systems.

The major part of the program carried out in the laboratory was devoted to an analysis of the spectrum of Jupiter. Its purpose was to identify all of the planetary absorptions occurring in the Jovian spectrum and to analyze the identified bands in an effort to derive an atmospheric temperature. The result of the first part of this study was that all of the previously unidentified spectral features contributed by the atmosphere of the planet in the region studied were found to be due to methane or ammonia. In the process, two new bands of ammonia were discovered and upper limits were set on the atmospheric D/H ratio and the abundances of a number of gases. The second part of the program succeeded when it was found that the  $3\nu_3$  band of methane occurring at  $1.1057\mu$  could be analyzed to yield an atmospheric temperature of  $200 \pm 25^\circ\text{K}$ .

With this study of Jupiter as background, low dispersion spectra of Jupiter and Saturn were obtained to determine whether any features not due to methane or ammonia would appear in the spectrum of the latter. The result was negative but the spectrum of Saturn's ring showed a broad absorption feature which has been found to correspond with a similar feature in the reflection spectrum of water ice. Low dispersion spectra of Io and Ganymede allowed an upper limit of 100 cm atm to be placed on the abundance of methane in possible atmospheres of these bodies.

A spectrogram of Mars obtained recently at the Mt. Wilson Observatory by Münch, Spinrad, and Kaplan revealed three rotational lines in the  $5\nu_3$  band of  $\text{CO}_2$ . This observation suggested that there was a much greater abundance of this gas in the atmosphere of the planet than had previously been assumed. As a result, an investigation was initiated to determine an independent value for this abundance. As part of this study, a spectrum of the sun at a very large air mass was obtained to test whether these  $\text{CO}_2$  lines would appear in the telluric spectrum. This attempt was successful and led to a very approximate value for the Martian  $\text{CO}_2$  abundance. A subsequent laboratory investigation resulted in a more precise determination of  $46 \pm 20$  m atm.

This research has indicated a number of areas where further work is needed. Among the required studies is a new model for the Jovian atmosphere based on additional measurements of temperature and abundances and their variation with time and position on the disk of the planet. Spectra of Mars obtained in the  $1.05\mu$  region should permit a more accurate determination of the  $\text{CO}_2$  abundance and the mean atmospheric temperature.



## 1. INTRODUCTION

The underlying purpose of the research reported in this dissertation has been the accumulation of additional knowledge about planetary environments. The dissertation itself is particularly concerned with properties of the atmospheres of Jupiter and Mars, but this work represents only a part of a continuing program which includes studies of the other planets as well.

One of the most powerful techniques for obtaining information about the atmosphere of a planet is modern spectroscopy as performed with large telescopes. Since the planets are at relatively low temperatures, one anticipates that the atmospheric gases will reveal their presence by absorbing the incident solar radiation at characteristic wavelengths. Some emissions will occur as a result of non-equilibrium excitation in the upper region of a planet's atmosphere but these will be difficult to detect against the strong solar background. This situation can be improved somewhat in the case of Venus by attempting to observe the unilluminated hemisphere, but such observations have not yet yielded unequivocal results.

The absorption bands which may be expected from the constituent molecules of an atmosphere are basically of

three types. In order of decreasing energy, these are due to electronic, vibrational, or rotational transitions. Only bands of the second type have been observed in the spectra of planets other than the Earth. This is not surprising since the electronic bands of most gases correspond to energies which are so high that the corresponding absorptions lie below the cut-off due to the (electronic) bands of telluric ozone. At the other extreme, the rotational lines occur at long wavelengths which are effectively blocked by absorptions due to the (rotational) spectrum of telluric water vapor. The ammonia band which has been detected in the spectrum of Jupiter at 1.28 cm is caused by a fourth type of transition known as an inversion.

The vibrational bands correspond to transitions with intermediate energies. Fundamental molecular vibrations give rise to absorptions at wavelengths greater than  $2\mu$ . The photographic plate can be used with difficulty to  $1.3\mu$  but its practical limit is closer to  $1.1\mu$ . Photographic spectroscopy (which is the technique used in the research described here) is thus limited to studies of overtones and combinations of the fundamental vibrations and their rotational fine structure. This is still a rich source of data, however, since in principle it is possible to deduce information about the chemical composition, abundance, temperature, pressure, and even certain dynamical properties

of the gases giving rise to the absorptions. When these gases are the constituents of the atmosphere of a planet, it is evident that a considerable amount of useful information characterizing the planetary environment can be obtained.

In practice, such deductions are often complicated by the lack of an adequate theory or difficulties in properly compensating for instrumental effects. Hence there is a definite need for a laboratory program which is directed toward the acquisition of spectra of gases subjected to simulated planetary conditions. Such a program requires two basic classes of equipment: absorption tubes and spectrographs. The former must be capable of producing long optical paths at a variety of temperatures. Since it is difficult for a single tube to meet both these requirements without compromise, it is more practical to have one tube (which remains at room temperature) for obtaining the longest possible optical paths and another tube which is sufficiently compact that it can be easily cooled or heated. The spectrographic equipment must at least be capable of duplicating the resolution of the planetary spectra which are being studied. When these spectra have been obtained with a powerful spectrograph at the coudé focus of a large reflecting telescope, matching the resolution becomes a significant challenge. Moreover, it is often valuable to be able to use even higher resolution in the laboratory in

order to examine features not clearly indicated in the planetary spectra.

A two-meter absorption tube was loaned to the Lunar and Planetary Laboratory by the National Research Council of Canada through the courtesy of Dr. Gerhard Herzberg. This tube had been used by Dr. Herzberg to study the pressure-induced dipole spectrum of hydrogen at the temperature of liquid nitrogen and thus was well suited to our purposes. It can produce a path length of 80 meters by means of a White mirror system. A Dewar was bought and a rack for supporting both tube and Dewar was constructed for low temperature work. The Herzberg tube has been used for studies of gases when relatively small path lengths or low temperatures were required but it is not suitable for investigations requiring long paths and low pressures. Hence a 72-foot absorption tube was built which has been used at path lengths up to 3.6 km.

The spectroscopic studies were begun with a Bausch and Lomb 1.5-meter concave grating spectrograph which has a dispersion of  $20 \text{ \AA/mm}$  in the first-order infrared. This instrument was adequate for comparisons with planetary spectra of moderate resolution but its limitations soon became apparent. Accordingly, a ten-foot plane grating instrument was constructed which has dispersions ranging from  $5 \text{ \AA/mm}$  to better than  $1 \text{ \AA/mm}$  depending on the order of the grating which is used.

With this equipment it has been possible to carry out a variety of investigations. Two typical problems which had been of particular interest to the writer were the identification of several features which had been discovered in the spectrum of Uranus several years ago and a direct determination of the mean temperature of the atmosphere of Jupiter from the absorption bands in its spectrum. Both of these problems have been solved (the Uranus study is reported elsewhere), and in the process, considerable additional information regarding the atmosphere of Jupiter has been acquired. At the time the laboratory program was begun, the atmosphere of Mars was considered to be relatively well understood. The recent observation of the  $5\nu_3$  band of carbon dioxide in a spectrogram of the planet obtained by Kaplan, Münch, and Spinrad (1964) has resulted in a rather drastic revision of a previously accepted estimate of Martian surface pressure and atmospheric composition. As a result, a laboratory study which had been initiated for the purpose of calibrating the intensities of the  $\text{CO}_2$  bands occurring at  $1.6\mu$  (with a lead-sulfide spectrometer) was expanded to include a direct abundance determination from the observation made by Kaplan et al.

These two studies (of Jupiter and Mars) form the body of the dissertation. They were originally written as separate articles for purposes of publication and this form has been retained. Thus the study of the spectrum of

Jupiter is broken down into several sections corresponding to individual papers. These papers are concerned with an identification of the absorptions which have been observed in the spectrum of the planet and an interpretation of the identified features in terms of atmospheric characteristics. This material is preceded by a review of previous investigations of planetary spectra and a description of the designs of the 72-foot absorption tube and the Czerny-Turner spectrograph. Three appendices are included to amplify certain points which were condensed for the sake of brevity in the main text.

## 2. HISTORICAL BACKGROUND

The study of planetary spectra began with the first applications of the spectroscope to an analysis of the light from astronomical sources. The initial observations were made visually with small telescopes. When the photographic process was developed, light-sensitive emulsions were used to record the spectra; in the blue and green regions at first, then further into the red and infrared as new sensitizing dyes became available. The improvement of photographic plates was roughly paralleled by improvements in the basic equipment used, culminating in the high-dispersion coude spectrographs and large reflecting telescopes of today. In this survey of the history of planetary spectroscopy, a brief account of the early work will be given followed by a more detailed review of the theoretical and observational results obtained in the last fifteen years. The latter section is divided into two parts corresponding to the concentration of the body of the dissertation on studies of the atmospheres of Mars and the Jovian planets. Within these two sections there is an emphasis on results which relate directly to the research described in the dissertation.

The first spectroscopic observations of the planets were probably those of Joseph Fraunhofer. In 1828 he

reported that "The spectra from the light of Mars and from that of Venus, contain the same fixed lines as the spectrum from sunlight, and in precisely the same place, at least as far as relates to the lines D, E, b, and F, of which the relative situation could be precisely determined" (Fraunhofer 1828).

Although he is not well known as a spectroscopist, Lewis Rutherfurd appears to have been the first person to detect non-solar absorptions in planetary spectra. In 1863 he wrote that in addition to the customary Fraunhofer lines, the spectrum of Jupiter contained ".... two bands in the red and orange, between C and D, which are not found in the solar spectrum." He suggested that these might be due to a Jovian atmosphere (Rutherfurd 1863).

The two most famous pioneers in the field of astronomical spectroscopy were Angelo Secchi of Italy and William Huggins of England. Both men recorded observations of planetary spectra. In 1863, Secchi published a brief article in the Astronomische Nachrichten describing his initial spectroscopic observations. In this report he mentions that he has observed the spectrum of Mars but this observation was made primarily as a check on the visibility of the Fraunhofer lines in astronomical sources with his instrument.

The following year, Huggins (1864) published the first account of his work. He pointed out that since lines



appear in the solar spectrum which are unquestionably due to the terrestrial atmosphere because they increase in strength as the sun approaches the horizon, it is not unreasonable to expect the atmospheres of other planets to reveal themselves in a similar fashion. With this thought in mind, he observed the spectra of the moon, Jupiter, Venus and Mars. He found no evidence of an atmosphere on Venus or the moon but discovered two lines in the red and orange region of the spectrum of Jupiter and suspected some augmentation of telluric features in the spectrum of Mars. The two lines in the Jovian spectrum are the same as those observed by Rutherford (of whose work Huggins was apparently unaware) and probably correspond to the  $6450 \text{ \AA}$  band of ammonia and the  $6190 \text{ \AA}$  band of methane, respectively. The Mars observations were undoubtedly erroneous but remained a source of controversy for some time. Later both Secchi (1869) and Huggins (1870) reported the presence of strong bands in the blue and green region of the spectrum of Uranus. All of these observations were made visually but Huggins was eventually able to photograph planetary spectra in the blue and green regions of the spectrum.

Other early observers who should be mentioned are Vogel (1895) and Keeler (1895). Vogel made a special study of planetary spectra using his own observations as well as those of Huggins and effectively summarized contemporary knowledge. Keeler used the Doppler effect to show

spectroscopically that Maxwell's hypothesis that the rings of Saturn consisted of separate particles was almost certainly correct. This result was subsequently confirmed by Campbell (1895).

The next active investigator of planetary spectra was V. M. Slipher of the Lowell Observatory. He summarized his observations, made over a period of thirty years, in the George Darwin lecture of 1933. During the course of his investigations, the wavelength range of the photographic emulsion was increased from an upper limit of 6000 Å to 10,500 Å. Slipher states that as the improved emulsions became available it was his "....custom at the Lowell Observatory to re-photograph the spectra of the planets whenever it has been possible to reach a little farther into the longer wavelengths, for every extension in that direction has added new planetary absorption bands." He was able to record the spectra of Venus and Jupiter to wavelengths slightly longer than 10,000 Å, the other planets being too faint even with the relatively low dispersions he employed. He notes the positions of the strong absorption bands in the major planets, pointing out that the bands are stronger in the spectra of the planets which are farther from the sun. Slipher's investigations also included a spectroscopic test for the rotation of Venus (giving a negative result) and an analysis of the spectrum of Mars.

which led him to conclude that the Martian atmosphere contained water vapor.

The absorption bands in the spectra of the major planets observed in the visible region by Huggins and Secchi and so prominent in the red and infrared spectra of Slipher were identified in 1932 by R. Wildt at Göttingen. Using Slipher's spectra as well as some of his own, Wildt was able to show that bands at  $6470 \text{ \AA}$  and  $7920 \text{ \AA}$  were probably due to ammonia while he identified the bands at  $5430 \text{ \AA}$ ,  $6190 \text{ \AA}$ ,  $7260 \text{ \AA}$ ,  $8650 \text{ \AA}$ , and  $8900 \text{ \AA}$  as due to methane. These identifications were accomplished by comparing wavelengths measured on spectra of the planets with the results of laboratory investigations of ammonia and methane made by Badger (1930) and Dennison and Ingram (1931), respectively. In the case of the methane absorptions, it was necessary to extrapolate from the only band observed photographically in the laboratory ( $8900 \text{ \AA}$ ) using a formula developed by Dennison and Ingram (loc. cit.) for the prediction of the positions of overtones of the methane fundamental at  $3.3\mu$  ( $\nu_3$ ).

The work on identifications was extended by Adel and Slipher (1934) who used a double-traversal absorption tube with a length of 22.5 meters which could be pressurized to about 45 atmospheres. With this apparatus they examined the spectrum of methane, ethane, and ethylene. They concluded that all of the methane bands they could observe in the laboratory were present in the planetary spectra while the

spectra of Uranus and Neptune contained additional bands in the blue and green region which they felt their path lengths were insufficient to produce. They remarked that the strongest of the ethylene and ethane bands were not present in the planetary spectra but did not try to set any abundance limits. This paper included an attempt to classify the methane bands in terms of combinations and overtones of the fundamental frequencies of the molecule. The attempt was subsequently criticized by Herzberg (1945) who suggested that there were not enough data available to support any general formula for the frequencies of the overtone and combination bands.

All of the investigations described so far were made with relatively low dispersion. High dispersion studies of planetary spectra were undertaken at the Mt. Wilson Observatory and the results of these studies have been summarized by Dunham (1952). A number of significant results were obtained including the identification of carbon dioxide bands in the spectrum of Venus and the establishment of new low upper limits on the water vapor and oxygen abundances in the atmosphere of Mars. The high dispersion spectra of Jupiter and Saturn revealed the individual lines making up the strong absorption bands thus permitting detailed comparisons with spectra of ammonia and methane obtained with the same spectrographic equipment and a double-pass absorption tube. These comparisons confirmed the earlier identifications made

by Wildt and indicated that intensity differences between the fine structure lines of ammonia in the spectra of Jupiter and Saturn and the laboratory spectra might provide an empirical means for estimating the temperatures of the planetary atmospheres. The spectrum of Jupiter was recorded out to 10,000 Å at a slightly higher dispersion than that used by Slipher but the absorption bands appearing in this region were not positively identified.

The early work on abundances of gases in planetary atmospheres was criticized by Herzberg (1952) on the grounds that the laboratory data were obtained at high pressures and consequently could not be expected to represent conditions in the atmospheres under investigation. The pressure broadening of the rotational lines made an accurate comparison of intensities between laboratory and planetary spectra virtually impossible. Modifying a design originally proposed by White (1942), Herzberg constructed multiple-path absorption tubes in which the light beam could make a large number of traversals through the gas being studied before leaving the tube for spectrographic analysis. Thus long path lengths could be achieved at relatively low pressures. The largest tube was 22 meters in length and had a maximum effective interior path length of 5500 meters. Among the results Herzberg obtained with this tube were a derivation of 2 km atmospheres for the abundance of CO<sub>2</sub> in the atmosphere of Venus and the detection of the (2,0) and (3,0)

quadrupole vibration-rotation lines of  $H_2$  (whose spectrum he had predicted several years earlier (Herzberg 1938)).

Kuiper (1952) used the same apparatus to determine the abundances of methane and ammonia in the atmospheres of the major planets and to set upper limits on the abundances of several gases in the atmospheres of the terrestrial planets. These results are summarized in a table on page 374 of the cited reference. This work was done at low and medium dispersion and took into consideration the theoretical study of van de Hulst (1952) which showed that abundances must be derived from the weakest of the absorption lines due to a particular gas which occur in the planetary spectrum. Reproductions of some of the laboratory spectra obtained in this program are presented in a review paper (Kuiper 1950) which includes summaries of current knowledge about the physical environments of the planets.

The increase in knowledge about the constituents of the atmospheres of the planets allowed a parallel advancement of understanding of atmospheric structure. On the basis of observations made at the telescope and in the laboratory, and with the help of the insight provided by advances in the science of terrestrial meteorology, it became possible to develop preliminary model atmospheres for those planets whose spectra were well observed.

## 2.1 Jupiter

In his original paper describing his identification of the absorption bands in the spectrum of Jupiter, Wildt (1932) derived a maximum ammonia abundance of  $0.03 \text{ gr/cm}^2$  by using laboratory data on the ammonia vapor pressure at a temperature near that ascribed to Jupiter by Pettit and Nicholson from their thermocouple measures. This procedure was reversed by Dunham (1933) who used the abundance of  $\text{NH}_3$  in the Jovian atmosphere as derived from laboratory comparisons to determine the temperature at which that amount of gas is in equilibrium with the solid. The temperature so derived is a minimum temperature for the layer in the atmosphere at the base of the ammonia column ( $150^\circ\text{K}$  assuming dilution by  $\text{H}_2$ ). Kuiper (1952) performed a more sophisticated analysis which involved the derivation of a preliminary model for the Jovian upper atmosphere. His starting point was a stratospheric temperature derived on the basis of the Gold-Humphreys interpretation of the terrestrial stratosphere. With two different assumptions for the atmospheric composition he computed the corresponding dry adiabatic lapse rates and used those to derive temperature vs. height profiles for the atmosphere below the "tropopause". Assuming saturation of the ammonia vapor above the cloud deck, the level of the latter corresponded to that distance below the tropopause at which the amount of ammonia vapor in a column of unit area was equal to the amount derived

from the spectroscopic abundance analysis. This point corresponds to a certain temperature as well, which is different for the two different compositions (lapse rates).

Hess (1953) obtained additional observational data by examining the variations in intensity of the ammonia and methane absorptions in the spectra of Jupiter and Saturn with respect to the projected position of the spectrograph slit on the planets' discs. He used a dispersion of  $43 \text{ \AA/mm}$  which meant that he could only determine the equivalent widths of each band as a whole, not of individual lines in a band. The purpose of his observations was twofold. He wanted to verify the surprising result obtained by earlier workers that the intensities of the absorptions did not increase near the limbs of the planets and he also hoped to be able to draw conclusions about the temperatures and elevations of the cloud layers at various positions on the discs. The latter deductions are possible because the amount of methane found above a given location is a measure of the height of the column above the location while the amount of ammonia depends on the surface partial pressure which in turn is essentially a function of temperature only. The difference arises because methane is uncondensed above the visible surface while ammonia is in equilibrium between the solid and gaseous states. Hess' conclusions were that "... the absorptions decrease slightly toward the edges of Jupiter but increase somewhat toward the edges of Saturn."



He interpreted this to mean that "... the cloud surface on Jupiter rises somewhat toward the limbs, but is more nearly level on Saturn. The ammonia results indicate a decrease in temperature from equator to poles on Jupiter. The morning limb is found to be cooler than the evening limb." Hess could not study the variation of the strength of the ammonia band in the spectrum of Jupiter because he found it too faint to measure accurately. We shall return to this point later.

Kuiper (1952) also looked for variations in the strengths of these two bands in the spectrum of Jupiter using a dispersion of  $110 \text{ \AA/mm}$ . He found variations amounting to a factor 2 in the intensity of the ammonia absorptions above the bright equatorial zone, sometimes occurring in a period of a week or two. The polar region showed a somewhat weaker absorption by about a factor 1.5. The strength of the methane band was found to be essentially constant with time and position on the disc. His conclusion, based on a comparison of cloud structure revealed in ultraviolet and infrared photographs as well, was that the top of the cloud layer was not sharp but diffuse and the constancy of the methane absorption with position on the disc is due to the fact that the light would penetrate the same distance into the haze layer at all positions on the disc. One could then explain the lower temperature found by Hess at the limbs as a natural result of the fact that this "penetration

level" would be higher above the cloud layer at the limbs than at the center of the disc simply as a result of the angle of observation (with respect to the local zenith). The difference in temperature between morning and evening limbs requires a different model, however.

Both of these interpretations were criticized by Squires (1957) who reinterpreted the observations of Hess "... taking into account the radiation conditions at the cloud surface, the apparent turbulence of the cloud layer, and possible temperature distributions. The only hypothesis found to be free from objection is that the cloud top is cumuliform." On this hypothesis, it is no longer possible to derive a temperature for the cloud layer from the spectroscopic measurements. In particular, these measurements are consistent with a temperature at the level of the main cloud deck considerably in excess of  $170^{\circ}\text{K}$ .

Additional attention has also been given to theoretical models for the Jovian atmosphere. Lorenz (1951) calculated a thermodynamic chart for Jupiter's atmosphere which was modeled on the pseudo-adiabatic charts in common use in terrestrial meteorology. His chart contained wet and dry adiabats and lines of constant mixing ratio superimposed on a grid of isobars and isotherms. The main conclusions which Lorenz drew from this work were the probable importance of changes of phase of ammonia in Jovian meteorology and the necessity for better knowledge of temperatures and

pressures in the Jovian atmosphere in order to properly understand the thermodynamic problems which the atmosphere presents.

Gallet (1963) has pointed out that conditions in the lower atmosphere (below the cloud deck) cannot be predicted on the basis of an extrapolation of the dry adiabatic lapse rate used by Kuiper for the upper atmosphere. Instead he proposed that the saturation adiabat must be followed to allow for condensation of ammonia (and at lower, warmer levels, of water vapor). In this way he finds that it is possible to reach high enough pressures at low enough temperatures that a solid mantle might exist below the atmosphere.

Lasker (1963) has suggested that a wet adiabatic model should be used for the atmosphere above the cloud layer as well since if one postulates sufficient turbulence in this region to keep the ammonia vapor in saturation equilibrium with the cloud particles, the heat balance established by the sublimation-deposition process will cause a significant departure from the dry adiabatic lapse rate.

Unfortunately, all these models depend on a knowledge of the composition of the Jovian atmosphere which is not yet well established. The principal uncertainty lies with the abundances of hydrogen and helium.

As stated above, Herzberg (1938, 1952) first predicted the wavelengths and intensities for the  $H_2$  quadrupole rotation-vibration spectrum and subsequently observed the (2,0) and (3,0) overtones in the laboratory. Kiess et al. (1960) detected the four strongest lines of the (3,0) overtone in the spectrum of Jupiter. Using their spectrum, Zabriskie (1962) derived a hydrogen abundance of 3.3 km atm and a rotational temperature of 170°K. He used a simple model atmosphere consisting of a clear layer of gas overlying a reflecting surface and the f-values derived by James and Coolidge (1938). He further assumed that the lines were not saturated. Spinrad and Trafton (1963) have made a new abundance determination based on an empirical comparison with Herzberg's laboratory spectra and supported by new work on the f-values for the transitions. They derived an abundance of 27 km atm using the same model as Zabriskie and also assuming no saturation. In the same paper they report the discovery of the (4,0) overtone of the  $H_2$  quadrupole system in spectra of Jupiter, Saturn, and Uranus. Foltz and Rank (1963) have cautioned that the hydrogen abundance derived by Spinrad and Trafton may still be too low by an order of magnitude since the mere presence of the (4,0) overtone implies immense amounts of gas.

Clearly a knowledge of the hydrogen abundance is critical for a proper understanding of the Jovian atmosphere since it is becoming obvious that hydrogen must be the major

atmospheric constituent. The main evidence for the presence of substantial quantities of helium (or some heavier gas) in addition to the hydrogen comes from an observation made by Baum and Code (1953). These authors were able to derive a value for the scale height in the upper atmosphere of Jupiter from a photometric observation of the occultation of the star  $\sigma$  Arietis by the planet. Using Kuiper's (1952) value of 86°K for the stratospheric temperature, they obtained a value of 3.3 for the mean molecular weight. Öpik (1963) has suggested that this figure should not be given undue weight since there are several ways in which a higher stratospheric temperature could be produced. The mixture of gases which Öpik uses to represent the atmospheric composition is based on Zabriskie's evaluation of the hydrogen abundance and thus is incorrect. It also results in a cloud-top pressure of 11 atmospheres which is not supported by a pressure-broadening analysis of the Jovian methane lines (Spinrad and Trafton 1963).

At the present time then, we have evidence for the presence of the following amounts of gases in the atmosphere of Jupiter:

H <sub>2</sub>	270 km atm	Foltz and Rank 1963
CH <sub>4</sub>	150 m atm	Kuiper 1952
NH <sub>3</sub>	7 m atm	Kuiper 1952

The atmosphere of Saturn is not as well analyzed. The presence of the (4,0) quadrupole band of H<sub>2</sub> (Spinrad and

Trafton 1963) again indicates large amounts of this gas but an abundance has not yet been derived. Dunham (1952) reported the presence of a small amount of ammonia but Spinrad and Münch (1963) have not been able to confirm this observation, in agreement with the result of Hess (1953). Spinrad (1963) has suggested that the abundance may be variable, depending on atmospheric temperature changes. Kuiper's (1952) determination of the  $\text{CH}_4$  abundance as 350 m atm appears to be the only reliable figure currently available.

From arguments based on cosmic abundances and theories of the origin of the solar system, it is possible to suggest approximate amounts of other gases which should be remnants of these planets' primeval atmospheres (Kuiper 1952, Urey 1951, Field 1963). In addition, from photochemical arguments Wildt (1937), Sagan (1960) and Cadle (1962) have shown that small amounts of more complex substances such as ethane, ethylene, and methylamine should be produced from the known constituents. Sagan's (1960) tentative identification of HCN on one of Kuiper's far infrared tracings is probably incorrect, however (Kuiper 1963). Sagan and Miller (1960) found that it was possible to produce active compounds such as acetylene and hydrazine in a mixture of hydrogen, methane and ammonia which was subjected to an electric discharge. Unfortunately, the hydrogen-methane ratio they used was smaller than that implied by the

discussion of Foltz and Rank (1963) by a factor 50. This interesting experiment should be repeated with a mixture of gases based on the new results.

Aside from chemical arguments, the presence of other atmospheric constituents can be suggested on the basis of the heat balance of the planet. As both Kuiper (1952) and Urey (1957) have stressed, neither methane nor ammonia absorbs strongly in the region where the black body curve corresponding to the temperature of the Jovian cloud layer has its maximum ( $\sim 18\mu$ ). Nevertheless, the measured Jovian temperatures are considerably in excess of those predicted from the radiation balance established by a rapidly rotating black body at the distance of Jupiter from the Sun (Kuiper 1952). This discrepancy has been explained by the proposal that Jupiter is still cooling down from an earlier high temperature stage (e.g., Kuiper 1952, Öpik 1963) but one cannot yet rule out the possibility that small amounts of other gases are present which absorb in the appropriate region thus producing the required "greenhouse effect". However, the suggestion by Zabriskie (1962) that the analysis of the Jovian spectrum carried out by Kiess et al. (1960) is indicative of the presence of a larger amount of methane than is generally accepted will be shown to be incorrect (Section 4.2). Spinrad (1962) has cast doubt on another result reported by Kiess et al., viz. the ultra-violet absorption continuum which they attribute to  $N_2O_4$ .

The determination of the atmospheric temperature has itself been a difficult problem. The early measurements of Menzel et al. (1926) gave a value of  $130^{\circ}\text{K}$  in the  $9\text{-}13\mu$  spectral region. Using the same technique, Pettit (1961) derived a value of  $150^{\circ}\text{K}$ . Working at the same wavelength but using a more sensitive instrument, Murray and Wildey (1963) found a temperature of  $128^{\circ}$ . Zabriskie (1962) used the rotational lines of the  $\text{H}_2$  quadrupole spectrum to derive a temperature of  $170^{\circ}\text{K}$  from an assumed Boltzmann distribution; Spinrad (1963) used the same lines (but measured on different spectra) and obtained a temperature of  $120^{\circ}\text{K}$ . The results derived in the microwave region are just as confusing and are summarized together with the others in Table 1.

The explanation for the multiplicity of temperatures appears to be threefold. On the one hand, some of the measurements are sufficiently difficult to be rather imprecise and thus the agreement among measurements made at a given wavelength may be better than it appears. Nevertheless, the vigorous activity observed in the cloud belts visually and photographically and the variability in the strength of the ammonia absorptions with time (see above) suggest that a real secular variation in temperature probably exists. Finally, the variation with wavelength is undoubtedly real and results from the fact that the different measurements correspond to different levels in the Jovian atmosphere as determined by the ammonia



Table 1

## JOVIAN TEMPERATURE MEASUREMENTS (a)

Temp. (°K)	Wave- length	Method	Identification and Central Wavelength of Relevant Absorber	Reference
170	.83 $\mu$	Analysis of (3,0) H <sub>2</sub> Quadrupole Lines	H <sub>2</sub> , S(0)-.83 $\mu$	Zabriskie 1962
120	.83 $\mu$	Analysis of (3,0) H <sub>2</sub> Quadrupole Lines	H <sub>2</sub> , S(0)-.83 $\mu$	Spinrad 1964
130	9-13 $\mu$	Thermocouple	NH <sub>3</sub> 10.5 $\mu$	Menzel et al. 1926
131	9-13 $\mu$	Thermocouple	NH <sub>3</sub> 10.5 $\mu$	Sinton & Strong 1960
150	9-13 $\mu$	Thermocouple	NH <sub>3</sub> 10.5 $\mu$	Pettit 1961
128 $\pm$ 2.3	9-13 $\mu$	Germanium Bolometer	NH <sub>3</sub> 10.5 $\mu$	Murray & Wildey 1963
144 $\pm$ 23	8.35 mm	Microwave Radiometer	NH <sub>3</sub> 1.28 cm	Thornton & Welch 1963
140 $\pm$ 38	3.15 cm	Microwave Radiometer	NH <sub>3</sub> 1.28 cm	Mayer et al. 1958a and b
145 $\pm$ 18	3.15 cm	Microwave Radiometer	NH <sub>3</sub> 1.28 cm	Mayer et al. 1958a and b

Table 1 (Continued)

Temp. (°K)	Wave- length	Method	Identification and Central Wavelength of Relevant Absorber	Reference
171 <u>±</u> 20	3.03 cm	Microwave Radiometer	NH <sub>3</sub> 1.28 cm	Giordmaine et al. 1959
173 <u>±</u> 20	3.17 cm	Microwave Radiometer	NH <sub>3</sub> 1.28 cm	Giordmaine et al. 1959
193 <u>±</u> 16	3.3 cm	Microwave Radiometer	NH <sub>3</sub> 1.28 cm	Bibinova et al. 1962
189 <u>±</u> 20	3.36 cm	Microwave Radiometer	NH <sub>3</sub> 1.28 cm	Giordmaine et al. 1959
200	3.75 cm	Microwave Radiometer	NH <sub>3</sub> 1.28 cm	Drake & Ewen 1958

absorption at the relevant wavelength (Kuiper 1952). This problem will be dealt with again in Section 4.4.

The intense activity of the Jovian atmosphere has manifested itself in another way. Spinrad (1962) measured the inclination of the ammonia lines on a high dispersion spectrum taken by Münch and found that the lines were inclined less than would have been expected from the known rotation rate of the planet. The reflected Fraunhofer lines in the same spectrum gave the expected value. To check this surprising result, Spinrad also measured a plate obtained by Dunham in 1934. Again a smaller inclination was found. Spinrad and Trafton (1963) discussed these observations in more detail and included additional measurements on spectra from the Victoria and Mt. Wilson Observatories. All the line tilt measurements made on spectra obtained prior to 1962 indicate significant deviations from the inclination expected from the rotation rate and always in the same sense - such that the ammonia appears to be rotating more slowly than the cloud layers. Two spectra obtained in 1962 showed no anomalous inclination which the authors interpret as evidence for "... noticeable changes in the rotation of the Jovian gases." As Spinrad and Trafton (1963) point out, an interpretation of these observations is difficult since a Doppler displacement requires a separation between the motions of the ammonia gas and the particles in the cloud layer which reflect the light. Owen and Staley (1963) have

suggested that if a Doppler shift is responsible, there may be an analogy with periodic winds in the Earth's stratosphere. An examination for periodicity was suggested as a test of this hypothesis. If the analogy with the telluric winds were rigorous, a maximum could be predicted for the fall of 1963. Giver (1964) reported no anomalously inclined lines in spectra obtained in August 1963, while Owen (unpublished) also found no deviation from normalcy in October 1963. Nishida and Jugaku (1964), however, apparently recorded a slight anomaly in November 1963. In apparent contradiction to this, Fehrenbach and Guerin (1964) have reported that no anomaly was present on a spectrum obtained some six days after the Japanese observation. These authors also found a normal inclination of the ammonia lines on two days in September 1963. It is possible that the effect is subject to rapid variations. In any case, more observations are needed before its magnitude and possible periodicity can be adequately determined.

## 2.2 Mars

The research on the Mars atmosphere which has been done for the dissertation is concerned with a derivation of the carbon dioxide content. Thus we shall only discuss that part of the extensive literature covering observational and theoretical research on Mars which is related to this topic.

Carbon dioxide was discovered in the Martian atmosphere by Kuiper in 1947 (Kuiper 1952). The observation leading to the discovery was made with a lead-sulfide spectrometer which recorded the CO<sub>2</sub> bands at 1.6μ. The Martian absorptions were calibrated by means of a curve of growth of the telluric CO<sub>2</sub> bands appearing in the solar spectrum with increasing intensity as the sun's zenith angle increases. This led to a preliminary estimate of 4.4 m atm for the CO<sub>2</sub> abundance in the Mars atmosphere.

Using this information and Dollfus' (1951) observation that the scattering power of the Mars atmosphere is 0.22 times that of the terrestrial atmosphere, Kuiper (1952) derived a mixture of 0.96 N<sub>2</sub>, 0.04 A, and 0.003 CO<sub>2</sub> (by volume) for the atmosphere.

Grandjean and Goody (1955) attempted to re-calibrate Kuiper's 1947 observations by working with the unresolved rotational lines in the two bands and considering the effects of pressure broadening. They derived a relation of the form

$$P_s^2 f = 1.6 \pm 0.5 \times 10^2 \text{ mb}^2$$

where  $P_s$  is the Martian surface pressure and  $f$  is the fraction by volume of CO<sub>2</sub> in the Martian atmosphere. Assuming a surface pressure of 100 mb as the most likely value they arrived at a Martian CO<sub>2</sub> concentration of 50 times the terrestrial value while the amount of the gas

would be 13 times or about 29 m atm. For a lower pressure, the concentration and amount of gas will increase.

The early work on the surface pressure of the Martian atmosphere has been reviewed by de Vaucouleurs (1954). This consisted of a determination of mean albedos (Menzel), polarization (Lyot and Dollfus), photographic and visual photometry (Barabascheff, Scharonow, Sytinskaya, Fessenkov (photographic), de Vaucouleurs (visual)), and a meteorological method involving observations of the heights of convective clouds (Hess). De Vaucouleurs rejects all of these results except the polarization measurements of Dollfus and his own photometric analysis, attributing greater significance to the former. The value derived from these measurements was  $85 \pm 4$  mb.

De Vaucouleurs' reasons for rejecting the other work range from criticism of the often made assumption of pure Rayleigh scattering (incorrect because of the violet haze which cuts the albedo way down in the blue) to inadequate observational data (e.g., the tiny photographic images the Russians had to work with; Hess' misinterpretation of an observation of a cloud by Antoniadi). He has several qualifications about the validity of his work as well, depending as it does on visual estimates of the variation of brightness of dark and light areas with position on the disk of the planet. His main reasons for accepting his result

are its agreement with the value derived by Dollfus and the fact that two different interpretations of his data lead to the same value.

Dollfus' polarization measurements also required certain assumptions before an atmospheric pressure could be deduced. The quantity Dollfus actually measured was the polarization of the disk as a function of phase angle, wavelength, and angular position on the disk. From measurements made with different values of each of these parameters he was able to derive four values for the ratio of the atmospheric and surface brightness. These gave a mean value of  $B_a/B_s = 0.037$ . Dollfus then used Russell's value for the magnitude of Mars at mean opposition to derive  $B_s$ . Assuming that the Martian atmosphere has the same scattering power as pure air, he concluded that its reduced thickness was 0.22 times that of the Earth and that the Martian surface pressure would be 85 millibars.

This was the situation in 1963 when Munch and Spinrad obtained a high resolution spectrogram of Mars in the N-plate region in order to look for water vapor lines. Their search was successful (Spinrad et al. 1963) but perhaps of even greater importance was their discovery that the R(8), R(10), R(12) lines of the  $5V_3$  overtone of  $CO_2$  appeared on their spectrogram. This implied immediately that the Martian abundance of this gas must be higher than had been previously estimated. Since the lines in this

band are unblended and very nearly unsaturated, they can be analyzed directly to give the abundance. When this datum is combined with observations of the strong, pressure broadened bands in the lead-sulfide region of the spectrum, an atmospheric pressure may be derived by means of a curve-of-growth analysis. Using laboratory data supplied by Rank; Kaplan, Münch and Spinrad (1964) first derived a  $\text{CO}_2$  abundance of  $50 \pm 20$  m atm or  $55 \pm 20$  m atm, the two values corresponding to assumed Martian atmospheric temperatures of  $200^\circ\text{K}$  or  $230^\circ\text{K}$ , respectively. They then selected the value corresponding to the higher temperature to derive a surface pressure of  $25 \pm 15$  mb. As we shall see in Section 6, it seems likely that a lower atmospheric temperature would be more suitable. The large discrepancy between the older polarimetric result for the surface pressure and the new value is almost certainly due to assumptions which must be made in order to interpret the data in the former case. A substantial percentage of carbon dioxide in the Martian atmosphere would increase the Rayleigh scattering coefficient and thus decrease the amount of gas required to produce a given atmospheric brightness. Hence the surface pressure would be lower. The presence of particles with radii substantially smaller than the wavelength at which the polarization measures are made will also lead to an overestimate of the amount of gas present. It is perhaps worthwhile to point out that Dollfus assigned no error to



his determination of surface pressure when he presented it in his thesis (1955). The probable error given above was assigned by de Vaucouleurs on the basis of an apparently close agreement between the four different techniques Dollfus used to measure  $B_a/B_s$ . Dollfus explicitly states that his results only "... establish orders of magnitude."

### 3. INSTRUMENTS

#### 3.1 A 72-Foot Multiple-Path Absorption Tube

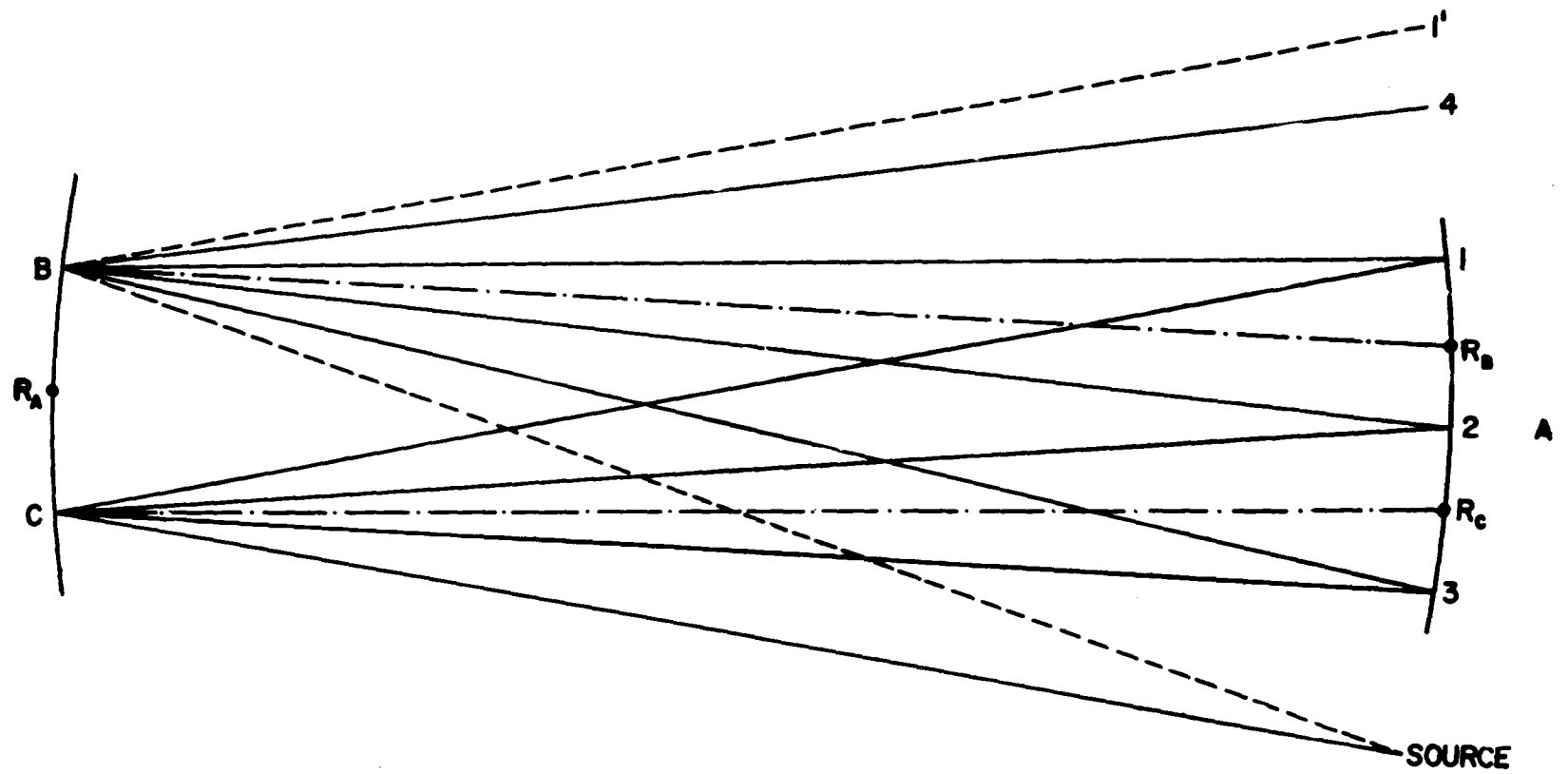
##### Introduction

In order to obtain absorption spectra which are similar to the spectra of the planets it is obviously necessary to have some means of obtaining long optical paths. The Lunar and Planetary Laboratory has been fortunate in having the use of a 2-meter absorption tube which is on loan from the National Research Council of Canada through the courtesy of Dr. Gerhard Herzberg. This tube is capable of producing a path length of 80 meters which is perfectly adequate for a variety of useful investigations. However, for problems which involve relatively large optical densities at low pressures (e.g., the calibration of the Martian CO<sub>2</sub> bands) a larger instrument is required. To meet this need, an absorption tube with a basic length of 72 feet was constructed. This paper describes the optical principles on which the design of the tube was based, some details of the design itself, and the technique to be followed in aligning and using the tube.

### Optical Principles

The experimental problem which this type of absorption tube is designed to solve is the achievement of long optical paths of large effective aperture within a relatively small linear distance. The first practical solution of this problem was accomplished by White (1942). He pointed out that an arrangement of three concave mirrors with equal radii of curvature could be used to give a large number of traversals of the fixed distance set by the radius of curvature. The basic principle underlying this technique is the simple rule that object and image points near the center of curvature of a spherical mirror always lie on a straight line whose midpoint falls on the center of curvature. The application of this rule to the problem at hand is illustrated in Figure 1. Light from the source is admitted at one side of the mirror A. It is reflected by mirror C and forms an image on mirror A at point (1), which is as far removed from the center of curvature of mirror C ( $R_C$ ) as is the source. An additional image of the source is formed by mirror B at point (1') which is removed from the optical train by a baffle. From point (1), the light is reflected to mirror B since the center of curvature of A ( $R_A$ ) lies midway between the centers of mirrors B and C. Mirror B forms an image at (2) which lies an equal distance from the center of curvature of mirror B ( $R_B$ ) as image (1). The light is now reflected to mirror C which returns it to A

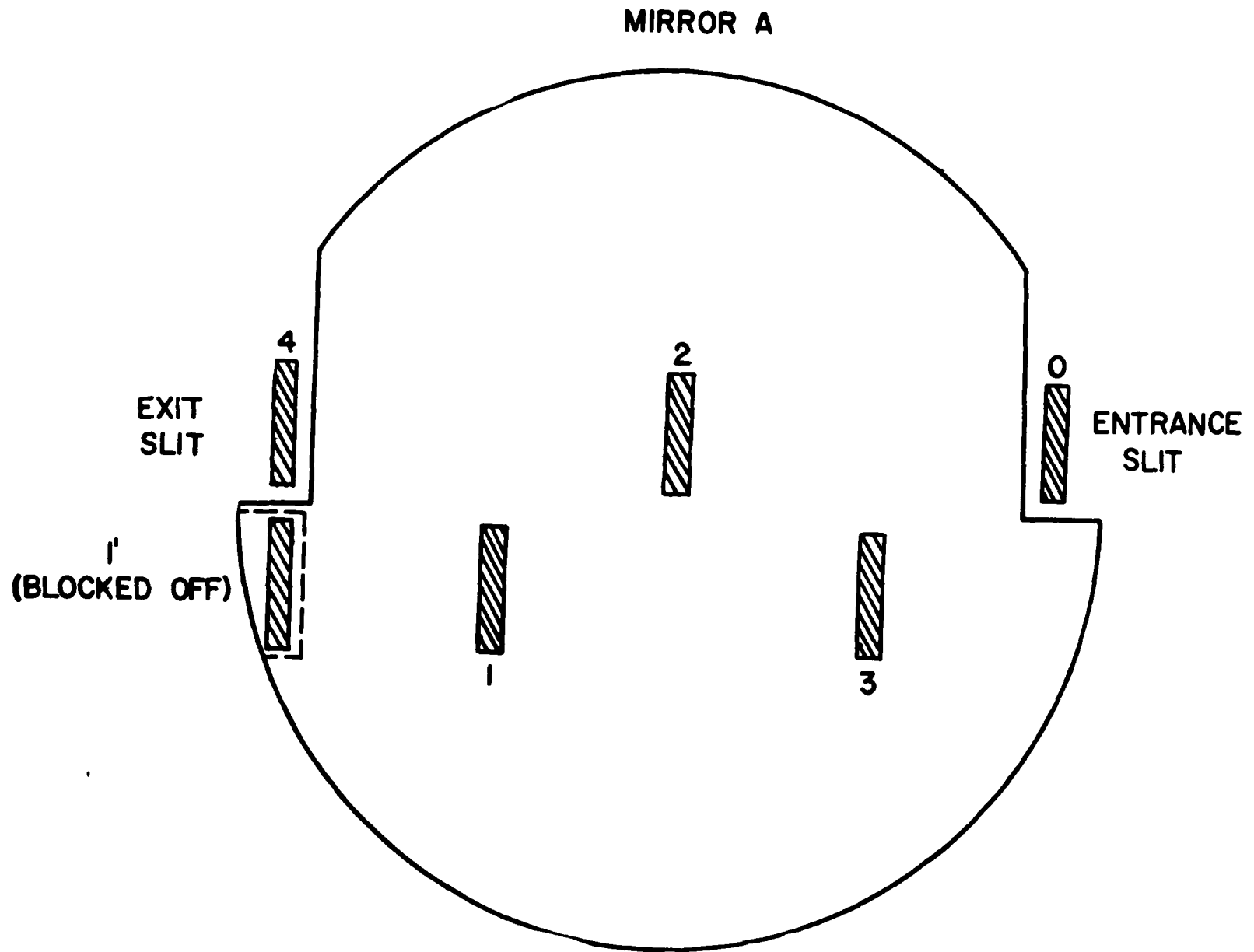
Fig. 1 Schematic Representation of White Mirror System (not to scale).



at (3). The image at point (3) is sufficiently far from  $R_B$  that the next reflection from mirror B takes it out of the tube at (4) where it may be examined. Thus with three images appearing on mirror A we have had eight traversals of the tube. To obtain a larger number of traversals it is only necessary to decrease the distance between  $R_C$  and  $R_B$  on mirror A which will result in a larger number of images on the latter. In general, if  $n$  images appear on mirror A, the number of traversals will be  $2(n + 1)$ .

White's basic design was modified by Bernstein and Herzberg (1948) to allow the accommodation of a larger number of images on the surface of mirror A. This was accomplished by tilting mirrors B and C to separate the even and odd images in two parallel rows. Inspection of Figure 1 indicates that images (1) and (3) are formed by mirror C while (2) and (4) come from mirror B. Thus one wishes to arrange the mirrors so that the even images fall on mirror A in a row which includes the entrance and exit slits while the odd images form a row directly below. An example of this configuration is shown on a front view of mirror A in Figure 2. The ultimate limitation to the number of traversals which can be achieved with this type of apparatus is set by the number of images which can be accommodated on mirror A. Thus this modification increases the utility of the instrument and also provides a convenient way of aligning the system by making it obvious which images are formed

Fig. 2 Front View of Mirror A with System Arranged for Eight Traversals ( $n = 3$ )  
in the Bernstein-Herzberg Modification .





by which mirrors. The number of traversals can be altered in much the same way as before. The simplest way of doing this is to keep mirror B fixed and only adjust mirror C. To achieve the largest possible number of traversals, the center of curvature of mirror B is set at the center of mirror A. This brings the unwanted primary image ( $1'$ ) to a point just below the exit slit where it must be masked off. Mirror C can now be rotated about an axis perpendicular to the plane of the page in Figure 1 which will cause its center of curvature to approach or recede from that of mirror B. The former direction causes an increase in the number of images and traversals, the latter a decrease.

#### The LPL 72-Foot Tube

Experience gained with the 2-meter absorption tube referred to in the introduction indicated that alignment procedures would be greatly simplified if the reflecting surface of mirror A could be inspected directly. With this idea in mind, a design was formulated which allowed all of the mirrors to be mounted outside the tube itself. Flanges welded to each end of the tube support circular plates whose centers are cut out to match the tube diameter. Four stainless steel rods are pressed into each plate and extend about 16" from the end of the tube before terminating in another metal plate which maintains their alignment. The mirror cells are attached to aluminum disks

which are free to slide along the rods (on ball bushings) to permit an adjustment of focus. These features are illustrated in Figures 3 and 4. The mirror cells each have three adjusting screws pushing against a compressed spring to permit alignment of the mirrors. A micrometer screw is provided for the appropriate adjustment of mirror C to allow the required precision in changing the number of traversals.

Two steel cannisters fit over the mirror support systems and are bolted to the metal plates which are attached to the tube flanges. Aluminum face-plates then fit over the ends of the cannisters to seal off the tube. All joints are provided with "O" ring seals which have proved adequate for both high and low pressure work. The entrance and exit windows are made of fused quartz and a third window is provided in the face plate behind mirrors B and C to allow inspection of the images on mirror A even when the tube is in use.

As of this writing, the tube has been used at path lengths up to 3.6 km. The number of traversals achieved depends critically on the quality of the reflecting coatings. Considering only losses due to reflection, the intensity of the light leaving the tube is given by the expression  $I = (R)^n I_0$  where  $R$  = the reflectivity of the mirror coatings,  $n$  = the number of reflections, and  $I_0$  is the incident intensity. For a 3.6 km path,  $n = 159$ , indicating the necessity for a high value of  $R$ . This means

Fig. 3 Front View of Mirror A in the LPL 72-foot Tube. Entrance Slit at Right  
of Mirror.



Fig. 4 Front View of Mirrors B and C in the LPL 72-foot Tube. Adjustable  
Mirror (C) at Left.



that for the largest number of traversals one must rely on a fresh silver coating to obtain usable intensities. If more moderate path lengths are required, aluminum is preferable since it is more stable and will be superior to a silver coat which has tarnished slightly.

A three-foot optical bench has been mounted in the ceiling at the entrance-exit end of the tube. Sliding supports attached to this optical bench are used to carry lenses and mirrors as well as a small incandescent lamp. This system includes a mirror which deflects the beam leaving the tube at a  $45^\circ$  angle which brings it down to a second mirror at the level of the optical path used in the laboratory. When sunlight is needed, a heliostat is set up on a support outside a laboratory window and the incandescent lamp is replaced by a mirror which reflects light from the heliostat through a lens and into the tube.

#### Alignment and Adjustment Procedures

In this section a list of the procedures to be followed in setting up and using the 72-foot tube is given. The given order of the steps has been found to be convenient but is not rigid in all cases. Two people are required to carry out the alignment.

1. Align mirror A such that it is perpendicular to the tube. This can be accomplished by sighting down the tube through the hole in the disk which

supports the cells of mirrors B and C while a second person adjusts mirror A. Sufficient alignment is achieved when the observer's eye is reflected back to him from mirror A through this hole.

2. Align the light source. This must be done in several steps. First, a rough alignment should be made by measuring the distance from the entrance slit in the back of the cell of mirror A to the south wall and the ceiling. These measurements should then be duplicated for the incandescent lamp and its lens. The optical axis of lens and lamp should lie one or two cm above the lower edge of the entrance slit. The lamp and lens can now be adjusted to form an image of the filament on the entrance slit. An easy way of doing this is to place a white card just in front of the surface of mirror A in line with the slit and focus on it. If the maximum number of traversals is to be obtained, the slit should be made as narrow as possible. This in turn requires a small image of the filament to permit the maximum intensity of light to enter the tube. The final step in the alignment of the light source is a check to make certain that the light is entering the tube properly. This can be done by using a large piece of paper as a projection



screen in front of mirrors B and C. When the light beam is properly adjusted, the screen should be uniformly illuminated.

3. Adjust mirror B. As illustrated in Figure 2, the image of the source which is reflected by mirror B ( $1'$ ) should fall below the exit slit cut into mirror A. To achieve this, one person should watch for this image with a piece of paper held in front of mirror A, or by looking down the tube, while the second person alters the alignment of mirror B by means of the adjustment screws. Once this image has been found, it is moved to a position which is just as far below the lower edge of the exit slit as the original image is above the lower edge of the entrance slit. In this position, the image may be blocked off by a small black card taped to the edge of the tube.
4. Adjust mirror C. This adjustment is essentially a repetition of that described for mirror B. The primary image of the entrance slit produced by mirror C ( $1$ ) should be at precisely the same level as that formed by mirror B ( $1'$ ). In this case, the image is not allowed to fall on the card, however.
5. With both primary images located, it is now possible to attach the cannister covering mirrors B and C. Minor adjustments of these mirrors may be necessary

after this operation to correct any misalignment which may have occurred.

6. Inspection of the reflecting surface of mirror A should now reveal two rows of images as illustrated in Figure 2. If the surface is very clean, it may be necessary to hold a card in front of it in order to see the images in which case it will not be possible to see all of them at once since an image projected on the card obviously ends the number of traversals. Tightening the micrometer screw adjustment on mirror C will cause the primary image (no. 1 in Fig. 2) to move to the left (towards the south wall of the tube). This motion compresses the space between successive images while allowing additional images to appear on mirror A, i.e., the rows become more densely populated.
7. In this condition, the rows should be checked carefully to be sure they are horizontal. One way of doing this is for the person observing mirror A to place his eye behind the exit slit and watch for any apparent motion of the images upwards or downwards as the other observer runs through successive images using the micrometer screw. If the mirrors are properly adjusted, no upward or downward migration of the images should occur. If such motion is observed, the lower (or upper) adjustment screw of

the cell of mirror C may be used to raise or lower the images the tiny amount required.

8. Final adjustments must be made with the face plate attached to the cannister covering mirrors B and C to eliminate the turbulence which otherwise accompanies the flow of air through the tube. In attaching this face plate, the rod which engages the micrometer screw in the back of mirror cell C should be pulled back through its seal so that no contact with the screw is made until after the plate is secured to the cannister. Care should be taken in this process not to bump the cannister as this is likely to throw the system out of alignment. The rod should now be carefully engaged to the micrometer screw.
9. If the rows of images do not appear horizontal (no migration of images) after the turbulence has been eliminated, the face plate must be removed and the adjustment procedures repeated. If the correct alignment has been achieved, the final adjustments of mirror A can be made. These consist of two steps. With a large number of images on mirror A, one of the two lower adjusting screws may be tightened or loosened while the intensity of the higher (numbered) images is inspected. This intensity should be a maximum if mirror A is properly aligned.

The second step is an inspection of the quality of the higher images. If there are any flares apparent, the upper adjustment screw should be used to eliminate them.

10. The cannister which covers the supports for mirror A may now be attached to the tube. To do this it is necessary to slide the illumination system back out of the way. Therefore it is best to have the tube set up such that a fairly high-order image (say No. 16) is coming out of the exit slit before attempting to put the cannister in place. Once this latter act has been accomplished, the visibility of the image can be used as a test for the accuracy of the alignment after the illumination system has been slid back into place. It should be pointed out that the most likely reason for the failure of the pre-selected image to appear in the exit slit is the misalignment of the illumination system. Hence care should be taken to preserve this alignment when moving the system along the optical bench.
11. After making any additional adjustments of the set screws in the cell of mirror A which may be necessary to improve the quality of the image as a result of the installation of the cannister, the face plate may be attached. The correct position of

this plate has the brass window-guards facing outwards from the tube. Again suitable precautions must be observed in order that the tube is not jarred during the installation. This step completes the alignment and assembly procedures.

The light leaving the tube should be reflected down to the level of the laboratory optical path at a right angle as described in Section 3.1, Optical Principles. At the correct level, a second mirror may be placed in the beam at  $45^\circ$  to deflect the beam along the optical path. Auxiliary mirrors may be added as needed to bring the beam into the proper position for entering the slit of whichever analyzing instrument is being used. A lens of appropriate  $f$ /ratio should be employed to form an image on the slit which will fill the collimator of the spectrograph or spectrometer. If all reflections occur at  $45^\circ$  angles (so the beam direction changes by  $90^\circ$ ) the image will not be rotated when it falls on the slit. This is an important consideration in achieving maximum illumination.

A large aperture valve and exhaust pipe are provided for evacuating the absorption tube. With the presently available pump, evacuation to  $P < 500\mu$  Hg takes approximately six hours. When the desired pressure has been achieved, the large aperture valve is closed, a second valve on the side of the exhaust tube is opened and the pump

turned off. The required amount of gas may now be admitted to the absorption tube. To set up the appropriate image, one person adjusts the micrometer screw on mirror C while the other watches for the image to be projected on the slit. The person adjusting mirror C can observe the position of image (1) on mirror A by looking down the tube through the window in the face plate at the east end of the tube. When this image is near the right hand side of mirror A, he should observe a flash of light at the exit slit on the upper left of mirror A. At the same time, the observer watching the slit of the spectrograph should see an image. This is the first image and may be used as a starting point for counting to higher images. With a little practice, it is possible to start with image 2 or 3 but this should not be attempted at first. Note that these images do not correspond numerically to the numbers in Figure 2. Thus the first image leaving the tube is No. 2, the second No. 4, etc.

One additional adjustment is provided for use in high-pressure work. This is a steel strap which surrounds the cannister covering mirrors B and C. This strap is connected to the ceiling by means of a turnbuckle which can be adjusted to compensate for a deviation of the optical path at high pressure. Under these conditions, the two rows of images have a tendency to rise on the surface of

mirror A. Tightening the turnbuckle will return the system to proper alignment.

It is recommended that the alignment of the analyzing instrument (spectrograph or spectrometer) be initiated with the image-forming lens out of the way. An image of the slit will then be formed somewhere on or near the collimator and may be centered before inserting the lens. It is best to use the first or second image for this purpose in order to have sufficient intensity. Placing the lens in the beam should now fill the collimator with light.

### 3.2 A 10-Foot Plane Grating Spectrograph

#### Introduction

The Lunar and Planetary Laboratory program of studies of the absorption spectra of gases for comparison with spectra of the planets was initiated with the help of a Bausch and Lomb 1.5-meter concave grating spectrograph. The limitations of this instrument rapidly became apparent and formed the basis of a set of prerequisites for a more powerful and more versatile spectrograph. An increase in dispersion from 20 Å/mm to 1-5 Å/mm while maintaining high resolution over a relatively large extent of the spectrum and without losing too much speed was perhaps the most important of the desired improvements. In addition, the frequency with which we found it necessary to change from

one wavelength region to another and one dispersion and/or resolution to another made it highly desirable that such operations could be accomplished with a minimum of readjustment. All of these criteria can be satisfied by the use of large-aperture, blazed plane gratings with a collimator and camera of relatively long focal length. Three 5-x 6-inch gratings blazed at  $2.0\mu$ ,  $1.6\mu$ , and  $1.0\mu$  had been ordered for installation in a lead-sulfide spectrometer (Binder, Cruikshank, and Kuiper 1964) so it was decided that the laboratory spectrograph should employ these same gratings as its dispersing elements. The design of this instrument and some examples of its performance are described in the following three sections.

### Design Considerations

#### a) Historical

The first successful use of concave mirrors as the collimator and camera elements of a plane grating spectrograph seems to have been accomplished by Ebert (1889). His design consisted of a single concave mirror which served both purposes and had the plate holder and slit on opposite sides of the grating. This design remained unnoticed for many years until it was independently discovered by Fastie (1952a) who altered Ebert's original design somewhat and gave a discussion of the aberrations of the system



(Fastie 1952b). As Fastie has pointed out, the great advantage of this configuration is the fact that images formed on-axis are free of aberrations since any aberrations introduced by the first reflection from the mirror will be cancelled by the second reflection, provided that the reflections are symmetric.

This property was well documented by Czerny and Turner (1930) who used separate mirrors for camera and collimator. These authors considered two basic arrangements of the optical elements (Fig. 5-a,b) and concluded on the basis of observational evidence (photographs of the image formed by the slit) that one of these configurations (5-b) was far superior to the other. This empirical evaluation was supported by a qualitative argument which indicated that in configuration 5-b the unsymmetrical distortions of the wave front introduced upon reflection from the mirrors are cancelled, whereas in 5-a they are not. This is basically due to an absence of symmetry in the latter design. Czerny and Turner concluded that many contemporary (1930) instruments were designed in such a way that they incorporated the bad qualities of configuration 5-a. As an alternative they suggested the design shown in Figure 6. As Fastie (1952a) has remarked, the Ebert system (of which Czerny and Turner appear to have been unaware) is a special case of the configuration shown in Figure 6 in which the two reflecting surfaces have coincident centers of curvature.

Fig. 5a  
and b

Two Configurations of Camera and Collimating  
Mirrors for a Plane-Grating Spectrograph.  
Grating is omitted since Only Symmetry  
of Mirror System is Considered.

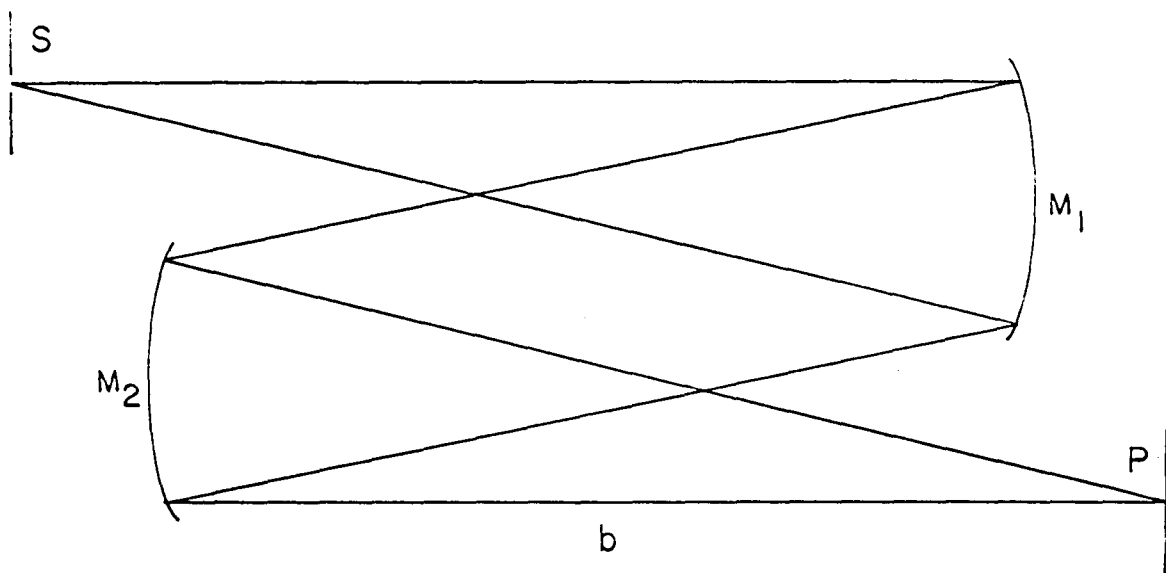
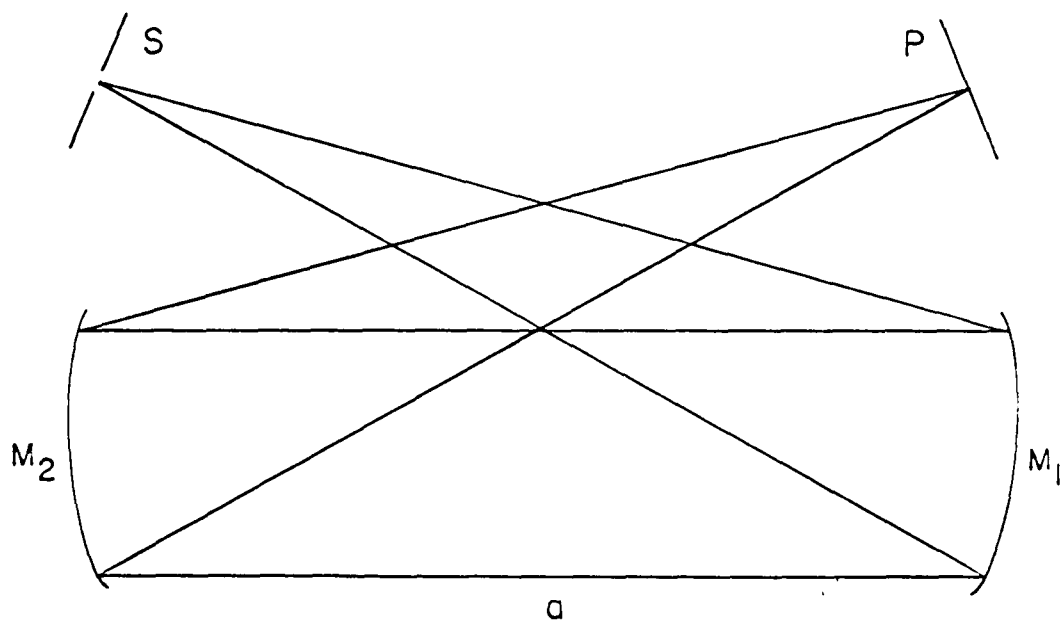


Fig. 6      The Czerny-Turner Design. The Angles Between  
the Mirrors and the Grating are  
Exaggerated.

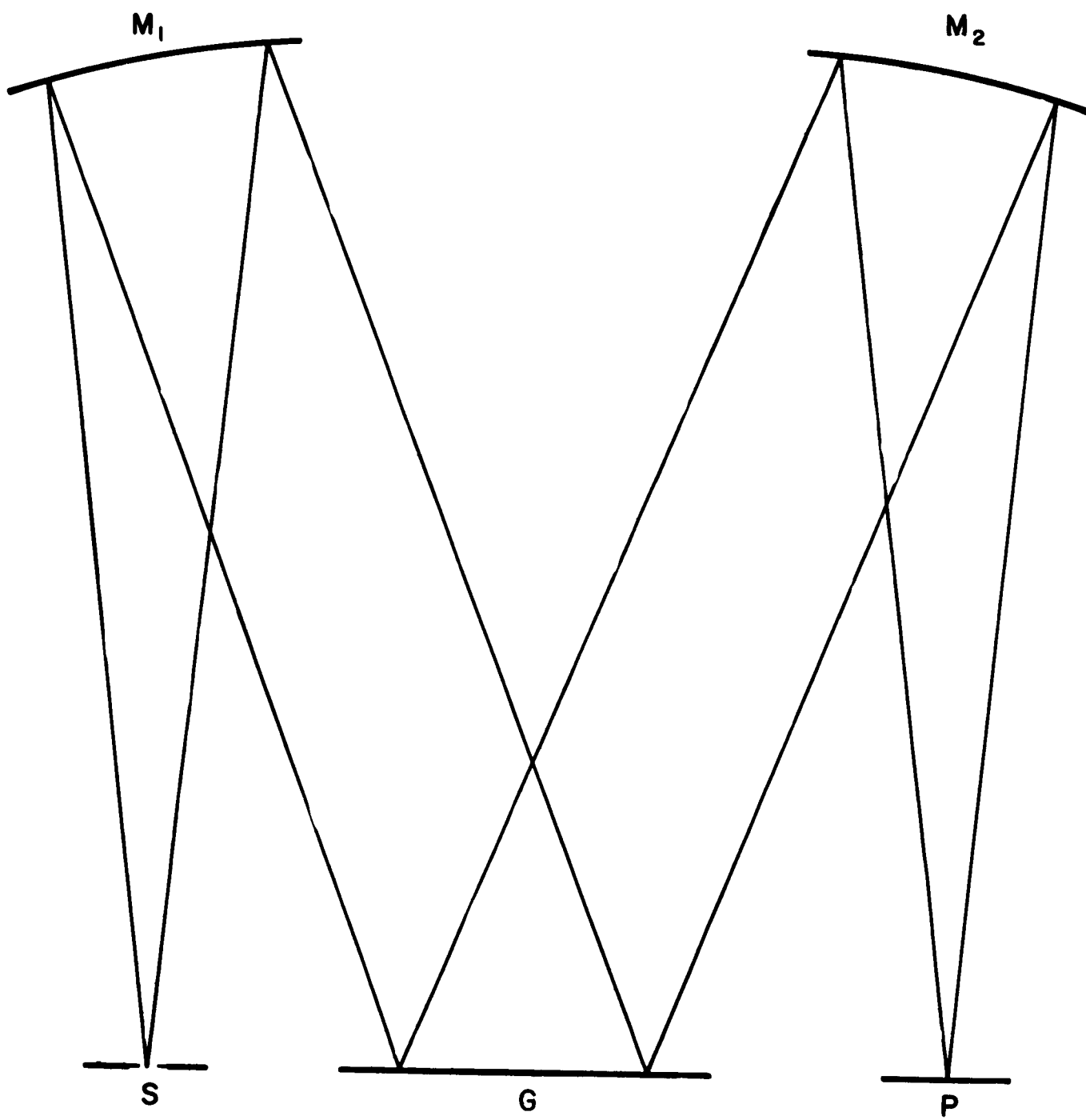
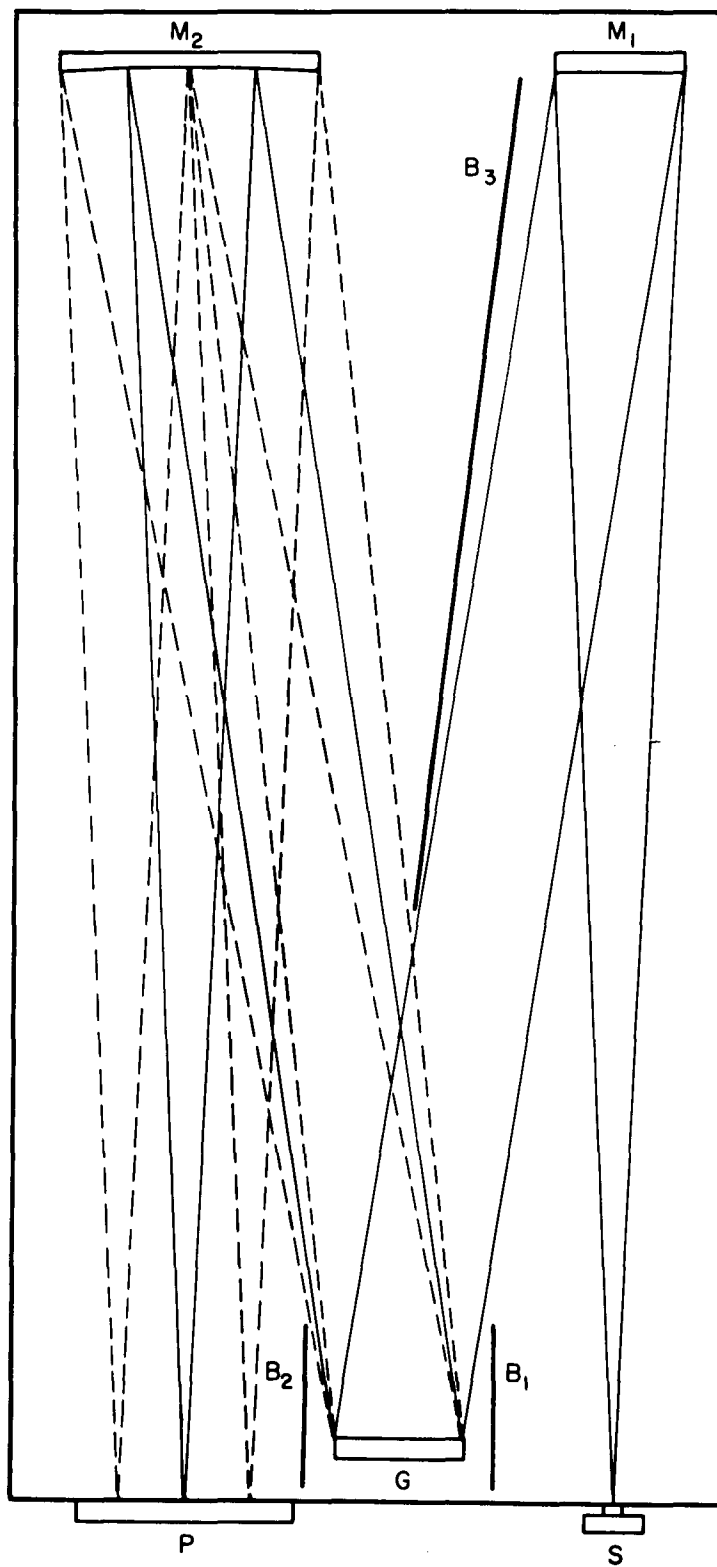


Fig. 7      The Lunar and Planetary Laboratory 10-foot  
Spectrograph (not to scale).



The practical advantage of the Czerny-Turner system lies in the fact that smaller mirrors can be used.

It should be pointed out that these instruments were all designed for use as spectrometers although Ebert's original design was a spectrograph. The cancellation of aberrations which makes this type of configuration so attractive is strictly valid only on the optical axis, thus favoring the spectrometer application. However, the use of a fairly high  $f$ /ratio allows one to work off-axis without violating the desired conditions of symmetry too severely. In addition, the fact that no refocussing is needed to move from one region of the spectrum to another (the grating is illuminated by a parallel beam) makes the absence of a large region of perfect definition acceptable. Thus it is not surprising that the largest of the modern high resolution solar spectrographs are built on the Czerny-Turner design (McMath and Mohler 1962).

#### b) The Laboratory Instrument

Returning to the criteria listed in the introduction, it is evident that they can be satisfied by the Czerny-Turner system if one can achieve a suitable compromise between the large focal length necessary for high dispersion and the small  $f$ /ratio required for high speed. Since we were going to use 5- x 6-inch gratings, a 6-inch mirror was required for the collimator in order that the parallel beam



would fully illuminate the grating. The focal length of both mirrors is set by the desired dispersion.

The angular dispersion of a diffraction grating is given by the equation

$$1) \quad \frac{d\theta}{d\lambda} = \frac{Nm}{A \cos \theta}$$

where  $N$  = total number of grating rulings contributing to the spectrum

$m$  = order of grating used

$A$  = linear aperture of grating (distance from first ruling counted for  $N$  to last)

$\theta$  = angle of diffraction.

The diffraction angle  $\theta$  for a particular wavelength  $\lambda$  and angle of incidence  $i$  is given by the grating equation:

$$2) \quad m\lambda = \frac{A}{N} (\sin i \pm \sin \theta).$$

In the Czerny-Turner design, both  $i$  and  $\theta$  change as the grating is tilted to change the orders but their combined values ( $i \pm \theta$ ) remain constant. The linear dispersion at the plate may be expressed as

$$3) \quad \frac{dx}{d\lambda} = f \cdot \frac{d\theta}{d\lambda} \frac{1}{\cos \gamma}$$

where  $f$  is the focal length of the camera and  $\gamma$  is the angle between the incident diffracted beam and the normal to the focal surface. In this case  $\gamma = 0$ .

Referring to equation (1), we see that the angular dispersion of the  $1.6\mu$  grating in the second order is  $1.2 \times 10^{-4}$  radian/ $\text{\AA}$  (600 lines/mm). Our goal is a linear dispersion of about  $2.5 \text{ \AA/mm}$ . If an f/20 system is used, the focal length  $f = 3.3$  meters. Considering the size of the grating holder and the gratings, it was possible to design the spectrograph with a distance of about 33 cm between the center of the grating and the slit. With the focal length given above, one then has  $i = \theta \sim 6^\circ$  with the grating adjusted for  $m = 0$ . Thus a normal spectrum ( $\theta = 0$ ) is obtained for  $i = 12^\circ$ . To find the dispersion obtained in this system at  $8000 \text{ \AA}$  in the second order we refer to equation (2). This gives us the condition  $\sin i + \sin \theta = 0.96$ . The zero order angle of  $6^\circ$  derived above gives the additional condition  $i + \theta = 12^\circ$ . Using these together we find  $i = 35^\circ$ ,  $\theta = 23^\circ$ . Solving equations (1) and (3) for this set of numbers then gives us a dispersion at the plate of  $\frac{dx}{d\lambda} = \frac{1}{2.3} \text{ mm/\AA}$ . Thus the adopted focal length will indeed result in the desired dispersion.

The aperture of the camera mirror is fixed by the length of photographic plate to be exposed to the spectrum. A 4-x 10-inch plate holder was available from another instrument. It was decided to restrict the area of best illumination to six inches in order to stay reasonably close to the optical axis. This requires a camera mirror of 12 inches aperture in order that the entire grating contributes

to the spectrum over the full six inches on the plate. The optical configuration is now defined and it is only necessary to arrange suitable mountings for the different components and a light-tight case for the entire system. A schematic drawing of the instrument is given in Figure 7. The baffles  $B_1$ ,  $B_2$ , and  $B_3$  are required to shield the plate from the collimator and a reflected image of the slit (in the camera mirror).

#### A Description of the Instrument

The mounted optical elements of the spectrograph are bolted to metal plates which are secured to a frame constructed of 3-inch I-beams. The frame is supported at all four corners by one inch diameter leveling screws. A box made of aluminum was built at each end of the frame with facing ends open so that the central part of the instrument (containing no optical parts) could be constructed of a light-weight aluminum shell. The mountings for the two mirrors and the gratings were purchased from the J. Unertl Company. The mirror mountings permit a fine-focussing adjustment along the optical axis in addition to providing the customary screws for altering the alignment of the mirror surfaces. The grating can be rotated about three perpendicular axes: in small amounts about the horizontal and normal axes, and  $180^\circ$  about the vertical axis. It is the latter adjustment, of course, which changes the orders.

The plate holder and bilateral slit were adapted from a Bausch and Lomb prism spectrograph of the Littrow type. The plate holder gives a slight curvature to the plates which doesn't quite match the focal surface of the present system. The effects of this only become noticeable near the edges of the plate but it is planned to make the necessary modifications to eliminate the present misalignment in the near future.

The entire instrument rests on a large, massive bench which is supported by six locking casters. This arrangement has been found to give adequate stability for the longest exposures.

#### Discussion of Performance and Results

The performance of the 10-foot spectrograph has been highly satisfactory. It was first used in an analysis of the Martian CO<sub>2</sub> abundance (Section 6), a problem which required a dispersion of at least 5 Å/mm at 8689Å and a rather high resolution. Using the 1.6μ grating in the second order, it was possible to match the resolution of a spectrogram obtained with the Mt. Wilson coude spectrograph by opening the slit to 100μ. As part of the same analysis, spectra of the CO<sub>2</sub> bands at 1.05μ were obtained with the 2μ grating in the second order (dispersion ~5 Å/mm). The effectiveness of the blaze is shown by the fact that these spectra were obtained in only 30 seconds compared to

exposures of the same region up to 45 minutes in length with the  $1.6\mu$  grating in the first order (same dispersion).

In these as in other programs, the resolution achieved has always been more than adequate for our purposes. The theoretical resolving power is simply  $Nm$ . For the  $1.6\mu$  grating in the fourth order this comes to  $3.7 \times 10^5$  (the grating is always fully illuminated). Examination of a plate obtained on a 103a-F emulsion in the fourth order near  $H\alpha$  indicates a resolution of about  $1.6 \times 10^5$ . This plate does not represent a maximum effort and it seems probable that a factor 1.5 could be gained by using an emulsion of finer grain under the best conditions. This would result in a resolution of about 0.65 that predicted by theory which is reasonably good. Aside from the difficulty with the curvature of the plate holder referred to earlier, the region of good resolution is found to extend across the full eight inches of exposed plate, i.e., four inches on either side of the optical axis.

Examples of spectra obtained with this instrument are given in Figures 8, 9, and 10 which represent respectively the H and K lines of calcium, the D lines of sodium, and Paschen 6 of hydrogen with some telluric water vapor lines in the  $1.1\mu$  region. Current programs include high dispersion mapping of the spectra of  $NO_2$  and  $CH_4$ .

Fig. 8 The H and K Lines of Ca II.  $1.6\mu$  Grating, 4th Order,  $10\mu$  Slit.

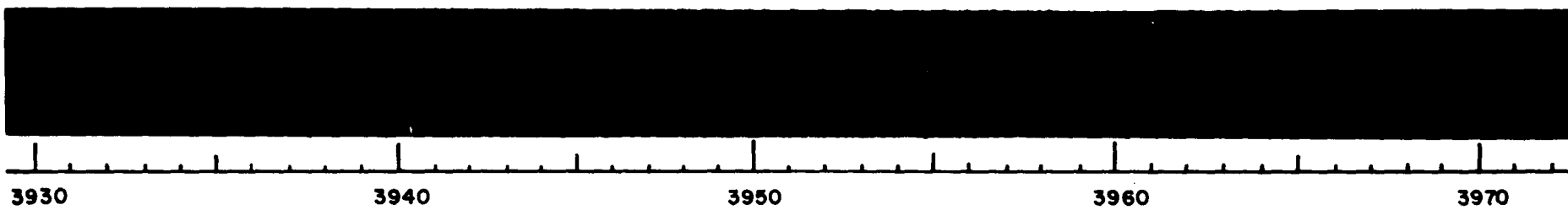


Fig. 9 The  $D_1$  and  $D_2$  Lines of Na I.  $1.6\mu$  Grating, 4th Order,  $10\mu$  Slit.



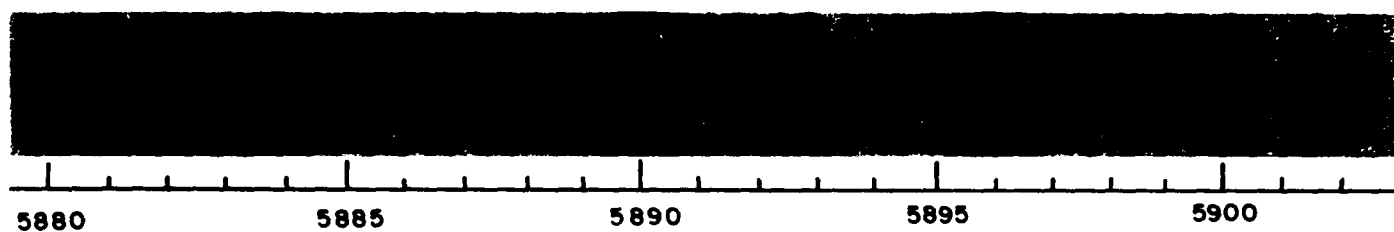
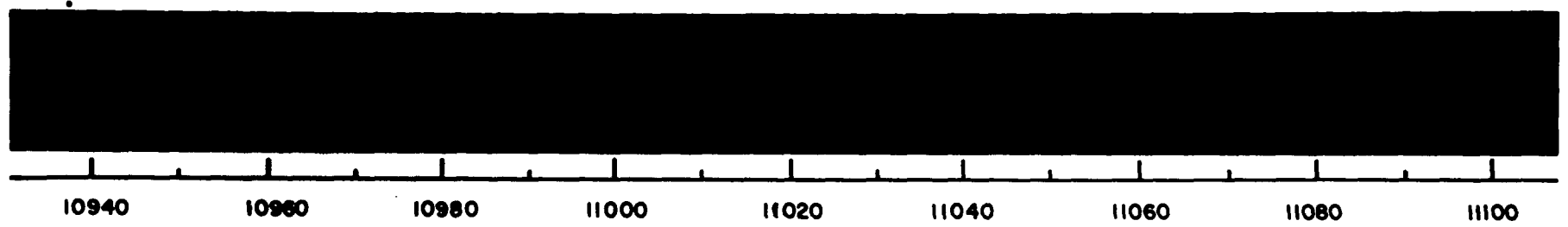


Fig. 10 Paschen 6 of H I and Telluric Water Vapor Lines.  $2.0\mu$  Grating, 2nd Order,  
 $50\mu$  Slit.



## 4. THE SPECTRUM OF JUPITER - IDENTIFICATIONS AND INTERPRETATIONS

### 4.1 A New Ammonia Band in the Jovian Spectrum

#### Introduction

While examining a high-dispersion spectrogram of Jupiter obtained by Dr. G. P. Kuiper at the McDonald Observatory, the writer noticed several faint lines in the region just short of the telluric A-band of oxygen which were not present in a solar comparison spectrum. Shortly thereafter, Dr. H. Spinrad sent a list of some thirty-seven lines which he had found in the Jovian spectrum in the A-band region which included those already mentioned. He had been unable to identify these lines by comparing the wavelengths he had measured with those reported in the literature for methane, ammonia, and a number of other gases. In addition to published data, Spinrad was able to use a spectrum of methane for this comparison which was obtained by J. Phillips at a long optical path with high resolution. Thus the negative result for methane appeared to be well founded. The situation was not quite as good with respect to the ammonia comparison and suggested that further laboratory studies of this gas should be made. As is shown below, these studies led to a positive identification

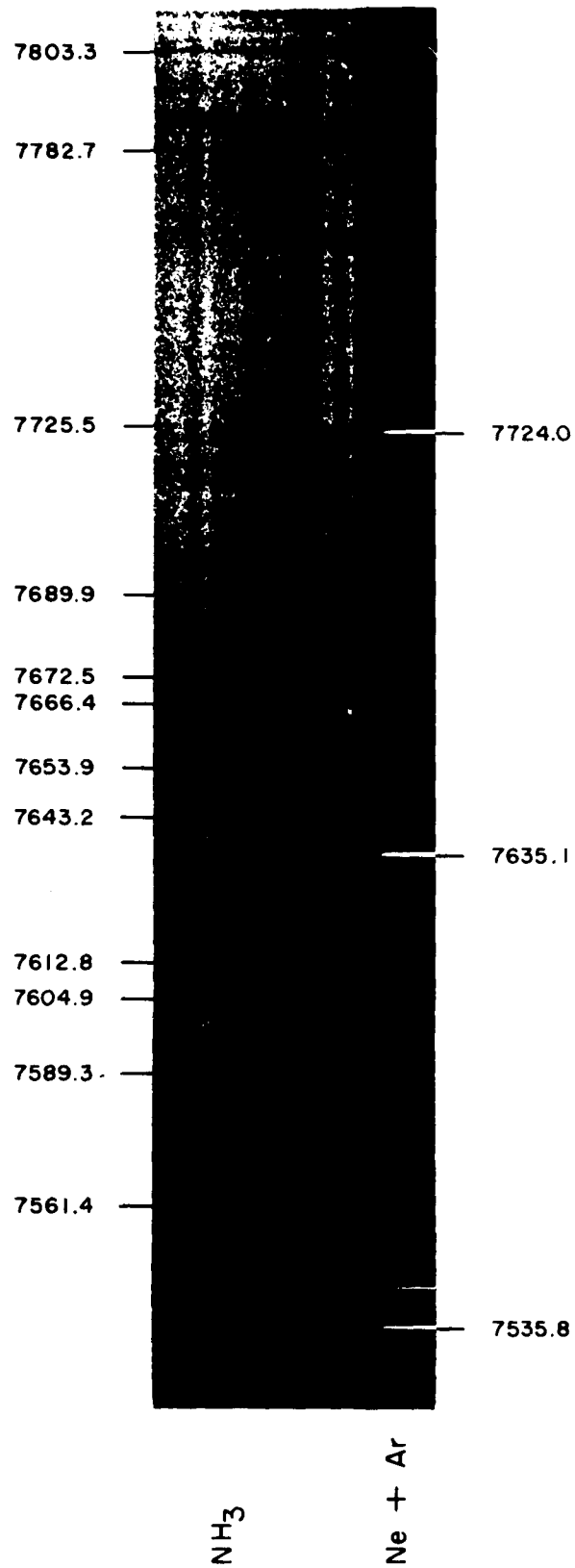
and the results of this work have been published (Owen, Richardson, and Spinrad 1964).

### 、 Laboratory Analysis

The photographic infrared spectrum of ammonia has been extensively investigated by Chao (1936). He did not list any absorption lines in the region of interest but used a maximum light path of only 8.6 m at atmospheric and less-than-atmospheric pressures. The amount of ammonia in the Jovian atmosphere has been estimated by Kuiper (1952) to be equivalent to 7 m atm (NTP). Thus weak ammonia lines in the Jovian spectrum should exhibit intensities corresponding to lines produced in the laboratory by roughly twice this amount of gas and could have escaped detection when smaller quantities were used. This possibility was investigated with the help of a 2-m multiple-path absorption tube with which an optical path of 80 m can be achieved. After passing through this tube, the light from a tungsten filament lamp was analyzed with a Bausch and Lomb 1.5-m grating spectrograph at a dispersion of  $20 \text{ Å/mm}$  in the first-order infrared. It was found that several faint lines indeed appeared in the  $7550 - 7750 \text{ Å}$  region when a 14 m-atm path length was used.

To obtain intensities which were more suitable for measuring purposes, a spectrum was obtained with a path of 80 m and a pressure of 350 mm Hg (Fig. 11). The lower

Fig. 11 Laboratory Spectrum of Ammonia in the Region 7535 Å to 7803 Å. Original  
Dispersion 20 Å/mm, Path Length 80 m, Pressure 350 mm Hg.



pressure permitted higher resolution by reducing the strong self-induced pressure broadening exhibited by ammonia. A slit width of  $10\mu$  and a IV-N emulsion were used to achieve a resolution comparable to that employed at the telescope.

The strongest of the lines appearing in this spectrogram were measured with a Gaertner measuring engine. The mean error associated with these measures is  $0.15 \text{ \AA}$ . Weak and diffuse lines were then measured on an enlarged high-contrast print, with a mean error estimated at  $0.3 \text{ \AA}$ . Wavelengths (in air) for all measured lines are given in Table 2. The measurements made on the plate are given to two decimal places, those made on the print are given to one place.

The laboratory wavelengths are compared in Table 3 with the wavelengths of the new Jovian lines measured by Spinrad on plates he had obtained at the Dominion Astrophysical Observatory and by Owen on the McDonald spectrogram. It seems safe to conclude from this comparison that the  $7654\text{-}\text{\AA}$  ammonia band is definitely present in the spectrum of Jupiter. It is equally obvious, however, that the two lists of lines do not exhibit a one-to-one correspondence. Some of the lines measured on the laboratory plate will be absent due to wavelength coincidences with members of the A-band of  $\text{O}_2$  and with various Fraunhofer lines. This is the case for the strong lines at  $\lambda 7604.9$ ,  $\lambda 7612.8$ , and  $\lambda 7653.9$ . Because of this overlapping, weak



Table 2

LABORATORY LINES OF THE 7654 Å BAND OF NH<sub>3</sub>

$\lambda_{\text{NH}_3}$	Notes	$\lambda_{\text{NH}_3}$	Notes
7554.3	Weak	7683.96	Weak
7561.43	Strong	7685.9	Very strong
7571.32		7688.20	
7574.8		7689.91	
7578.1		7690.9	Very weak
7582.1		7694.0	Very weak
7583.64	Strong	7697.4	
7586.41	Weak	7699.45	Diffuse, weak
7589.25	Strong	7701.45	Diffuse
7604.87	Very strong	7713.88	Diffuse, strong
7612.84	Very strong	7716.92	Diffuse, strong
7616.4	Strong	7719.9	
7618.5	Strong	7722.60	Diffuse
7623.9	Strong	7725.50	Diffuse
7625.7	Strong	7731.1	Very weak
7643.22		7733.5	Diffuse, weak
7648.96		7738.8	Diffuse, weak
7651.00		7745.0	Diffuse, weak
7653.89	Very strong	7748.3	Diffuse, weak
7666.36	Strong	7763.1	Diffuse
7667.7	Weak	7776.6	Diffuse
7670.1	Weak	7782.7	Diffuse
7672.45		7785.9	Diffuse, weak
7673.2	Weak	7789.4	Diffuse
7675.98		7795.8	Diffuse
7678.74		7797.2	Diffuse
7681.03		7803.3	Strong

Table 3

A COMPARISON OF JOVIAN AND LABORATORY  
AMMONIA WAVELENGTHS

$\lambda$ Jup (Spinrad)	Notes	$\lambda$ Jup (Owen)	$\lambda$ NH <sub>3</sub>	Notes NH <sub>3</sub>
7561.35	Diffuse	7561.52	7561.43	Strong
7571.88	Diffuse	7571.77	7571.32	
7577.24	?			
7578.46	?		7578.1	
7581.88	Strong	7582.03	7582.1	
7589.54	Sharp	7589.12	7589.25	Strong
7666.70		7666.57	7666.36	Strong
7668.07		7668.61	7667.7	Weak
7672.48		7672.59	7672.45	
7673.61		7673.78	7673.2	Weak
7678.44		7678.30	7678.74	
7679.41		7679.68		
		7681.56		
7684.12	?	7684.64	7683.96	Weak
7684.82	?			
7686.08		7686.10	7685.9	Very strong
		7690.57		
7693.03				
7694.20			7694.0	Very weak

Table 3 (Continued)

$\lambda$ Jup (Spinrad)	Notes	$\lambda$ Jup (Owen)	$\lambda$ NH <sub>3</sub>	Notes NH <sub>3</sub>
7696.87				
7697.84	?		7697.4	
7706.17	Diffuse			
		7713.66		
7716.57		7716.84	7716.92	Diffuse, strong
7717.64		7717.91		
7720.92	o?*			
7725.33	Diffuse, strong	7725.26	7725.50	Diffuse
7728.61				
7729.86	CH <sub>4</sub> ? †	7729.73		
7731.44	CH <sub>4</sub> ?	7731.39	7731.1	Very weak
7734.40				
7752.37	?			
7753.34		7753.39		
7755.47				
7757.00				
7758.11				
7763.03		7762.83	7763.1	Diffuse

\* o? = possible solar line.

† CH<sub>4</sub>? = possible methane line.

Table 3 (Continued)

$\lambda$ Jup (Spinrad)	Notes	$\lambda$ Jup (Owen)	$\lambda$ NH <sub>3</sub>	Notes NH <sub>3</sub>
7765.14				
7767.14	?			
		7772.78		
7777.24	Strong	7777.48		

ammonia lines in the region  $\lambda 7600$ - $\lambda 7643$  were not measured. There are also a number of lines which were observed in the Jovian spectrum which do not correspond to any of the ammonia lines. The spectrogram of methane obtained by Phillips (referred to above) with a path length of 700 m atm and a dispersion of  $2.5 \text{ \AA/mm}$  shows a weak band of several lines in the region  $7725$ - $7780 \text{ \AA}$ , but between this point and  $\lambda 7640$ , the spectrum is virtually blank. Thus we are left with eleven lines whose identity remains uncertain. Since all the Jovian lines are very weak, the principal cause for the differences in the relative intensities of lines observed in the laboratory spectrum compared with those in the spectrum of Jupiter must be the difference in the local temperatures at which the two spectra are produced. Thus one may speculate that some of the as-yet unidentified lines could be members of the  $7654\text{-}\text{\AA}$  ammonia band lying below the present limit of laboratory resolution for the intensities corresponding to the laboratory temperature. Spectra of higher resolution obtained with the more versatile spectrograph described in Section 3.2 should settle this question.

## 4.2 The Spectrum of Jupiter from 7750-8800 Å

### Introduction

This region of the spectrum of Jupiter contains a number of strong bands due to methane and ammonia. These bands were first identified by Wildt (1932) and the identification was subsequently verified at higher dispersion by Dunham (1933). A comprehensive investigation which included studies of the spectra of Saturn, Uranus, and Neptune was carried out by Adel and Slipher (1934) who made assignments of overtones and combinations of the vibrational frequencies of methane to the planetary absorption features. The most recent study of this region of the spectrum of Jupiter has been made by Kiess, Corliss, and Kiess (1960) who used dispersions of 5 Å/mm and 2 Å/mm. They measured large numbers of lines and attempted to identify these with the help of laboratory measures of methane and ammonia wavelengths published by Vedder and Mecke (1933) and Chao (1936), respectively. Although Kiess et al. found a very good agreement to exist between the laboratory and Jovian ammonia wavelengths, many of the lines in bands which have been attributed to methane by earlier observers (at low dispersion) remain unidentified. This lack of correspondence has been considered as possible evidence for the presence of an amount of methane in the Jovian atmosphere which is much larger than the commonly accepted value (Zabriskie 1962)

which makes the identification of these lines a particularly interesting problem.

Perhaps the first point to consider is the adequacy of the laboratory comparisons. Vedder and Mecke (1933) obtained their laboratory spectra at a maximum equivalent path length of 85 m atm while the amount of methane in the atmosphere of Jupiter would require a path of at least 300 m atm for the weaker lines (Kuiper 1952). The effect of such differences has already been illustrated in the case of ammonia (Owen 1963, Owen, Richardson, and Spinrad 1964). It thus seemed worthwhile to obtain laboratory spectra of methane and ammonia at more suitable path lengths to see if the unidentified lines were in fact due to these gases. In the process of carrying out this program, several spectra were obtained at higher resolution using the Sun as a source of illumination. The richness and complexity of the methane bands on these plates make clear the necessity for obtaining Jovian spectra of the highest possible resolution to remove all ambiguities in identification. The purpose of the present paper is simply to elucidate the reasons for the current uncertainties and to resolve as many of these as possible. A complete line-by-line analysis should await better spectra of Jupiter and the aid of an automatic measuring program!

### Experimental Procedure

In addition to the wavelengths tabulated by Kiess et al., reference was made in the present study to a spectrum of Jupiter obtained by Dr. Gerard P. Kuiper and kindly made available by him for this purpose. This plate (McDonald D520) was used in a previous study (Owen 1963) and its characteristics are described more fully there. It has a dispersion of  $9.8 \text{ \AA/mm}$  on a hypersensitized I-N emulsion. This dispersion is obviously less than that used by Kiess et al., but part of this disadvantage is made up for in the present application by the greater width of the McDonald spectrum which increases the reliability of the identifications.

The methane and ammonia spectra were obtained with the 2-meter and 22.5-meter multiple-path absorption tubes of the Lunar and Planetary Laboratory using both low and high resolution equipment. The high resolution work ( $2.5 \text{ \AA/mm}$  dispersion) was carried out at pressures which were equal to or less than 700 mb in order to minimize the effects of pressure broadening. All of these spectra were obtained at room temperature.

Both sets of spectra have been analyzed in several ways. Some measurements were made on the original plates and some on enlarged prints. Neither of these methods was found to be completely satisfactory since at low resolution the rotational lines are blended together into broad, often



diffuse features which are difficult to measure while at high resolution the number of lines is immense. These two extremes embrace a number of intermediate stages in which different groups of lines will blend together when analyzed at a given resolution and be measured as individual features whose wavelengths will not necessarily correspond to those measured at some other resolution. Blending remains a problem for identifications even when the resolution at the telescope is perfectly matched in the laboratory since the relative intensities of the fine structure lines making up the blends will be different owing to differences in temperature between the planetary atmosphere and the laboratory. Thus a compromise was followed in which some of the more prominent blends were measured while the fine structure of the bands was studied by direct comparison of prints of the Jovian and laboratory spectra.

#### Discussion of Results

Kiess et al. discussed six absorption bands in their paper: the ammonia bands at  $6450 \text{ \AA}$  and  $7900 \text{ \AA}$ , and methane bands at  $6190 \text{ \AA}$ ,  $7250 \text{ \AA}$ ,  $8414 \text{ \AA}$ , and  $8606 \text{ \AA}$ . There is no serious identification problem with the two ammonia bands although the  $7900 \text{ \AA}$  band may be subject to some misinterpretation as is mentioned below. The methane bands at  $6190 \text{ \AA}$  and  $7250 \text{ \AA}$  are not included in the present study since adequate laboratory spectra are not yet available.

The 7250 Å band is particularly difficult to analyze because of its coincidence with a region of strong telluric water vapor absorptions. The latter may account for some of the unidentified lines in the list of Kiess et al. The 8414 Å and 8606 Å methane bands are discussed below.

a) The 7900 Å band of  $\text{NH}_3$

This band has been carefully studied by Chao (1936) at high resolution and, as Kiess et al. point out, there is a good correspondence between their measures of wavelengths in the spectrum of Jupiter and the measures of Chao. There is a weak methane band which overlaps this region, however, with several relatively strong absorptions near 7840 Å. Kiess et al. have ignored this system even though some of its members were tabulated by Vedder and Mecke (1933). This system is responsible for the unidentified line measured by Kiess et al. at 7826.26 Å and undoubtedly contributes (by blending) to several other lines which have been identified as due to ammonia, particularly those at 7837.25 Å, 7839.58 Å, and 7840.32 Å.

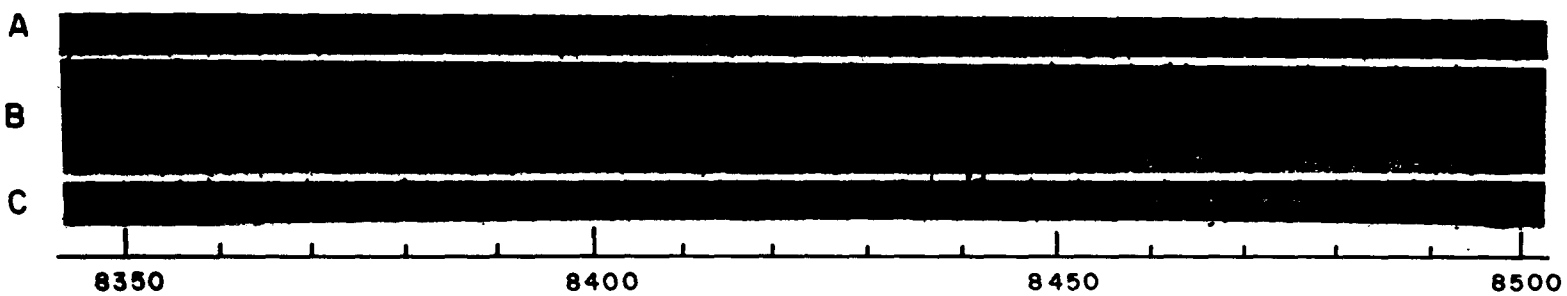
This methane band has led to a misidentification in the spectrum of Saturn as well. The lines are considerably stronger there owing to the greater amount of methane in the optical path and apparently led Dunham (1952) to assume that the absorptions in this region were due to ammonia as in the case of Jupiter.

b) The CH<sub>4</sub> band at 8414 Å

This band is dominated by two roughly antisymmetrical groups of three strong features, each of which is seen to be composed of several lines at high resolution. In addition, there is a large number of lines both shortward and longward of these groups. Kiess et al. have identified four of the six principal features of the band. The absorption at 8387.65 Å was presumably overlooked because it is blended with a solar line; the blend at 8420.25 Å is listed but unidentified.

Kiess et al. tabulate wavelengths for this band running from 8371.29 Å to 8443.20 Å (the measures for the 8606 Å band begin with 8455.59 Å). Comparison of their wavelengths with the plate material used for this discussion reveals no absorption which cannot be explained as being due to methane with the possible exception of a few lines whose relative intensities are 2 or less. (Kiess et al. use an intensity scale in which a given line in a band is compared with other lines in the same band - not to the solar lines.) The same holds true when a comparison of the McDonald spectrogram with the laboratory plates is made. An example of the latter is presented in Figure 12. The comparison spectra of the Sun (A) and Sun plus methane (C) were obtained at considerably higher resolution than the spectrum of Jupiter (B). Close inspection of the methane spectrum reveals that many faint lines occur throughout this

Fig. 12 Spectra of the Sun (A), Jupiter (B), and 313 m atm (NTP) of CH<sub>4</sub> Plus  
Sunlight (C), 8350 Å to 8500 Å.



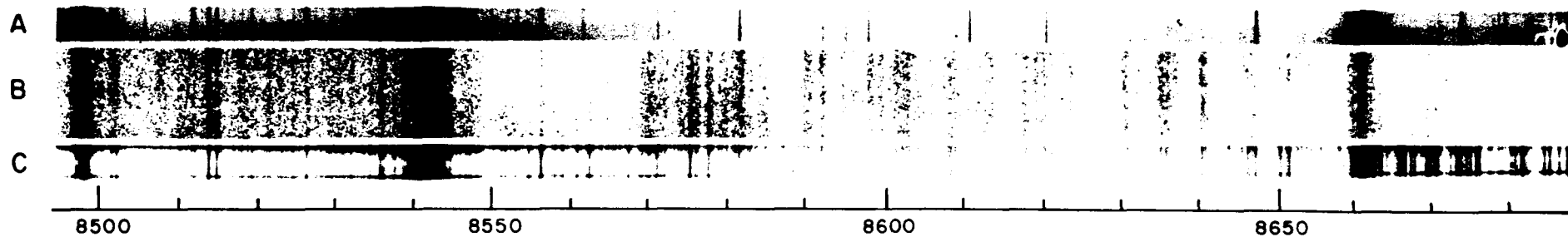
spectral region. In no case is there a non-Fraunhofer absorption in the Jovian spectrum which is not attributable to methane. In addition to the features listed by Kiess et al., there are relatively strong methane absorptions at 8364 Å, 8450 Å, 8457 Å, 8463 Å, and 8473 Å in the spectrum of Jupiter.

c) The CH<sub>4</sub> band at 8606 Å

This band is one of the strongest features in the spectrum of Jupiter below 8800 Å. It is complex even at relatively low dispersion. Kiess et al. list twenty-four features in the region 8543.74 - 8666.93 Å, the long-wave cut-off presumably being set by the characteristics of their plates. The McDonald plate indicates that the methane absorptions are prominent all the way to 8800 Å, where the members of the very strong 8873 Å band establish the longward limit of the plate. All of the absorptions tabulated by Kiess et al. appear to be due to methane but there are a great many omissions from their list and some considerable discrepancies in intensity. Examples of omissions are the features at 8602 Å, 8608 Å, and 8618-20 Å, all of which appear quite strong both on the laboratory plates and the McDonald spectrum. Another region rich in lines where none is recorded occurs between 8647.36 Å and 8666.93 Å.

Reference is made to Figure 13 which shows a comparison similar to that of Figure 12 for the region 8500 - 8685 Å. The intensity discrepancies referred to are most clearly

Fig. 13 Spectra of the Sun (A), Jupiter (B), and 313 m atm (NTP) of CH<sub>4</sub> Plus  
Sunlight (C), 8500 Å to 8685 Å.





illustrated in the case of the features at  $8632 \text{ \AA}$  and  $8648 \text{ \AA}$ . Kiess et al. assign these two features a relative intensity of 2 while on the McDonald plate they appear to have intensities equivalent to or stronger than the absorptions at  $8641.95 \text{ \AA}$  and  $8666.93 \text{ \AA}$  to which Kiess et al. have assigned a value of 10. These authors have also omitted the feature at  $8637 \text{ \AA}$  which is one of the strongest methane absorptions in this region.

Although it appears from Figure 13 that methane is responsible for all of the non-Fraunhofer absorptions, this is not quite true. There is an ammonia band at  $8800 \text{ \AA}$  which has some isolated, outlying members which overlap the region under discussion. Most prominent of these is a line at  $8590.3 \text{ \AA}$ . Inspection of Figure 13 indicates that this line may contribute to the absorption at this wavelength but it is evident that higher resolution is required to distinguish it from the methane lines. Other (weaker) ammonia lines occur at  $8635 \text{ \AA}$  and  $8652 \text{ \AA}$ . The more prominent features of this band begin to appear at  $8781 \text{ \AA}$ .

d) Assignments of vibrational frequencies (methane bands)

Kiess et al. suggest that the assignments made by Adel and Slipher (1934) are incorrect and offer new ones in their place. Herzberg (1945) has also criticized the results of Adel and Slipher but cautioned that the complexity of the bands made the alternative assignments which he

presented tentative. Kiess et al. note that Adel and Slipher assign absorptions at 798, 788 and 782  $\mu$  to methane and suggest that these "... are to be regarded as blends of strong lines in the  $\text{NH}_3$  band rather than as members of  $\text{CH}_4$  bands." As we have seen, while the first two of these features are indeed due to ammonia the third is at least partially due to methane.

Concerning the four methane bands in which they have measured individual wavelengths, Kiess et al. state that they have been able to determine the positions of the maximum absorptions with greater precision than has been possible before. On the basis of these measurements, they make new assignments for the overtone and fundamental frequencies responsible for the bands. Their results are reproduced in Table 4. Rea (1962) has already remarked that with the exception of the band at 8618  $\text{\AA}$  (our 8606  $\text{\AA}$ ) these assignments must be wrong since they suggest a negative or zero anharmonicity acting to make the calculated overtone or combination wave numbers lower than (or equal to) the observed values. In fact the anharmonicities act in just the opposite sense. It remains to point out that the frequency  $\nu_1$  is inactive in the infrared since it involves no change in the dipole moment. Thus the assignment of  $4\nu_1$  for the band at 8618  $\text{\AA}$  is also incorrect. Inspection of Figure 13 suggests that this band is far too complex to be a pure

Table 4

THE ASSIGNMENT OF VIBRATIONAL FREQUENCIES  
TO BANDS OF CH<sub>4</sub> IN THE SPECTRUM OF JUPITER

Wave-length (air)	Wave No. (vac)	Assignment (Kieess = K)	Assignment (Herzberg = H)
8871	11270 H		$3\nu_1 + \nu_3 = 11763$
8618	11600 K	$4\nu_1 = 11657$	$2\nu_1 + 2\nu_3 = 11869$
8423	11869 K	$2\nu_1 + 2\nu_3 = 11869$	$\nu_1 + 3\nu_3 = 11975$
			$4\nu_3 = 12081$
7838	12755 H		$3\nu_1 + \nu_3 + \nu_4 = 13069$
			$2\nu_1 + \nu_2 + 2\nu_3 = 13395$
7270	13750 K	$3\nu_2 + 3\nu_3 = 13660$	$4\nu_1 + \nu_3 = 14677$
			$3\nu_1 + 2\nu_3 = 14783$
6205	16112 K	$5\nu_1 + \nu_2 = 16103$	

overtone in any case. Until detailed analyses are carried out which result in the identifications of the individual lines, it seems that the assignments suggested by Herzberg are probably the best available.

### Conclusions

It has been shown that the unidentified absorption lines listed by Kiess, Corliss, and Kiess (1960) in the region of the methane bands at  $8414 \text{ \AA}$  and  $8606 \text{ \AA}$  are primarily due to methane with some contribution (in the latter case) from ammonia. The presence of an overlapping methane band in the region of the strong  $7900 \text{ \AA}$  band of ammonia has also been pointed out. The assignment of overtone and combination frequencies to the various methane bands has been criticized as unrealistic. There appears to be no need to invoke the presence of other gases in the Jovian atmosphere to account for the absorptions observed in this region of the spectrum. Nevertheless, the fact that in some cases the methane and ammonia lines are so badly blended that they are inseparable suggests that absorptions due to other gases could be present in this region and escape detection. This is a strong argument for the use of the highest possible resolution in obtaining planetary spectra. This study has also indicated the need for laboratory spectra obtained at conditions which approximate

those existing in the atmosphere of the planet as closely as possible when attempting to identify and interpret the absorptions observed in the planetary spectrum. Low temperature spectra of the type needed for these comparisons would also provide the necessary data for the assignment of rotational quantum numbers to the fine structure lines. This in turn should lead to a better understanding of the fundamental frequencies involved in these transitions.

#### 4.3 The Spectrum of Jupiter from 9000 - 10100 Å

##### Introduction

The region of the Jovian spectrum which is the subject of this investigation is of particular interest for two reasons. First, it has not been thoroughly studied in the past and contains a number of absorption features which have not been positively identified. Second, there is the possibility of detecting gases which may be expected to be present in the Jovian atmosphere in addition to the well-known constituents since some of these gases have relatively strong absorptions in this wavelength interval. Bardwell and Herzberg (1953), in discussing the possibility of detecting  $\text{SiH}_4$  and  $\text{CH}_3\text{D}$  in the atmospheres of the outer planets, gave a brief list of absorption bands occurring in this region of the Jovian spectrum which they had compiled from the work of several observers. They noted that Vedder

and Mecke (1933) had reported a strong absorption due to methane at  $9706 \text{ \AA}$  from a laboratory investigation of this gas and concluded that methane was responsible for the band at  $9700 \text{ \AA}$  which had been observed in the spectrum of Jupiter. The identification of the other absorption features was secondary to these authors' purpose and consequently was not pursued. In the present paper, recently obtained laboratory spectra of several gases are compared with spectra of Jupiter taken by Dr. G. P. Kuiper at the McDonald Observatory in 1954 and 1955. These spectra are of a higher quality than those published previously, and permit a detailed identification of the various absorptions occurring in this region, as well as provide a means for setting upper limits on the abundances of certain gases considered to be probable constituents of the Jovian atmosphere.

#### Equipment and Experimental Procedure

Absorption spectra of the gases investigated were obtained with the help of a 2-meter multiple path absorption tube on loan from the National Research Council of Canada through the courtesy of Dr. G. Herzberg. The design of this type of apparatus has been described elsewhere (Herzberg 1952); its great advantage lies in the possibility of obtaining long optical paths in a relatively small space. With this particular tube a total path length of 80 meters

is attainable. It is also possible to vary the pressure and temperature of the gas in the tube so that a wide variety of physical conditions can be reproduced. In the present investigation the tube was allowed to remain at room temperature at all times, and except for methane (which required a pressure of 5 atm to match the Jovian amount) all gases were studied at atmospheric pressure. A simple tungsten-filament lamp served as a light source.

The spectra were produced by a Bausch and Lomb 1.5-meter spectrograph, using a grating blazed at  $7000 \text{ \AA}$  with a dispersion of  $20 \text{ \AA/mm}$  in the region of interest. A plate holder designed by Dr. A. B. Meinel has been substituted for the film holder supplied with the spectrograph, permitting the use of thin plates curved to fit the focal surface of the grating. A list of the plates obtained for this study is given in Table 5.

The laboratory spectra were compared with spectra of Jupiter and the moon made available by Dr. G. P. Kuiper. The four plates used in this work are described in Table 6. Plate D520 is included for the discussion of abundances even though it does not overlap the region of the spectrum chosen for particular study in this paper. The long-wavelength limit of the present analysis is set by the characteristics of the laboratory spectrograph which prevent the study of the spectrum beyond  $1.01\mu$  without considerable

Table 5

## LABORATORY SPECTRA OF GASES

Plate No.	Gas	Equivalent Path Length	Emulsion*
67	$C_2H_4$	8 m atm	I-N
74	$CH_4$	400	I-Mh
77	$CH_4$	400	I-Zh
90	$NH_3$	16	I-Zh
95	$NH_3$	16	I-Mh
99	$C_2H_6$	16	I-Zh
100	$C_2H_4$	16	I-Zh
101	$CH_3NH_2$	16	I-Zh
102	$CH_3NH_2$	8	I-Zh
103	$C_2H_6$	8	I-Zh

\*h = hypersensitized with ammonia solution.



Table 6  
SPECTRA OF JUPITER (a)

Plate No.	Dispersion (Å/mm)	Wave- length Range (Å)	Emulsion	Exposure (min.)	Date
D520	9.8	6600-8800	I-Nh	240	1/24/54
D521	35.9	8700-9720	I-Mh	145	1/24/54
D522*	35.9	7200-9950	I-Mh	45	1/24/54
1169	71	9700-11200	I-Zh	360	2/11/55

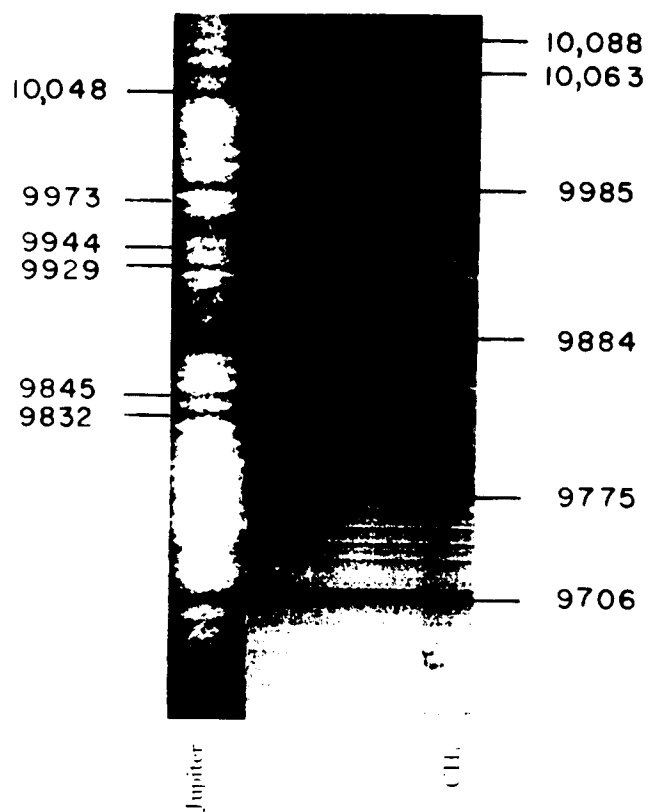
\* Lunar spectrum for comparison.

adjustment. The 9000 Å limit marks the onset of the strong 8873 Å band of CH<sub>4</sub>. At shorter wavelengths, Jovian spectra of much higher dispersion (such as plate D520) are available which require better laboratory spectra for their interpretation (cp. Section 4.2). The region of the Jovian spectrum which extends to the practical limit of the photographic infrared is discussed in Section 4.4.

### Identifications

Since methane and ammonia are both known to be present in the Jovian atmosphere, these gases were investigated first. It became apparent almost immediately that the strong absorptions in the region 9700-10100 Å were nearly all due to methane. This is made clear in Figure 14 which shows the laboratory spectrum of methane compared with plate 1169 of Jupiter. Since the dispersion achieved in the laboratory is considerably higher than that used at the telescope, a larger number of bands are visible in the laboratory methane spectrum than appear in the spectrum of Jupiter. The comparison is also hindered by the difference in the manner of formation of the absorption lines in the two cases which leads to differences in their relative intensities. Nevertheless, the presence of the strong features at 9706 Å, 9984 Å, and 9985 Å in both spectra, together with the large number of other coincidences, makes the identification of those features appearing in both spectra quite

Fig. 14 Spectra of Jupiter and Methane, 9630 Å to 10100 Å.

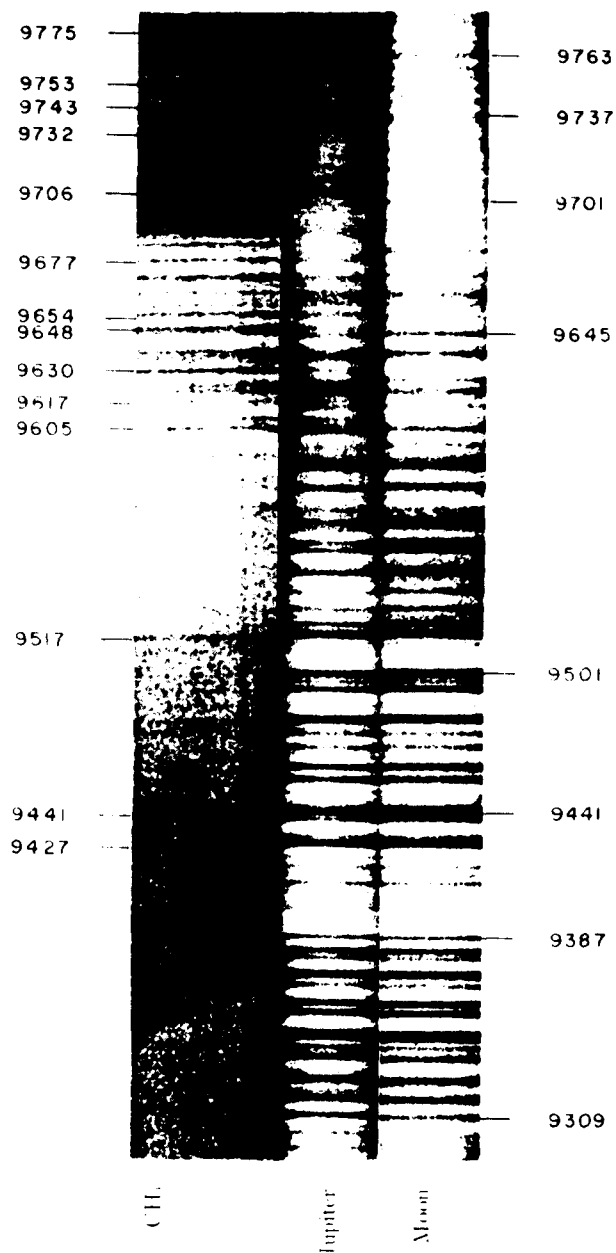


definite. A possible exception is provided by the band at  $10048 \text{ \AA}$  which is obviously much stronger in Jupiter than the weak line appearing in the laboratory spectrum. This difference is partly a result of the low contrast of the laboratory plate in this region, but is also due to the intensity differences referred to above. In addition, the strong Fraunhofer line at  $10049 \text{ \AA}$  (Paschen 7 of hydrogen) will contribute to the  $10048 \text{ \AA}$  absorption in the spectrum of Jupiter. The ammonia spectrum reveals a large number of lines in the region  $9770 - 10100 \text{ \AA}$ , but none of these is clearly separated from the strong methane absorptions in this same wavelength interval.

The region from  $9000 - 9775 \text{ \AA}$  could be studied in greater detail owing to the higher dispersion of plates D521 and D522. Although there is serious interference from the  $\rho$  band of telluric water vapor, some additional members of the  $9706 \text{ \AA}$  band of methane are visible and give added support to the identification. This is indicated in Figure 15 which includes the lunar spectrum for comparison.

In the course of studying the spectrum of ammonia produced by 16 meters of this gas (for comparison with the 14 meters expected in the spectrum of Jupiter (Kuiper 1952a)), two band systems were found which were not reported by Chao (1936), whose longest path length was 8.6 meters. Both of these systems are present in the spectrum of

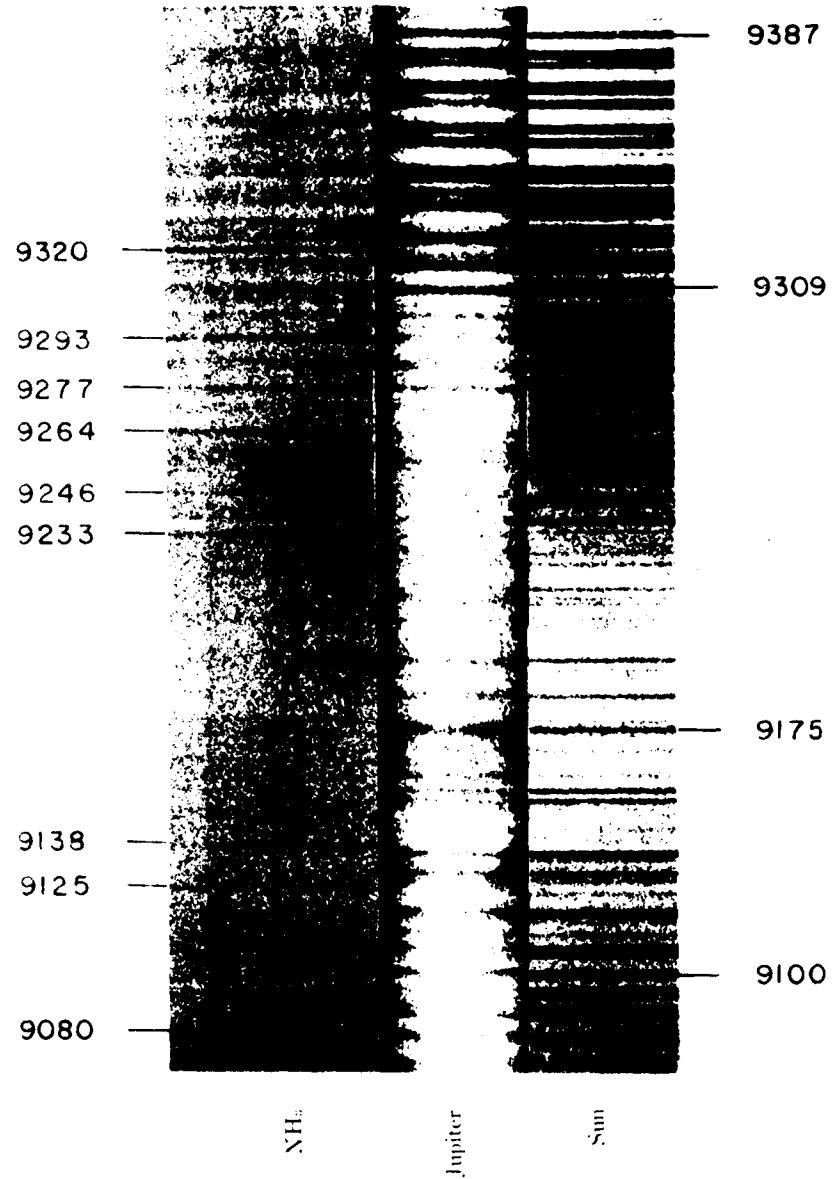
Fig. 15 Spectra of Methane, Jupiter, and the Moon, 9300 Å to 9775 Å .



Jupiter, one of them falling in the region discussed here (the other was described in Section 4.1). The strongest member of this system at room temperature has a wavelength of  $9320 \text{ \AA}$ ; using the frequencies of the fundamental vibrations of the ammonia molecule given by Herzberg (1945a), one is led to the assignment of  $3\nu_1 + \nu_2$ . As both Herzberg (1945b) and Wu (1946) have stressed, however, the complexity of the ammonia spectrum makes any such assignment uncertain, particularly in the present case where no fine-structure analysis was carried out. Wavelengths of the strongest members of this system are given in Figure 16 which indicates their presence in the Jovian spectrum. A spectrogram of the sun taken with the laboratory spectrograph has been substituted for the lunar comparison in this case since the latter contains a serious plate defect in this spectral region. The higher resolution of the solar and ammonia spectra should be kept in mind when comparing them with the spectrum of Jupiter. The comparison reveals an unfortunately large number of wavelength coincidences between the ammonia and Fraunhofer lines, but the consequent enhancement of these blends (e.g.,  $9233 \text{ \AA}$ ,  $9293 \text{ \AA}$ ) compared with their appearance in the solar spectrum, as well as the presence of an unblended ammonia line at  $9264 \text{ \AA}$  is quite convincing. The apparent absence of the strong line at  $9320 \text{ \AA}$  in the Jovian spectrum is somewhat disturbing; it may



Fig. 16 Spectra of Ammonia, Jupiter, and the Sun, 9080 Å to 9455 Å.



be a result of the difference in the temperatures at which the two spectra are produced. At the low temperature expected in the Jupiter atmosphere, the line could conceivably be weak enough to be lost in the "wings" of the strong telluric blends centered at 9317 Å and 9324 Å. This hypothesis will be tested by means of low-temperature laboratory spectra. Observations of Jupiter with higher resolution would also be helpful.

#### Upper Limits

Kuiper (1952b) has given an extensive list of gases which could be considered as possible constituents of various planetary atmospheres. Many of these can be eliminated as subjects for the present investigation because of the reducing nature of the Jovian atmosphere. Of the remaining gases, those which are most likely to be present as a result of reactions of the known constituents can be selected on the basis of photochemical arguments such as those presented by Wildt (1937) and Cadle (1962), and from the experimental work of Sagan and Miller (1960). The list is further narrowed by the requirement that the gas must have at least one strong absorption band in the region of the spectrum being studied which is visible at the dispersions employed - this requirement has been relaxed to permit the inclusion of  $C_2H_4$  and HD. We are left with six gases for which data were either obtained in the present

investigation or are available from other sources. These are listed in Table 7 and discussed below. The limits given in the table are intended as a first approximation only; they are based on a simplified model atmosphere in which the gas is assumed to lie above a reflecting surface and to contain no particles which scatter light in the wavelength interval under consideration. Since the gases investigated were not detected, it is clear that we are dealing with weak lines which if present would have intensities corresponding very nearly to the intensities of lines produced by the path lengths used in the laboratory (van de Hulst 1952). Additional corrections should be made for the difference in pressure and temperature between the laboratory and planetary environments. The limits presented here are based on the laboratory values of these parameters; they were not corrected to N.T.P. since the information required was not available for three of the gases. The effect of such a correction will be to lower the limits somewhat, by a factor 0.85 for the first three gases. An effective path length of two air masses has been assumed since the planet is observed as an extended disk.

Methylamine ( $\text{CH}_3\text{NH}_2$ ): The 9950 Å band consists of several Q branches on either side of an intensity minimum. It should be noted that there is strong overlapping in this region from  $\text{CH}_4$ ; otherwise a more sensitive determination would be possible.

Table 7

UPPER LIMITS ON THE ABUNDANCES OF SIX GASES  
IN THE JOVIAN ATMOSPHERE

Gas	Band Used	Abundance Limit	Comparison Plate
$\text{CH}_3\text{NH}_2$	9950 Å	8 m atm	1169
$\text{C}_2\text{H}_4$	8715	2	D520
$\text{C}_2\text{H}_6$	9060	4	D521
$\text{SiH}_4$	9738	20	D521
$\text{CH}_3\text{D}$	9936	30	1169
HD	7377	500	D520
	7464		

Ethylene ( $\text{C}_2\text{H}_4$ ): The band at  $8715 \text{ \AA}$  consists of several members of which a broad feature centered at  $8693 \text{ \AA}$  and two sharper absorptions at  $8715 \text{ \AA}$  and  $8724 \text{ \AA}$  are the strongest. The limit in the table allows for the higher dispersion used at the telescope in this case.

Ethane ( $\text{C}_2\text{H}_6$ ): The  $9060 \text{ \AA}$  band is unresolved on the laboratory plates, but causes a wide ( $50 - 100 \text{ \AA}$ ) depression in the continuum. Such a depression was searched for without success in the spectrum of Jupiter. The limit given takes into account the slight interference caused by the  $8873 \text{ \AA}$  band of  $\text{CH}_4$ .

Silane ( $\text{SiH}_4$ ): It is not possible to add to the discussion of Bardwell and Herzberg (1953), even though the spectrum of Jupiter available for the present study is of a higher quality than the spectra which they were able to use. This lack of precision is due to the presence of strong absorptions at  $9737\text{-}38 \text{ \AA}$ , due both to telluric  $\text{H}_2\text{O}$  and Jovian  $\text{CH}_4$  which require the use of very high dispersion to lower substantially the limit set by these authors.

Methyl deuteride ( $\text{CH}_3\text{D}$ ): The most favorable of the absorptions listed by Bardwell and Herzberg (1953) is the one at  $9936 \text{ \AA}$ , since it is essentially free from interference by  $\text{CH}_4$ . This is evident from inspection of Figure 14, which also shows the absence of the  $\text{CH}_3\text{D}$  absorption. It is difficult to set a limit in this case since the

spectrum was not shown in the original article. The maximum path length used was 90 meters, and the absorption at 9936 Å was classified as medium in strength. From this and the fact that Childs and Jahn (1936, 1939) apparently observed bands in this region with a path length of only 6 meters (but with much higher dispersion), it seems safe to conclude that the amount given in the table would have been visible if present.

Deuterium hydride (HD): The (3,0) rotation-vibration band of this gas falls in the wavelength region of principal interest but consists of sharp, widely separated lines which would not be detectable at the dispersions used here. The (4,0) band occurs in the N-plate region where higher dispersion can be employed. It is assumed that the 1000 m atm path used in the laboratory by Durie and Herzberg (1960) would lead to detectable absorptions on plate D520. This assumption is supported by the fact that the intrinsically very narrow S(0) and S(1) lines of the (3,0) band of the quadrupole rotation-vibration spectrum of H<sub>2</sub> are visible on this plate. The wavelengths given in the table refer, respectively, to the R(0) and P(1) lines of the (4,0) band.

It is possible to set a very rough upper limit on the Jovian deuterium-hydrogen ratio from the last two results. The amount of methane present is 150 m atm. Hence we have the ratio  $\text{CH}_3\text{D}/\text{CH}_4 < 1/5$ . This leads in turn to the

ratio  $D/H < 1/23$ . HD provides a more sensitive test, leading to a ratio of  $D/H < 1/100$  if the 27 km atm abundance of molecular hydrogen given by Spinrad and Trafton (1963) is adopted. This is still almost two orders of magnitude greater than the terrestrial ratio of  $1/6400$  which would allow only 1/5 m atm of  $CH_3D$  and 17 m atm of HD in the optical path which produces the Jovian spectrum. It is clear that only very high dispersion spectra and considerable deuterium enrichment would permit these gases to be detected in this part of the spectrum. Kuiper (1952c) has suggested that enrichment could have occurred if there was a sufficient interval of time in the planet's early history when  $H_2$  could just escape from the atmosphere while the escape of HD was negligible. At the moment, the best hope for lowering this crude abundance limit would seem to be furnished by the possibility of observing further in the infrared where smaller quantities of both gases produce detectable absorptions. The limiting factor in such work will probably be the extensive overlapping of the strong  $CH_4$  and  $NH_3$  absorption bands which occur in this spectral region.



#### 4.4 The Spectrum of Jupiter from 9700 - 11200 Å

##### Introduction

This paper extends the study of the Jovian spectrum to the longest wavelengths which have been recorded photographically. The observational material consists of McDonald Observatory Plates 1169 and 1221 obtained by Dr. Gerard P. Kuiper in 1955 and kindly made available by him for this study. These plates are compared with a series of spectrograms taken at the Lunar and Planetary Laboratory by the writer.

In continuing the investigation initiated (chronologically) in Section 4.3 (hereafter referred to as Paper I) the absorption features occurring in this region of the Jovian spectrum are identified and upper limits are set on the abundances of several gases. In addition, the relatively simple structure of the methane band at 11057 Å is analyzed to allow a derivation of the temperature of the planet's upper atmosphere.

##### Observational Material and Experimental Procedure

The McDonald spectrograms were both taken with the slit of the spectrograph placed along the equator of the planet such that the entire width of the disc was passed by the slit. Because of the much greater sensitivity of the

Z emulsion in the range 10400 - 11200 Å and the strength of the planetary absorptions occurring from 9700 - 10400 Å, the former region must be overexposed in order to register the latter clearly. Thus two exposures of different lengths are needed to define the spectrum over the entire wavelength interval. In addition one must consider the strong telluric water vapor bands at  $0.94\mu$  (ϑ) and  $1.13\mu$  (ϕ). In this respect plate 1169 is particularly noteworthy since it was obtained at a temperature of 10°F so the water vapor absorptions are relatively weak. This circumstance has contributed significantly to the amount of information which can be derived from the spectrogram. The pertinent data describing the two plates are summarized in Table 8. As it is important to the calibration of these plates which is described later, we point out here that both were obtained with the modern Z emulsion, I-Z (II) as it was originally designated.

Two alterations in the laboratory procedure described in Paper I were introduced in the present investigation in order to obtain spectra which would be more nearly comparable to the spectrum of Jupiter. In order to match the line widths the resolution of the laboratory spectrograph was decreased by using a wider slit ( $300\mu$  vs  $60\mu$ ). To match the line intensities, the amount of gas in the optical path was reduced. The principal features in the

Table 8

## SPECTRA OF JUPITER (b)

Plate No.	Dispersion (Å/mm)	Wave- length Range (Å)	Emulsion	Exposure (hours)	Date
1169	71	9700-11200	I-Zh	6	2/11/55
1221	71	10150-11100	I-Zh	1.5	2/13/55

region of the spectrum discussed here consist of very strong systems, so it is not surprising that the amount of gas needed to produce the appropriate line intensities is considerably less than that deduced to be present above the cloud layer from an analysis of weaker bands. This effect is not due to an increased atmospheric opacity in this wavelength region since ammonia lines which are weak in both the laboratory and planetary spectra require much longer laboratory paths to produce a good match in intensity.

In addition to the room temperature spectra, methane was examined at  $\sim 210^\circ\text{K}$  to provide an empirical check on the temperature analysis given later in this paper. This was accomplished by supporting the absorption tube in an upright position so that it could be encased by a Dewar except for its uppermost end. The Dewar was then filled with a mixture of dry ice and alcohol which was allowed to come to equilibrium with the tube and its content of gas. A rough check on the resulting gas temperature was achieved by measuring the pressure after the tube had regained room temperature since it was sealed off from the gas cylinder during the experiment.

#### Identifications

A line-by-line analysis of the Jovian spectrum in this wavelength region is presented in Table 9. The lines

Table 9

IDENTIFICATION OF ABSORPTION LINES IN THE SPECTRUM  
OF JUPITER FROM 9690 Å TO 11206 Å

λ	Ident.	Rem.	λ	Ident.	Rem.
9690	CH <sub>4</sub> + Atm?		9944	CH <sub>4</sub>	
9706	CH <sub>4</sub>	very strong	9953	CH <sub>4</sub>	
9732	CH <sub>4</sub> + Atm?		9962	CH <sub>4</sub>	
9743	CH <sub>4</sub> + Atm		9974	CH <sub>4</sub>	
9753	CH <sub>4</sub> + Atm?		9986	CH <sub>4</sub>	
9764	CH <sub>4</sub>		9993	CH <sub>4</sub>	
9775	CH <sub>4</sub> + NH <sub>3</sub> ?		10004	CH <sub>4</sub>	
9806	CH <sub>4</sub>		10014	CH <sub>4</sub>	
9818	CH <sub>4</sub>		10021	CH <sub>4</sub>	defect
9832	CH <sub>4</sub>	strong	10032	CH <sub>4</sub>	very weak
9845	CH <sub>4</sub>	strong	10041	CH <sub>4</sub>	very weak
9855	CH <sub>4</sub>		10048	CH <sub>4</sub> + e	
9863	CH <sub>4</sub>		10064	CH <sub>4</sub>	
9884	CH <sub>4</sub>	very strong, broad	10077	CH <sub>4</sub>	
9902	CH <sub>4</sub>	broad	10089	CH <sub>4</sub> + NH <sub>3</sub> ?	
9915	CH <sub>4</sub>	broad	10098	CH <sub>4</sub>	broad
9923	CH <sub>4</sub>		10118	CH <sub>4</sub>	very broad
9930	CH <sub>4</sub>		10140	CH <sub>4</sub> + NH <sub>3</sub>	
			10147	CH <sub>4</sub>	

Table 9 (Continued)

$\lambda$	Ident.	Rem.	$\lambda$	Ident.	Rem.
10161	CH <sub>4</sub>		10444	NH <sub>3</sub>	very weak
10170	NH <sub>3</sub>		10463	NH <sub>3</sub>	weak
10177	CH <sub>4</sub> + NH <sub>3</sub>		10480	NH <sub>3</sub>	weak, broad
10194	CH <sub>4</sub> + NH <sub>3</sub>	very broad	10582	NH <sub>3</sub> + $\odot$	broad
10210	CH <sub>4</sub> + NH <sub>3</sub>		10593	NH <sub>3</sub>	weak
10219	NH <sub>3</sub>		10603	$\odot$	weak
10227	CH <sub>4</sub> + NH <sub>3</sub>		10661	$\odot$	weak
10250	CH <sub>4</sub> + NH <sub>3</sub>	broad, weak	10678	NH <sub>3</sub> + $\odot$	weak, broad
10267	CH <sub>4</sub> + NH <sub>3</sub>		10687	NH <sub>3</sub> + $\odot$	weak, broad
10284	NH <sub>3</sub>		10707	NH <sub>3</sub> + $\odot$	weak
10298	NH <sub>3</sub>	broad	10718	NH <sub>3</sub> + $\odot$	weak
10324	NH <sub>3</sub>	very broad	10727	NH <sub>3</sub> + $\odot$	
10347	NH <sub>3</sub>		10749	$\odot$	weak
10357	NH <sub>3</sub>	broad	10772	NH <sub>3</sub> + Atm	weak
10389	NH <sub>3</sub>	very weak	10786	NH <sub>3</sub> + Atm	weak
10407	NH <sub>3</sub>	weak	10795	NH <sub>3</sub> + Atm	weak
10416	NH <sub>3</sub>	very weak	10810	NH <sub>3</sub> + Atm	broad
10422	NH <sub>3</sub>	very weak	10820	NH <sub>3</sub>	
			10827	$\odot$	weak
			10869	$\odot$	defect(?)
			10889	NH <sub>3</sub> + Atm	

Table 9 (Continued)

$\lambda$	Ident.	Rem.	$\lambda$	Ident.	Rem.
10900	NH <sub>3</sub> + Atm	weak	11048	CH <sub>4</sub>	
10923	CH <sub>4</sub> + Atm	R(9)	11057	CH <sub>4</sub>	Q
10937	CH <sub>4</sub>	R(8)broad, strong	11081	CH <sub>4</sub>	strong, broad
10951	CH <sub>4</sub>	R(7)broad	11095	CH <sub>4</sub>	
10962	CH <sub>4</sub>	R(6)	11109	CH <sub>4</sub>	
10969	CH <sub>4</sub>	weak	11124	CH <sub>4</sub>	
10975	CH <sub>4</sub>	R(5)	11140	CH <sub>4</sub>	strong, broad
10981	CH <sub>4</sub>		11157	CH <sub>4</sub>	
10986	CH <sub>4</sub>	R(4)	11164	CH <sub>4</sub> + Atm	
10996	CH <sub>4</sub>		11174	CH <sub>4</sub>	
11000	CH <sub>4</sub>	R(3)	11191	CH <sub>4</sub> + Atm	
11013	CH <sub>4</sub>	R(2)	11198	CH <sub>4</sub> + Atm?	
11024	CH <sub>4</sub>	R(1)	11206	CH <sub>4</sub>	
11037	CH <sub>4</sub>	R(0)			

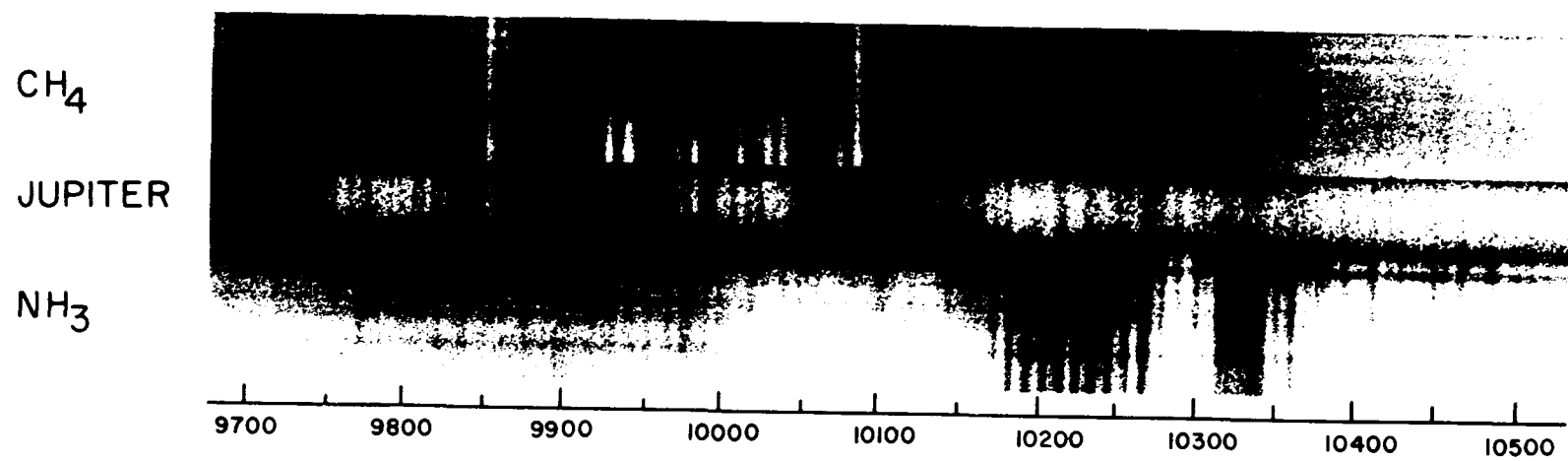
were measured on enlarged high contrast prints which were calibrated by means of easily identified Fraunhofer and methane lines. The mean error in the measurements is estimated at  $1 \text{ \AA}$  for well-defined lines; for wide, diffuse or weak features the error is somewhat larger. It is evident from inspection of the table that methane and ammonia absorptions can account for all features not due to telluric lines or the reflected solar spectrum.

The most interesting spectral regions are reproduced in Figures 17 and 18. Figure 17 shows the close match between the spectrum of Jupiter and laboratory spectra of 170 m atm of methane and 3.4 m atm of ammonia (NTP) in the interval  $9700 - 10400 \text{ \AA}$ . A comparison of this illustration with Figure 14 of Paper I indicates the usefulness of the modifications in laboratory procedure described above. In particular, the uncertainty concerning the identification of the line at  $10048 \text{ \AA}$  has been resolved in favor of methane.

On the other hand, it is clear that there are still differences in intensity between individual lines in the laboratory spectra compared with those in the spectrum of Jupiter. Examples are the ammonia lines at  $10170 \text{ \AA}$  and  $10219 \text{ \AA}$  and the methane line at  $10291 \text{ \AA}$  which is apparently completely absent from the Jovian spectrum. In assessing these differences one should bear in mind that we are considering only one plate (1169) of rather low dispersion on



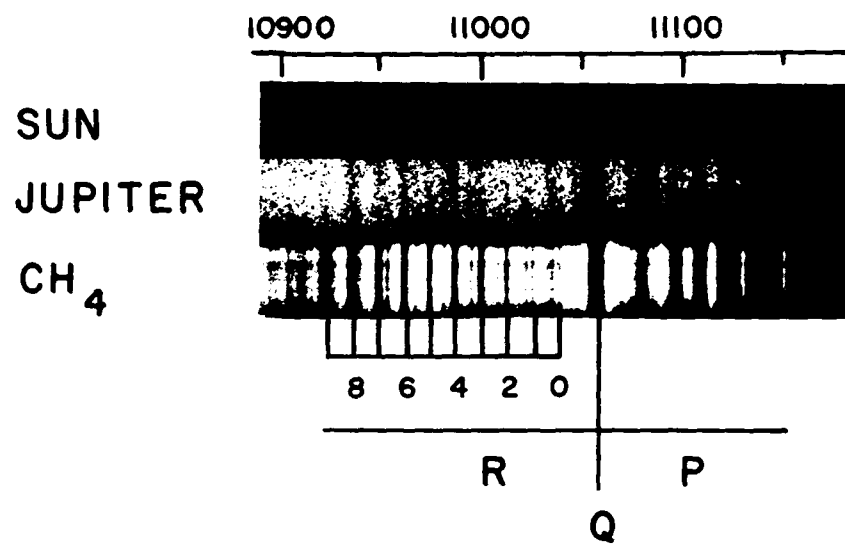
Fig. 17 Spectrum of Jupiter with Comparison Spectra of 170 m atm of Methane and 3.4 m atm of Ammonia (NTP), 9700 Å to 10500 Å.



a grainy, hypersensitized emulsion. It would obviously be helpful to have additional data. It is felt that despite these uncertainties the differences in intensity may well be real since similar effects have been observed in other parts of the spectrum (Dunham 1952). Furthermore, it will be shown that intensity variations can be analyzed in a meaningful way within certain limitations. One is thus led to ascribe at least some of the intensity differences to the different temperatures at which the two spectra were obtained. This supposition is supported by the fact that the lines in question have roughly the same intensity in the laboratory spectrum as others which present the same appearance in both laboratory and planetary spectra. Hence the intensity variation seems unlikely to be due to a difference in the process of line formation in the two cases. The complete absence of the 10291 Å methane line is still puzzling, however, since this represents a remarkable decrease in intensity. This line shows no apparent weakening in a laboratory spectrogram obtained at  $\sim 210^\circ\text{K}$ . If this result is interpreted strictly in terms of temperature differences it implies a temperature for the Jovian atmosphere which is distinctly lower than  $210^\circ\text{K}$ . This point will be referred to again below.

Figure 18 shows a region near the long wavelength end of the McDonald spectrogram which is beginning to show

Fig. 18 Spectrum of Jupiter with Comparison Spectra of Sun and 340 m atm of Methane (NTP), 10900 Å to 11175 Å.



the effects of the decreasing sensitivity of the Z emulsion and the strong  $\Phi$  band of telluric water vapor. The comparison spectra in this case were both obtained with higher resolution than the spectrum of Jupiter in order to clearly delineate the fine structure of the methane and water-vapor band systems in this region. One is immediately struck by the regularity of the methane absorptions. As indicated in the illustration, this regularity reflects the fact that these absorptions are the R and Q branches of the second overtone of the fundamental frequency  $\nu_3$ . There is some overlapping from the methane combination band  $\nu_1 + 2\nu_3$  centered at 11230 Å which (with the  $\Phi$  band of telluric H<sub>2</sub>O) obscures the P branch of the  $3\nu_3$  system. The basic structure is nevertheless apparent. This band was first observed in the laboratory by Childs (1936) and the J numbers given follow his assignment (see also Herzberg 1945, p. 457).

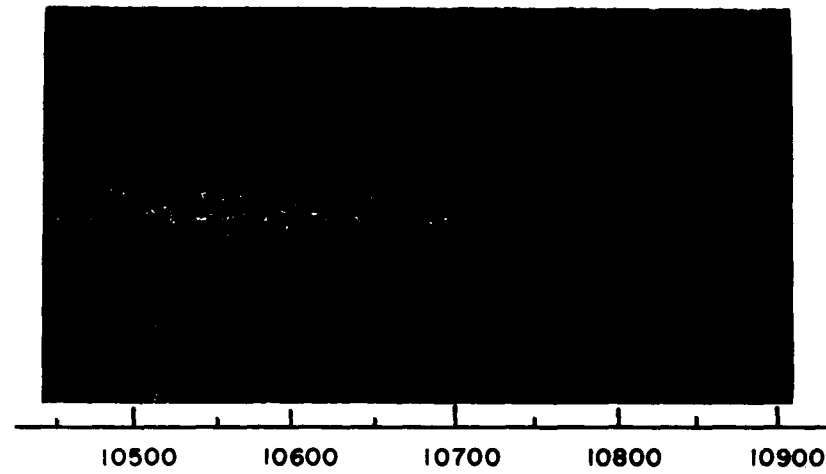
The intermediate region of the spectrum is presented for the sake of completeness in Figure 19. It contains a few ammonia lines in addition to the solar absorptions. This illustration was made from McDonald Observatory plate 1121 while the other two were taken from plate 1169. As in the case of Figure 19, the comparison spectra printed here were obtained at considerably higher resolution than that of the Jovian spectrogram. All

Fig. 19 Spectrum of Jupiter with Comparison Spectra of Sun and 13.6 m atm of  
Ammonia (NTP), 10500 Å to 10900 Å.

SUN

JUPITER

NH<sub>3</sub>





features occurring in this region are relatively weak and hence the identification and wavelengths are somewhat less certain than in the other two spectral regions. Identifications were verified on strongly exposed prints of plate 1169 wherever possible.

### Upper Limits

Of the gases for which upper limits were determined in Paper I, only methylamine has a stronger absorption in this region. The Q branch of  $3\nu_3$  of  $\text{CH}_3\text{D}$  falls at  $11084 \text{ \AA}$  (Childs and Jahn 1939) which is unfortunately well within the region overlapped by  $\nu_1 + 2\nu_3$  of  $\text{CH}_4$  and the telluric water vapor band ( $\phi$ ). However, the second overtones of  $\text{C}_2\text{H}_2$  and  $\text{HCN}$  - both gases which are likely to be present in the Jovian atmosphere (Sagan 1960, Sagan and Miller 1960) - occur in a relatively open spectral region. The absence of  $\text{HCN}$  is in agreement with Kuiper's (1963) improved spectrometer tracings of the  $1.53\mu$  region of the Jovian spectrum which indicate that Sagan's (1960) tentative identification of this feature as due to  $\text{HCN}$  is probably incorrect.

As in Paper I, the limits presented here are derived on the assumption that particle scattering plays no role in the formation of the absorption lines. This assumption is reconsidered in the concluding section of the present paper. In Paper I, the effective air mass was assumed to be 2. Subsequent considerations have indicated that this is

probably too low unless a narrow slit is used. For weak lines, the effective air mass is equal to 3.14 when the spectrograph slit is positioned limb to limb on a planet's disk (Owen and Kuiper 1964). In the present case, limb darkening will tend to decrease this value while the relatively wide slit of the spectrograph will tend to increase it. Considered together, these effects suggest a value of about 3.

Another point which requires correction is the limit to the abundance of deuterium derived in Paper I. Foltz and Rank (1963) have pointed out that the  $H_2$  abundance derived by Spinrad and Trafton (1963) (and used for the derivation of the deuterium abundance) may be too low by as much as an order of magnitude. Taken literally, this leads to a maximum value of 270 km atm of hydrogen in the Jovian atmosphere. On the basis of their original estimate, Spinrad and Trafton (1963) concluded that the H/C ratio for Jupiter was roughly 5.5 times smaller than that for the Sun. An increase in the amount of hydrogen obviously decreases this discrepancy; as a working hypothesis we will assume the two ratios are equal. Using Kuiper's (1952) value for the abundance of  $CH_4$  (150 m atm), the amount of molecular hydrogen turns out to be 190 km atm, or roughly 7 times the original estimate. This value is in better agreement with the results of Foltz and Rank and suggests a solar-type

composition for the atmosphere of Jupiter. The D/H ratio presented in Paper I must then be corrected to  $D/H < 1/1300$  (the terrestrial value of  $D/H = 1/6400$ ). In this case, since a narrow slit was used (McDonald plate D520), the limb darkening will be dominant and a factor 2 for the effective air mass is probably more appropriate. The precision of the D/H limit can be improved by additional work on the Jovian  $H_2$  abundance and spectra of the planet obtained at higher resolution.

In Table 10 we present a summary of the upper limits on the various gases which have been considered in both papers, making use of the corrected air mass where appropriate. The gases studied particularly for this region of the spectrum are described below.

Methylamine ( $CH_3NH_2$ ): At the resolution used in the laboratory, the band at  $10325 \text{ \AA}$  appears as an intense, unresolved absorption with a width of about  $120 \text{ \AA}$  at a path length of 8 m atm. With 4 m atm the appearance of the band resembles that of the strong  $NH_3$  absorption centered at the same wavelength. The limit given represents an effort to take into account the lower quality of the plates in this region and the interference caused by the overlapping ammonia band.

Acetylene ( $C_2H_2$ ): The fine structure of the P and R branches of the band at  $10372 \text{ \AA}$  is well resolved on the

Table 10

UPPER LIMITS ON THE ABUNDANCES OF EIGHT GASES  
IN THE JOVIAN ATMOSPHERE

Gas	Band Used	Abundance Limit	Comparison Plate
$C_2H_2$	10372 Å	3 m atm	1169
$C_2H_4$	8715	2	D250
$C_2H_6$	9060	4	D521
$CH_3NH_2$	10325	3	1169
$CH_3D$	9936	20	1169
HCN	10385	2	1169
$SiH_4$	9738	20	D521
HD	7377, 7464	500	D250

laboratory plates. It is thus possible to use the rotational lines corresponding to low values of  $J$  (largest population at anticipated Jovian temperatures) to set the limit.

Hydrogen cyanide (HCN): The limit set for this gas is estimated from a spectrum of the  $3\nu_3$  band at  $10385 \text{ \AA}$  published by Herzberg and Spinks (1934). These authors used a dispersion of  $5.4 \text{ \AA/mm}$  and a path length of  $1.5 \text{ m atm}$ . The figure given in the table was derived by comparing this spectrum with one of the acetylene band at  $10372 \text{ \AA}$  reproduced at a similar scale (Herzberg 1945, pp. 383, 385).

#### The $3\nu_3$ Band of $\text{CH}_4$ and a Determination of Mean Temperature

A molecule which has all three principal moments of inertia equal is called a spherical top. This is the case for the methane molecule which has a tetrahedral shape. This molecule has four fundamental vibrational frequencies which are illustrated in Figure 20. Of these frequencies,  $\nu_2$  is doubly degenerate while both  $\nu_3$  and  $\nu_4$  are triply degenerate. Only the latter two are active in the infrared since they are the only two which are anti-symmetric with respect to the center of symmetry and thus result in a change in the dipole moment. Two or more of these frequencies or their overtones can be excited together to give combination bands while pure overtones occur only for the frequencies  $\nu_3$  or  $\nu_4$ . An added complication is introduced

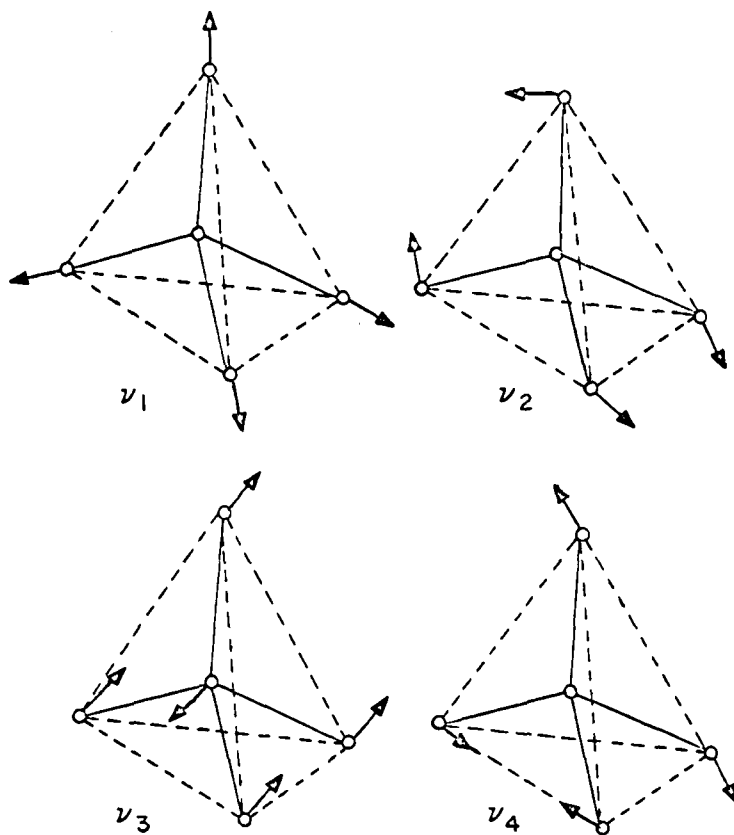


Fig. 20 Normal Vibrations of a Tetrahedral Spherical Top Molecule.

by the fact that the inactive fundamentals have frequencies sufficiently close to  $\nu_3$  and  $\nu_4$  that the rotational levels of the latter are subject to a Coriolis perturbation. This causes a splitting of the rotational lines which can produce very complicated band systems. Unfortunately for the planetary astronomer, the methane bands which occur in the easily accessible part of the spectrum of Jupiter are combination bands whose fine structure is very difficult to analyze. It is therefore not surprising that as yet no determinations of the mean atmospheric temperature of Jupiter have been made using these bands.

As was pointed out above, the  $3\nu_3$  overtone at  $11057 \text{ \AA}$  has a relatively simple, open structure which is susceptible to analysis. The basic theory required was developed by Wilson (1935) and Jahn (1938) and has been applied by Childs and Jahn (1939) to the laboratory spectrum of the fundamental  $\nu_4$  of methane. In the same paper the latter authors point out that their analysis also provides a remarkably good interpretation for the appearance of the  $3\nu_3$  band. They attribute this to the basic symmetry of the methane molecule and the fact that the resultant perturbation to which the rotational levels are subject is apparently no larger than that affecting the levels of the fundamental.

The Coriolis perturbation is actually negligible for our purposes since the resolution of the McDonald spectrograms is insufficient to show the splitting of the rotational lines. The problem is thus reduced to a prediction of the relative intensities of the R-branch lines as a function of temperature. The following discussion is based on the analysis of Childs and Jahn (1939) and the review by Herzberg (1945).

Since the molecule has spherical symmetry, any axis through the center serves as an axis of rotation. The energy associated with the various rotational levels of a spherical top can be expressed as

$$1) \quad F(J) = BJ(J+1)$$

where the rotational constant B is given by

$$2) \quad B = \frac{h}{8\pi^2 cI}$$

the moment of inertia I being the same for any set of three mutually orthogonal axes. To take account of non-rigidity the small correction term  $-DJ^2(J+1)^2$  may be added to (1). The fact that the molecule has such a high degree of symmetry means that in addition to a  $2J+1$ -fold space degeneracy, every rotational level of a given J has an additional  $2J+1$ -fold degeneracy. The first corresponds to the fact that the angular momentum vector  $\vec{J}$  may have  $2J+1$  orientations with respect to a fixed direction in space,



the second indicates that  $\bar{J}$  may have  $2J + 1$  orientations with respect to a fixed direction within the molecule. Hence the statistical weight of a given rotational level is  $(2J + 1)^2$ .

Up to this point we have not considered the effect of the spin of the nuclei. The total angular momentum of the system must consist of the sum of molecular rotation and nuclear spin. This means that the factor by which the space degeneracy is multiplied is no longer just  $2J + 1$ . For a tetrahedral molecule such as methane, there are three types or species of rotational levels denoted A, E, and F corresponding to no degeneracy, double degeneracy and triple degeneracy, respectively. Thinking in terms of the orientation of the nuclear spin vectors, A corresponds to all vectors parallel, total spin  $T = 2$  ( $C^{12}$  has spin  $I = 0$ ,  $H^1$  has  $I = 1/2$ ), E to two parallel, two anti-parallel,  $T = 0$ , and F to three parallel one anti-parallel,  $T = 1$ . The next step is a determination of the number of levels of species A, E, and F corresponding to a given  $J$  for the molecule under consideration. Using group theory, Wilson (1935) has deduced that in the case of  $XY_4$  molecules with  $I = 1/2$  (e.g.,  $CH_4$ ), the statistical weights of the A, E, and F levels are 5, 2, and 3 respectively. Thus the statistical weight for a given  $J$  may be written as  $5a + 2b + 3c$  where  $a$ ,  $b$ , and  $c$  are the number of rotational

levels of types A, E, and F, respectively. The total statistical weight is then simply  $(2J + 1)(5a + 2b + 3c)$ .

The intensity of the rotational lines will be proportional to the product of the statistical weight and the Boltzmann factor  $\exp - E/kT$  where  $E = F(J)hc$  is the energy of the  $J$ th level. Thus we may write (using Eq. (1) ):

$$3) \quad I_J \propto (2J + 1)(5a + 2b + 3c) \exp [-BJ(J + 1)hc/kT]$$

In this approximation we are assuming that there is an equal transition probability for all the lines in a band. This is actually not the case and the variation with  $J$  and  $\Delta J$  has been considered by Jahn (1938). He found that the proper value for the space degeneracy was as follows:

R branch ( $J' - J'' = + 1$ ),  $(2J + 3)$

Q branch ( $J' - J'' = 0$ ),  $(2J + 1)$

P branch ( $J' - J'' = -1$ ),  $(2J - 1)$

where  $J'$  denotes the  $J$  number in the upper stage,  $J''$  in the lower. Since we are only considering the R branch in the  $3\nu_3$  band, the complete expression for the intensity variation becomes

$$4) \quad I_J \propto (2J + 3)(5a + 2b + 3c) \exp [-BJ(J + 1)hc/kT].$$

The type and number of the rotational levels corresponding to the different values of  $J$  have been given by Childs and Jahn (1938). Thus the product  $(2J + 3)(5a + 2b + 3c)$  can be tabulated and relative values of  $I_J$  calculated for various temperatures using Equation 4.

With this information available, it should now be possible to derive a rotational temperature from the Jovian  $\text{CH}_4$  band. In principle it is only necessary to determine the relative intensities of the rotational lines and compare them with the theoretical values. In practice, this procedure is complicated by the fact that plate 1169 did not have a wavelength-dependent calibration at the time it was taken. The wavelength region under consideration occurs just at the "shoulder" of the sensitivity curve for the I-Z emulsion where one can anticipate that the value of gamma for the plate is changing rapidly with wavelength. Thus some kind of estimate of this variation of gamma is essential in order that meaningful intensities can be derived. Accordingly, several I-Z plates were hypersensitized independently and exposed to spectra of the Sun with the laboratory spectrograph. Development was also independent but an attempt was made to duplicate the conditions of development of the McDonald plate. Densitometer tracings of these spectra were made and HD curves were constructed for two of the plates at five different wavelengths covering the spectral region under study. The wavelengths were chosen with the help of the Mt. Wilson Atlas of the Solar Spectrum to ensure that they represented the true continuum. A plot could then be made of the variation of gamma with wavelength. While this variation was considerable, it repeated reasonably well

from plate to plate indicating that average values taken from this plot could be considered as reliable representations of I-Z characteristics within the associated error.

A further problem results from the presence of the overlapping fine structure lines from the  $\nu_1 + 2\nu_3$  band discussed above. A laboratory plate obtained at a higher resolution than plate 1169 indicated that the  $J = 0, 1, 2$  and  $J > 6$  lines of  $3\nu_3$  would all be blended with lines from the other band (Fig. 18). Hence the determination must be made from the relative intensities of the  $J = 3, 4, 5$ , and 6 lines. The profiles of even these lines are distorted by the close proximity of the  $\nu_1 + 2\nu_3$  lines, however, so it was necessary to measure line strengths  $(1 - I_L/I_C$  at the line centers) rather than the equivalent widths. As was stated previously, the Jovian spectrogram was obtained on a cold night when the telluric water vapor absorptions were exceptionally weak. There is no evidence in the densitometer tracings of blending with water vapor lines or even for the presence of such lines in parts of the continuum undisturbed by the  $\text{CH}_4$  absorptions. Hence it appears safe to neglect them in determining the intensities.

As a check on the general procedure, two laboratory spectrograms were reduced using the gammas derived in the manner outlined above. The calibration plates were obtained from a different shipment than the plates used for the

laboratory spectrograms and thus should not have characteristics more typical of the latter than of plate 1169 (unless long-term variations in the manufacture of the I-Z emulsion have occurred).

The laboratory spectra chosen for analysis were obtained at room temperature ( $\sim 295^\circ\text{K}$ ) and at a temperature somewhat higher than that assumed by a dry ice-alcohol mixture ( $\sim 210^\circ\text{K}$ ). In both cases the laboratory resolution was roughly equivalent to that of the McDonald plates. The results are shown in Figures 21 and 22 which give schematic representations of the  $J = 3, 4, 5$ , and 6 lines normalized to  $I_4 = 8.0$  for the two spectra. For comparison, theoretical intensities of the lines in this band are shown in the same figures. It is apparent that while the agreement is not perfect, it is sufficiently good to allow considerable confidence to be placed in the technique. In particular, attention is called to the striking decrease in relative intensity exhibited by  $J = 6$  with the decline in temperature represented in going from Figure 21 to Figure 22. A slight increase in the relative intensity of  $J = 3$  also occurs in this temperature range. Examining these diagrams more closely, the relative intensities of  $I_6$  and  $I_3$  in Figure 21 suggest that the laboratory temperature was significantly lower than  $295^\circ\text{K}$ , while in Figure 22 it is apparent that the intensities of these same lines in the low temperature

Fig. 21 Normalized Intensities of Rotational Lines of the  $3\nu_3$  Band of  $\text{CH}_4$ :  
A Comparison of Theoretical and Laboratory Intensities at  $T = 295^\circ\text{K}$ .

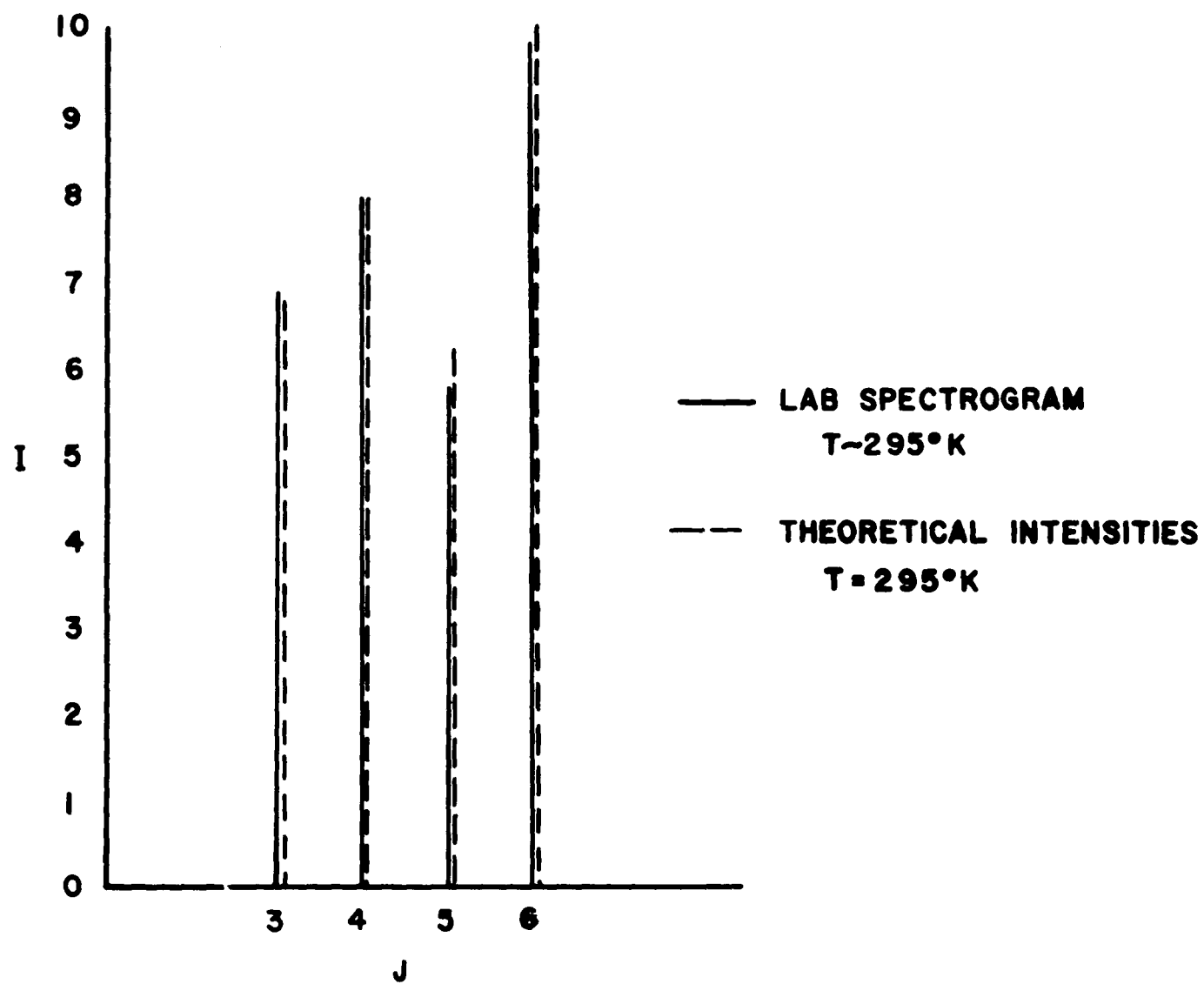
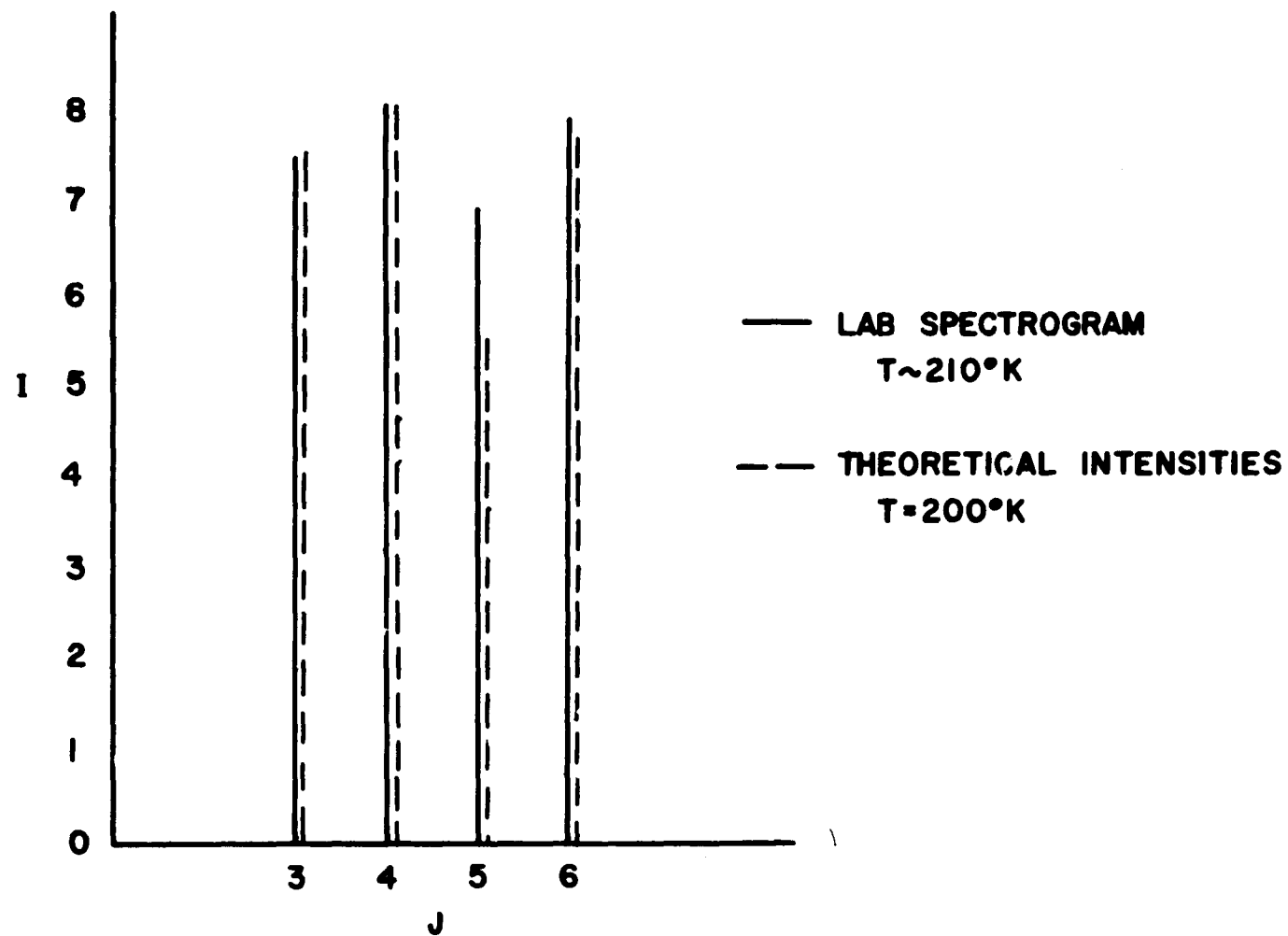


Fig. 22 Normalized Intensities of Rotational Lines of the  $3\nu_3$  Band of  $\text{CH}_4$ :  
A Comparison of Laboratory Intensities at  $T \sim 210^\circ\text{K}$  with Theoretical  
Intensities at  $T = 200^\circ\text{K}$ .

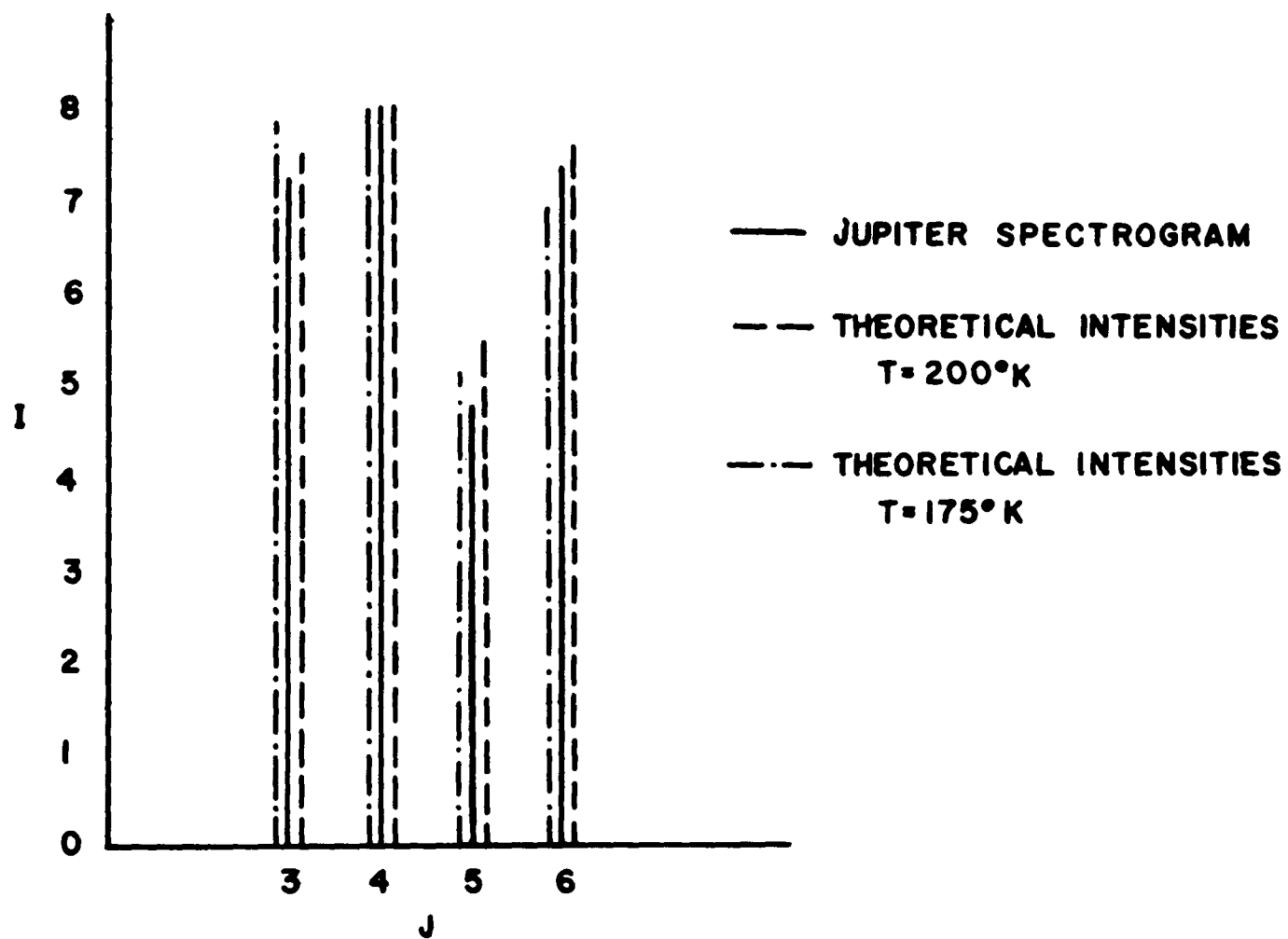




laboratory spectrum imply that in this case the gas had a temperature which was slightly higher than 200°K. While the former conclusion seems unlikely to be correct, the latter is in agreement with the conditions of the experiment. Thus the reliability of the method appears to be about  $\pm 15^\circ\text{K}$  simply on the basis of these two measurements. The anomalously high intensity of  $J = 5$  in Figure 22 has not been accounted for but is not a critical factor in the temperature determination.

Figure 23 gives the same representation for Jupiter. The theoretical intensities for 200°K and 175°K are included for comparison. Again the match with theory is not as good as one would like but it is evident that the Jovian temperature has a value near 200°K. At this temperature, the theoretical intensity of  $J(6)$  is slightly greater than that of  $J(3)$ ; at  $T = 175^\circ\text{K}$ , the intensities are emphatically reversed. In the spectrum of Jupiter the two lines have relative intensities similar to the theoretically predicted values for the higher temperature although both lines are weaker with respect to  $J(4)$  than theory would predict. It is perhaps worthwhile to point out explicitly that in order for the temperature to be substantially lower,  $I_6$  would have to be much less and  $I_3$  greater. In other words, the intensities of both lines must change and in opposite ways.

Fig. 23 Normalized Intensities of Rotational Lines of the  $3\nu_3$  Band of  $\text{CH}_4$ :  
A Comparison of Intensities in the Spectrum of Jupiter with  
Theoretical Intensities at  $T = 200^\circ\text{K}$  and  $T = 175^\circ\text{K}$ .



This temperature is decidedly higher than that which would be deduced from the absence of the 10291 Å methane line referred to earlier, suggesting that the latter anomaly is due to other than temperature induced causes. However, one is left with some doubt as to the accuracy of intensity measures obtained from this plate. Such considerations plus the uncertainties in the calibration procedure and the actual measurements of the intensities suggest that the error associated with this determination is of the order of 10%. Thus the temperature derived from the  $3\nu_3$  band of  $\text{CH}_4$  may be expressed as

$$T = 200 \pm 25^\circ\text{K} .$$

### Discussion of Results

#### a) Abundances

The abundance limits given in Section 3 are based on a simple model atmosphere in which the absorbing gas is assumed to lie above a reflecting layer and to contain no scattering particles. There is considerable observational evidence, however, which favors a model in which the gas is contaminated by a haze of particles producing multiple scattering. Under these conditions, the intensities of rotational lines should be proportional to the square root of the number of molecules in a given rotational state rather than directly proportional as would be the case for

the "clear gas" model (van de Hulst 1952, Chamberlain and Kuiper 1956, also see Appendix A). The effect of this square-root dependence would be to even out the differences in intensity, i.e., the theoretical intensities would all be raised slightly relative to  $I_4$ . This would increase the present discrepancy between the observed and theoretical intensities. Thus the simplified model appears to give a better fit to the results reported here and it becomes necessary to attempt to explain the observations suggesting a haze-layer model in other ways.

These observations are basically of three types: photographs at different wavelengths, polarimetry, and center-to-limb variations in the strength of absorption lines. Perhaps the best examples of the first of these are the Palomar Telescope photographs presented by Humason (1960). Plates 13 and 14 of this reference are particularly striking in showing the great increase in detail which appears on the plate taken in red light compared to that in blue. There is no doubt that an atmospheric haze is present which is more deeply penetrated in red light. The polarization observations are similarly strongly suggestive of the presence of a haze in that the polarization starts out negative as the phase angle increases from  $0^\circ$  (Dollfus 1961). It must be remembered that these observations are limited to visual light, however, while the region of the

spectrum examined in this discussion lies far out in the infrared. The photography suggests that the haze is relatively well penetrated at  $.65\mu$ ; at  $1.1\mu$  we are probably looking still deeper into the atmosphere and the particles indicated by both of the above techniques may play an insignificant role in the process of line formation here.

This brings us to the spectroscopic results. Squires (1957) has shown that the observations of Hess (1953) which indicated a decrease in the strength of  $\text{CH}_4$  and  $\text{NH}_3$  absorptions from center to limb could be better explained from a meteorological standpoint by a model in which the cloud layer exhibited considerable vertical structure than by a change in the mean height of the cloud layer or by the presence of a thick haze. Hess' observations have been confirmed by Münch and Younkin (1964) who also favor Squires' interpretation.

It thus seems safe to conclude that the simple "clear gas" model will be an adequate first approximation for the determination of upper limits to abundances in this part of the spectrum. It is also apparent that the Jovian cloud structure is probably more complex than has been generally assumed and may consist of several layers of different morphological cloud types containing particles of different sizes. Such configurations are frequently

encountered in terrestrial meteorology. The fact that the temperature derived in the present paper is slightly above the melting point of ammonia ( $195.5^{\circ}\text{K}$  at 1 atm) supports these ideas by suggesting the presence of droplet clouds (e.g., cumuli) in the lower levels of the atmosphere.

#### b) Temperature

A summary of modern measurements of Jovian temperatures is given in Table 11 which is based in part on a similar table published by Mayer (1961) (cp. Table 1). It is evident that there is a rather wide range of values and that the temperature derived in the present paper is at the upper end of this range. However, a closer look at these measurements indicates that they are consistent with present knowledge about the wavelength dependence of the atmospheric absorption coefficient and the composition of the atmosphere. It is probably premature at this point to derive a detailed model atmosphere but this general consistency can be described.

Beginning with the shorter wavelengths, the temperatures determined from the hydrogen quadrupole lines are unreliable for two reasons. The narrowness of the lines makes it extremely difficult to determine the equivalent widths precisely. Even if this were possible, however, the work of Foltz and Rank (1963) referred to earlier suggests that these lines are strongly saturated in which case they



Table 11

## JOVIAN TEMPERATURE MEASUREMENTS (b)

Temp. (°K)	Wave- length	Method	Identification and Central Wavelength of Relevant Absorber	Reference
170	.83 $\mu$	Analysis of (3,0) H <sub>2</sub> Quadrupole Lines	H <sub>2</sub> , S(0)-.83 $\mu$	Zabriskie 1962
120	.83 $\mu$	Analysis of (3,0) H <sub>2</sub> Quadrupole Lines	H <sub>2</sub> , S(0)-.83 $\mu$	Spinrad 1964
128 $\pm$ 2.3	9-13 $\mu$	Germanium Bolometer	NH <sub>3</sub> 10.5 $\mu$	Murray & Wildey 1963
144 $\pm$ 23	8.35 mm	Microwave Radiometer	NH <sub>3</sub> 1.28 cm	Thornton & Welch 1963
140 $\pm$ 38	3.15 cm	Microwave Radiometer	NH <sub>3</sub> 1.28 cm	Mayer et al. 1958a and b
145 $\pm$ 18	3.15 cm	Microwave Radiometer	NH <sub>3</sub> 1.28 cm	Mayer et al. 1958a and b
171 $\pm$ 20	3.03 cm	Microwave Radiometer	NH <sub>3</sub> 1.28 cm	Giordmaine et al. 1959
173 $\pm$ 20	3.17 cm	Microwave Radiometer	NH <sub>3</sub> 1.28 cm	Giordmaine et al. 1959
193 $\pm$ 16	3.3 cm	Microwave Radiometer	NH <sub>3</sub> 1.28 cm	Bibinova et al. 1962

Table 11 (Continued)

Temp. (°K)	Wave- length	Method	Identification and Central Wavelength of Relevant Absorber	Reference
189+20	3.36 cm	Microwave Radiometer	NH <sub>3</sub> 1.28 cm	Giordmaine et al. 1959
200	3.75 cm	Microwave Radiometer	NH <sub>3</sub> 1.28 cm	Drake & Ewen 1958

can't be used for a simple temperature analysis. Thus the disagreement between the two determinations is understandable and reflects the uncertainty in the data and the method. It seems advisable to assign these determinations relatively low weight.

In the 9-13 $\mu$  region, the atmospheric opacity is determined by ammonia which has a double fundamental ( $\nu_2$ ) centered at 931.6  $\text{cm}^{-1}$  and 968.1  $\text{cm}^{-1}$ . As Kuiper (1952) has pointed out, the presence of this strong ammonia band means that temperatures obtained in this region of the spectrum must refer to a level well above the cloud layer. This results from the fact that 1 cm atm of ammonia is opaque at these wavelengths while the weaker bands reveal an abundance of roughly 7 m atm of this gas in the Jovian atmosphere. In other words, at some wavelengths outside this region the light reflected by the planet has reached much lower levels of the atmosphere.

In the microwave region, the dominant absorber is again ammonia which has a strong inversion transition at 1.28 cm. This absorption will be pressure-broadened in the Jovian atmosphere and has an intrinsically unsymmetrical profile, rising steeply on the shortwave side, reaching its maximum and then tapering off gradually toward longer wavelengths (Cleeton and Williams 1934). One would therefore expect that observations of the planet should show

increasing temperatures with increasing wavelength separation from the absorption maximum. The values given in Table 11 appear to confirm this expectation in a qualitative way and are distinctly higher as a group than the 9-13 $\mu$  measures. At longer wavelengths the spectrum is dominated by non-thermal radiation; it is generally assumed that the latter makes a negligible contribution at 3 cm.

In a more recent discussion of their microwave results, Alsop and Giordmaine (1961) suggest that some of the variability in their measurements may be related to visible activity on the surface of the planet. Thus an anomalously high value of temperature ( $268^{\circ} \pm 14^{\circ}\text{K}$ ) was derived from observations made on May 1, 1958 shortly after an outbreak of activity in the South Equatorial Belt when the disturbed region was in full view. In addition, the authors note that their entire series of measurements was made within four months of the outbreak and led to an average temperature of  $177^{\circ}\text{K}$  as compared with  $145^{\circ}\text{K}$  derived by Mayer the preceding year (1957). While stating that it is impossible to say with certainty that their average temperature is definitely higher than Mayer's, they add that the suggestion is an obvious one and that the problem should be pursued.

One thus gains a definite impression of rising temperatures with increasing penetration into the atmosphere

and there appears to be a definite possibility of both long- and short-term variations. There is one other piece of evidence which is strongly indicative of a warm lower atmosphere. Murray, Wildey, and Westphal (1963) observed a large increase in radiation inside the shadows of satellites II and III in transit across the disk of the planet as compared to the general background. This increase corresponds to a temperature of 190°K or 160°K depending on whether it is interpreted as coming just from the umbra or the penumbra as well. The authors tentatively suggest that the high temperatures are either due to an upwelling of warmer gas from lower layers as a result of an induced instability or an actual decrease in atmospheric opacity within the shadows, allowing the radiometer to "see" to lower warmer levels. In either case these remarkable observations present strong evidence for relatively high temperatures at levels below the normal penetration depth of  $10\mu$  radiation.

From the standpoint of current atmospheric models, we are again led to favor the more complex picture of the cloud layer offered by Squires (1957). In this model, the cloud layer is characterized as cumuliiform with the tops of the cumuli reaching 20-30 km above the main cloud deck. Squires notes that if the ammonia vapor in the space between the cumulus towers is well below saturation and the

towers themselves shield the main deck, the temperature of the latter may be as high as  $230^{\circ}\text{K}$ .

It must be kept in mind that numbers such as this last one are strongly dependent on the spectroscopically determined abundance of ammonia which is not a precise quantity and is probably variable with time and with position on the disk (Kuiper 1952, Hess 1953). Thus ideally one would like to have spectroscopic observations in several wavelength regions and several positions on the disk all obtained on the same night. It would then be possible to construct a consistent model for conditions at that time. At present we only wish to suggest that there appears to be good observational evidence for temperatures of  $175^{\circ}\text{K}$  and higher in the Jovian atmosphere above the main cloud layer and that such temperatures are compatible with an existing model for the cloud deck. Attention is again called to the fact that the temperature derived in this paper is based on intensities at  $1.1\mu$ , a wavelength at which the Jovian atmosphere should be relatively transparent to incident solar radiation. Thus the effective absorbing layer for these lines will be much lower than (say) the  $130^{\circ}\text{K}$  level determined by the  $\nu_2$  band of  $\text{NH}_3$  at  $10.5\mu$ . It is hoped that future observations of the  $3\nu_3$  methane lines with higher angular and spectral resolution will allow a more precise determination of Jovian temperature and its variation over the disk at this wavelength.

## 5. LOW-DISPERSION INFRARED SPECTRA OF JUPITER, SATURN, IO AND GANYMEDE

### Introduction

Low-dispersion infrared spectra of Saturn, Jupiter, and the Galilean satellites of Jupiter have been published by Kuiper (1952). The spectra of the two planets were obtained on M plates and thus are cut off near  $10,000 \text{ \AA}$  by the decrease in plate sensitivity. Subsequent to this publication, Kuiper has obtained additional spectra of Jupiter at higher resolution covering the range of  $8800 - 11200 \text{ \AA}$ . These plates have been analyzed in Sections 4.3 and 4.4 and constitute the standards for the present work. It was felt that since the Jovian spectrum was relatively well understood in this region, it would be interesting to compare low-dispersion spectra of Jupiter and Saturn to see if the latter showed any new detail.

The spectra of the Galilean satellites obtained by Kuiper were recorded on N plates which have a long-wave cut-off near  $8800 \text{ \AA}$ . On the basis of these spectra, Kuiper was able to set a limit of 200 cm atm on the abundance of  $\text{CH}_4$  in possible atmospheres of these bodies. Since  $8800 \text{ \AA}$  is just at the beginning of a very strong methane band, it seemed

worthwhile to attempt to record the spectra of the satellites on M plates which would allow this band to be completely bracketed.

Both of these projects were carried out at the Kitt Peak Observatory with the Cassegrain spectrograph of the 36" reflector. Details of the exposures are given in Table 12. Instrumental difficulties prevented the completion of the satellite program but it is hoped that this can be pursued during the next opposition of Jupiter.

### The Observations

#### a) Jupiter and Saturn

A comparison of M-plate spectra of Jupiter and Saturn is presented in Figure 24. These spectra show the customary telluric features:  $O_2$  at 7600 Å,  $H_2O$  at 8200 Å, 9150 Å, 9350 Å, and beyond to the plate limit where methane absorptions are dominant. It is easy to distinguish the planetary absorptions in the Saturn spectra by their absence from the spectra of the rings. The principal methane bands occur at 7840 Å, 8414 Å, 8606 Å, 8873 Å, and 9706 Å. The continuation of the spectra of the rings beyond the cut-off of the ball at long wavelengths is an indication of the presence of a strong methane band system in this region. Reference is made to Figures 14-16 for spectra of Jupiter and methane in this spectral region obtained at



Table 12

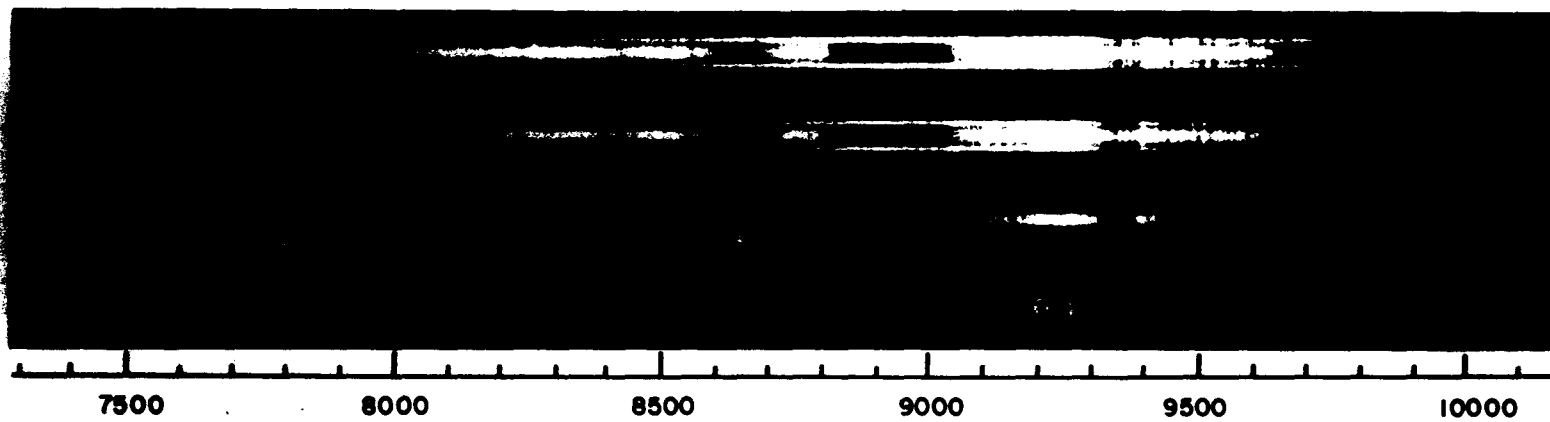
LOW DISPERSION SPECTRA OBTAINED AT  
THE KITT PEAK OBSERVATORY

Plate No.	Subject	Exposure	Emulsion	Date
A-853	Saturn	5m	I-Mh	9/5-6/64
	Saturn	10	I-Mh	9/5-6/64
	Saturn	20	I-Mh	9/5-6/64
A-855	Io	119	I-Mh	9/5-6/64
	Ganymede	90	I-Mh	9/5-6/64
	Jupiter	8	I-Mh	9/5-6/64
A-856	Saturn	90	I-Zh	9/19-20/64
A-857	Jupiter	2	I-Mh	9/19-20/64
A-984	Jupiter	45	I-Zh	12/2-3/64

Fig. 24 Spectra of Jupiter and Saturn (three exposures) on I-M Emulsions, 7300 Å  
to 9900 Å.

SATURN

JUPITER



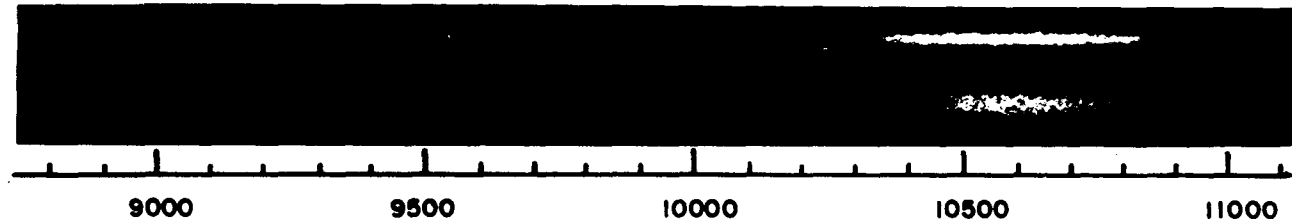
higher dispersion. The secondary features at the long wavelength end of the spectrum at 9660 Å and 9830 Å are apparently due to blends of strong methane "lines". The reflectivity of the ring appears to be slightly less than that of the ball throughout this region.

Spectra of Jupiter and Saturn obtained on I-Z plates are compared in Figure 25. These spectra are of rather poor quality and only permit gross features to be identified. The broad absorption system extending roughly from 9700 - 10400 Å is due to methane and its appearance in the Jovian spectrum at higher dispersion has been described in some detail in Section 4.4. It is doubtful that ammonia contributes to this system in the spectrum of Saturn as it does in Jupiter since the presence of this gas in the atmosphere of Saturn now appears doubtful (Munch and Spinrad 1964, cp. Section 4.2). The only other feature of interest is the low reflectivity of the ring in the region 10400 - 10900 Å, first pointed out by Fredrick (1963). In this wavelength region, the sensitivity of the I-Z emulsion rises to its maximum and then drops steeply toward longer wavelengths. This behavior is well illustrated by the spectra of Jupiter and the disk of Saturn, but the ring exhibits a nearly uniform brightness across the plate indicating a definite drop in reflectivity in the region referred to.

Fig. 25 Spectra of Jupiter and Saturn on I-Z Emulsions, 8800 Å to 11000 Å.

SATURN

JUPITER



Kuiper (1952) has suggested that the particles making up the ring are covered by frost (if not composed of ice) on the basis of their low reflectivity near  $1.5\mu$ . To test whether this deduction might also explain the present observation, reflection spectra of  $H_2O$  ice,  $CO_2$  ice, and  $H_2O$  ice crystals were obtained in the laboratory, at a resolution comparable to that of the planetary spectra. The ice crystals were formed in a thin layer on a metal plate cooled by a piece of "dry ice", while blocks of the two ices were used for the other comparisons. In each case, a comparison spectrum of sunlight reflected from a layer of  $MgO$  deposited on a metal plate was obtained on the same plate as the spectrum of sunlight reflected from the sample under investigation. An effort was made to keep the densities of the two spectra as equal as possible in the "neutral" region ( $\lambda < 10,000 \text{ \AA}$ ). The author is indebted to Mr. J. V. Marshall for his valuable assistance in obtaining these spectra.

Reproductions of the three sets of spectra obtained by this method are presented in Figure 26 at a slightly smaller scale than the spectra of Figure 25. The telluric features referred to earlier are quite prominent. It is readily apparent from inspection of this illustration that the reflection spectrum from the ice block (C) gives the best match to the absorption observed in Saturn's ring (the

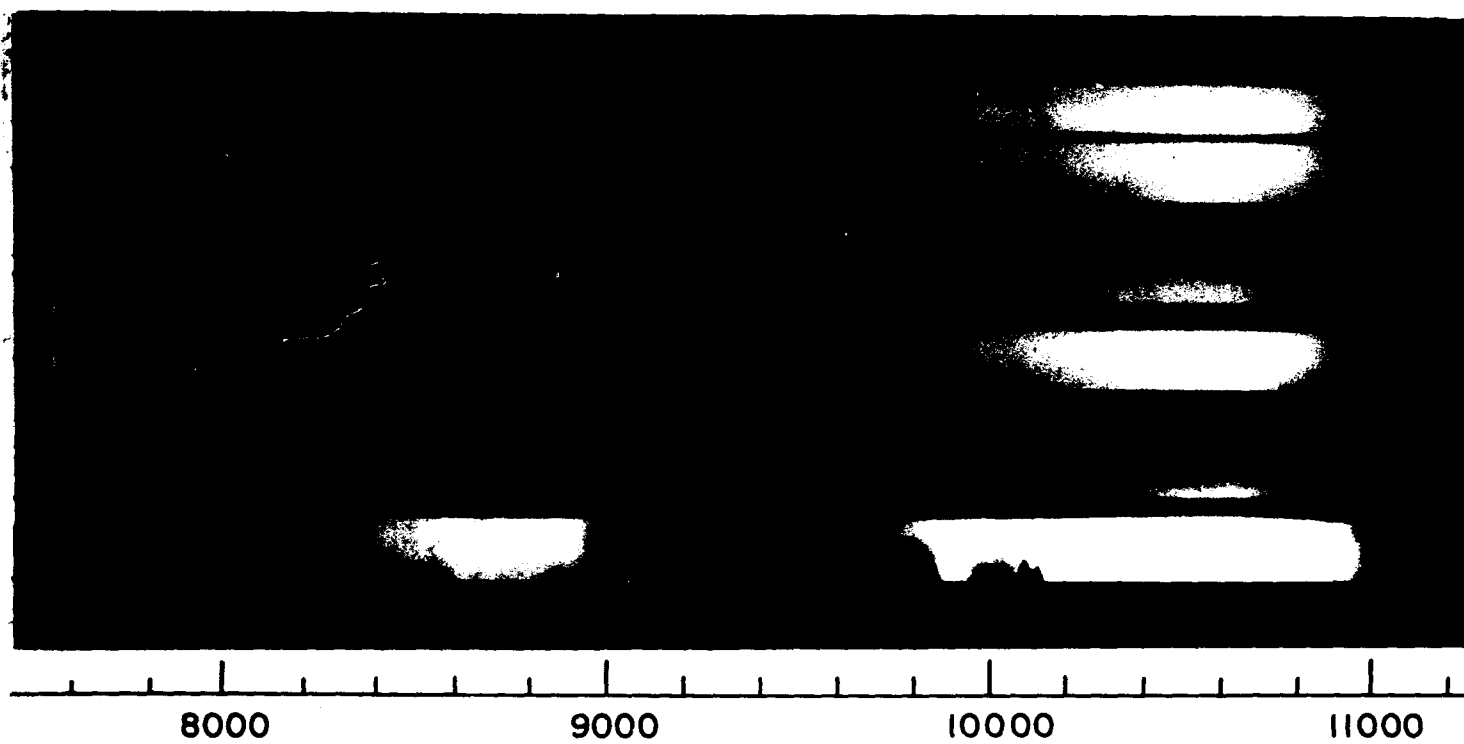
Fig. 26 Laboratory Spectra for Comparison with Plate II. These are Pairs of Spectra of Sunlight Reflected by a Layer of MgO (lower, wider spectrum in each case) and an Ice (upper, narrower spectrum) as follows: A) CO<sub>2</sub> Ice Block, B) H<sub>2</sub>O Ice Crystals, C) H<sub>2</sub>O Ice Block.



**A**

**B**

**C**



irregular features in the MgO comparison at 9800 Å and 10000 Å are due to hypersensitizing). A slight weakening is noticeable in the appropriate region of the spectrum from the ice crystals while the CO<sub>2</sub> block gives an essentially neutral spectrum. Densitometer tracings bear out these conclusions. The spectrum from the ice block is somewhat weaker than the comparison spectrum from MgO in the neutral region. Thus one would anticipate (assuming no absorption) that the ratio of the densities at 10600 Å and 8900 Å would be higher for the ice block spectrum than for that from MgO, since the latter is closer to saturation. In fact the reverse is true. The ratio for MgO is a factor 1.5 greater than that for the ice block. In the case of the other two pairs of spectra, these ratios are very nearly equal. Thus Kuiper's original conclusion is substantiated by these results. The observation of a second absorption at the correct wavelength makes it virtually certain that the absorbing substance associated with the ring particles is indeed water ice. The fact that the ice block gives a better match than the ice crystals simply indicates that the light path in the latter was insufficient, i.e., the layer of crystals was too thin. Spectra of the ring obtained at about the same dispersion but at a larger scale should permit an accurate photometric comparison with laboratory spectra to determine a water cell equivalent for the ice

absorption. This, in turn, could be used to give a minimum thickness for the particles making up the ring assuming they were composed entirely of ice and occurred in a single-particle layer.

b) Io and Ganymede

Kuiper (1952) has developed an order for the probability of retention of an atmosphere for the major planets and satellites of the solar system. This order is based on Jeans' criterion for atmospheric stability over periods of time comparable to the age of the solar system, viz:

$$V_m < 0.2 V_{esc}$$

where  $V_m$  is the root mean square velocity of the molecules and  $V_{esc}$  is the escape velocity for the planet or satellite. Since  $V_m \propto T^{1/2}$  and  $T \propto (1-A)^{1/4} r^{-1/2}$  where  $A$  is the albedo and  $r$  is the distance to the Sun, the various bodies may be ordered according to their values of  $V_{esc} (1-A)^{-1/8} r^{1/4}$  which is what Kuiper has done. On this basis, using the new values of albedo tabulated by Kuiper (1964) we find the following order for Titan and the Galilean satellites: Titan, JIII, JI, JII, JIV. This is identical with Kuiper's original listing except for the interchange of JII and JIV. Titan is known to have an atmosphere. Thus JIII and JI (Ganymede and Io) are logical first choices in this program.

It must be borne in mind that this ordering is only a first approximation, however, since heating of an exosphere by photochemical effects has been ignored. Without this refinement the likelihood of atmosphere-retention varies so little for the four satellites that all of them should be examined.

Figure 27 contains reproductions of M-plate spectra of Io, Ganymede and Jupiter. One spectrum of Jupiter was deliberately over-exposed to show the appearance of the strongest member of the  $8873 \text{ \AA}$  methane band at this dispersion (and temperature). It is clearly absent from the spectra of the two satellites although the quality of the latter could be improved slightly even at this dispersion. (The spectrum of Io is terminated on the short wavelength side by a hypersensitizing defect.) A comparison of these spectra with laboratory spectra of methane obtained at approximately the same resolution indicates that there must be less than 4 m atm of this gas in the optical path intercepted by the slit of the spectrograph. Since the latter passed nearly the entire disks of both satellites, the effective air mass was about four (no limb darkening) and thus the abundance of methane in possible atmospheres of these objects is less than 100 cm atm.

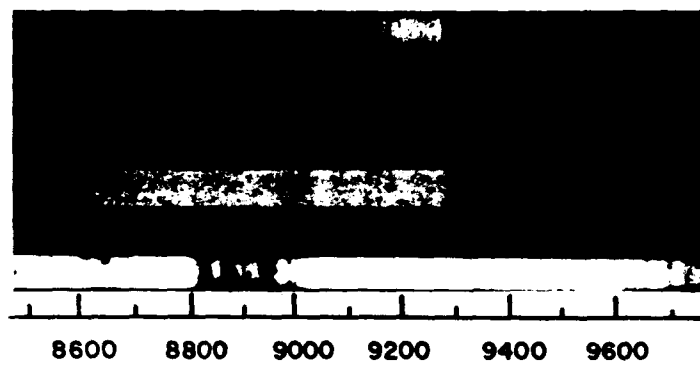
Fig. 27 Spectra of Jupiter and Satellites Io (JI) and Ganymede (JIII) on I-M Emulsions, 8500 Å to 9700 Å. The Lower Spectrum of Jupiter is Deliberately Overexposed to Show Details of 8873 Å Methane Band.

JUPITER

J III

J I

JUPITER



## 6. A DETERMINATION OF THE MARTIAN CO<sub>2</sub> ABUNDANCE

### Introduction

In two papers published elsewhere (Kuiper 1964, Owen and Kuiper 1964) new spectra of the planet Mars in the 1.0 - 2.5 $\mu$  region obtained by Kuiper and their laboratory calibration with a long absorption tube have been presented. This calibration leads to a relationship between total atmospheric pressure and CO<sub>2</sub> abundance. Before the atmospheric pressure (and, by inference, an approximate composition) can be found, independent data on the Martian CO<sub>2</sub> abundance are required. The best source of this information at present is the Martian 8689 Å CO<sub>2</sub> band observed by Kaplan, Münch, and Spinrad (1964) (referred to hereafter as KMS). These authors themselves calibrated this CO<sub>2</sub> band from laboratory observations supplied by Rank, but because of the peculiar role played in this band by the effects of blending by solar Fraunhofer lines it appeared important to recalibrate the spectrum in such a manner that the effects of solar blending would be accurately allowed for. The interest in the 8689 Å band stems from the fact that the lines in this band are very weak so there is almost no saturation. Thus they are on the linear part of the curve of growth and their intensities are directly proportional to the abundance.

After calculating the effective air mass corresponding to the Martian observation and making slight corrections for collisional broadening and saturation effects due to the narrowness of the lines, KMS derived a value of  $55 \pm 20$  m atm for the  $\text{CO}_2$  abundance. This value corresponds to an assumed temperature of  $230^\circ\text{K}$  in the Martian atmosphere. For  $200^\circ\text{K}$ , the corresponding value was  $50 \pm 20$  m atm. The principal reason cited for the large probable error associated with these values was the difficulty in determining the equivalent widths of the weak  $\text{CO}_2$  lines.

The new calibration of the Mt. Wilson spectrogram was done in two steps. A preliminary calibration was made prior to the completion of our high-dispersion laboratory spectrograph by means of observations of the  $8689 \text{ \AA}$  band of  $\text{CO}_2$  in the solar spectrum at sunrise. When the spectrograph was finished, laboratory spectra of  $\text{CO}_2$  were obtained from which a more precise value for the Martian abundance could be derived. For the sake of completeness and because of the intrinsic interest in the solar observation, both of these techniques are described below.

#### Observations and Experimental Procedure

The observations of the Sun were made with the McMath Solar Telescope of the Kitt Peak National Observatory. The 30-foot spectrograph employed with this



instrument gives a dispersion of  $1 \text{ \AA/mm}$  when the grating is used in the first order (blaze at  $8000 \text{ \AA}$ ). The solar spectrum was obtained by setting up the image of the eastern horizon on the spectrograph with the slit oriented parallel to the horizon and just above it, slightly southwest of the sunrise point. The Sun was allowed to drift past the slit during the course of the exposure, which was made at a fixed zenith angle. The heliostat was then moved to position the slit ahead of the Sun and the procedure was repeated. In this way a series of exposures corresponding to decreasing values of zenith angle could be obtained within a few minutes while conditions were optimum.

The laboratory work was carried out with the help of the 72-foot multiple path absorption tube described in Section 3.1. The aim of the program was the acquisition of a series of spectra of different amounts of  $\text{CO}_2$  that could be compared directly with the Mt. Wilson spectrogram of Mars. To achieve this end, spectra were obtained at a range of pressures between 10 and 20 cm Hg and a corresponding range of path lengths using the Sun as a light source. The laboratory spectrograph is of the Czerny-Turner type and has a 10-foot focal length. A 600 line/mm grating blazed at  $1.6\mu$  was used in the second order to produce a dispersion of  $2.5 \text{ \AA/mm}$ . This configuration matched the resolution of the Mt. Wilson spectrogram rather well when the slit was opened

to  $100\mu$ . As a final precaution, hypersensitized IV-N, the type of emulsion that recorded the spectrum of Mars, was employed for the laboratory work.

### The Martian $\text{CO}_2$ Abundance

#### a) The Solar Observations

The most suitable solar spectra for the present purpose were obtained on November 12, 1963. A reproduction of the spectrum corresponding to the largest zenith angle is given in Figure 28 together with a comparison spectrum taken with the Sun two hours past the meridian. These spectra indicate one of the problems encountered in the calibration of the intensities of the Martian  $\text{CO}_2$  lines by revealing the large number of faint solar lines which occur in this spectral region. Nevertheless, the interval between the two lines at  $8689.79 \text{ \AA}$  and  $8692.34 \text{ \AA}$  is clear, and on the spectrum obtained with the Sun at the horizon, the  $J = 8, 10, \text{ and } 12$  lines of the R branch of the  $5\nu_3$  band of  $\text{CO}_2$  are faintly visible. The presence of R(4) is revealed by the enhancement of the solar line at  $8693.15 \text{ \AA}$ . The many weak solar absorptions in this region essentially exclude the P branch lines of the  $\text{CO}_2$  band from consideration in the abundance determination. A comparison of these spectra with the spectrum of Mars reproduced in Figure 29 reveals that the resolution of the former is considerably higher (the

Fig. 28 Spectra of the Sun Obtained at Two Zenith Angles ( $z$ ) to Show the Presence of Telluric CO<sub>2</sub> Absorptions with a Large Air Mass.

CO<sub>2</sub> — 5V<sub>3</sub>

10 6 2

LOW SUN

$z = 89^\circ 57'$

HIGH SUN

$z = 32^\circ 30'$

8680 8690 8700 8710 8720 8730 8740 8750 8760

group of lines at  $8680 \text{ \AA}$  is a good indicator). It is evident that the telluric  $\text{CO}_2$  lines are considerably weaker than those in the spectrum of Mars, even at this large zenith angle. This difference is easily seen by comparing the intensity of R(10) with the solar lines at  $8682.99 \text{ \AA}$  and  $8728.60 \text{ \AA}$  on each spectrum. From such a comparison it is possible to estimate that the telluric lines are weaker by a factor of about 4. This indicates that at normal air paths the Martian  $\text{CO}_2$  lines will be roughly 100 times stronger than the telluric equivalents. Thus there should be no problem due to blending with the telluric features.

To proceed from these observations to a rough estimate of the Martian  $\text{CO}_2$  abundance, it is necessary to know the air mass through which the observations were made. For such large zenith angles it is no longer possible to use the customary approximations employed in calculating air masses for use in photometric extinction determinations. Instead, a graphical interpolation method was employed based on data tabulated by Allen (1963). The zenith angles were computed from readings of the setting circles and verified by calculation of the position of the center of the Sun's disk from the recorded times (correcting for refraction). The air mass was then read from a plot of zenith angle vs air mass constructed from Allen's data and corrected for the local temperature and pressure. This led to a value of  $30 \pm 3$  air

masses which corresponds to roughly 66 m atm of  $\text{CO}_2$ . Thus the Martian  $\text{CO}_2$  lines would require about 264 m atm or roughly 73 m atm of  $\text{CO}_2$  in the atmosphere of Mars when account is taken of the geometry of the Mars observation (see below). This admittedly crude determination served to verify the result of KMS to the extent that it supports the requirement for a larger amount of Martian  $\text{CO}_2$  than previously expected.

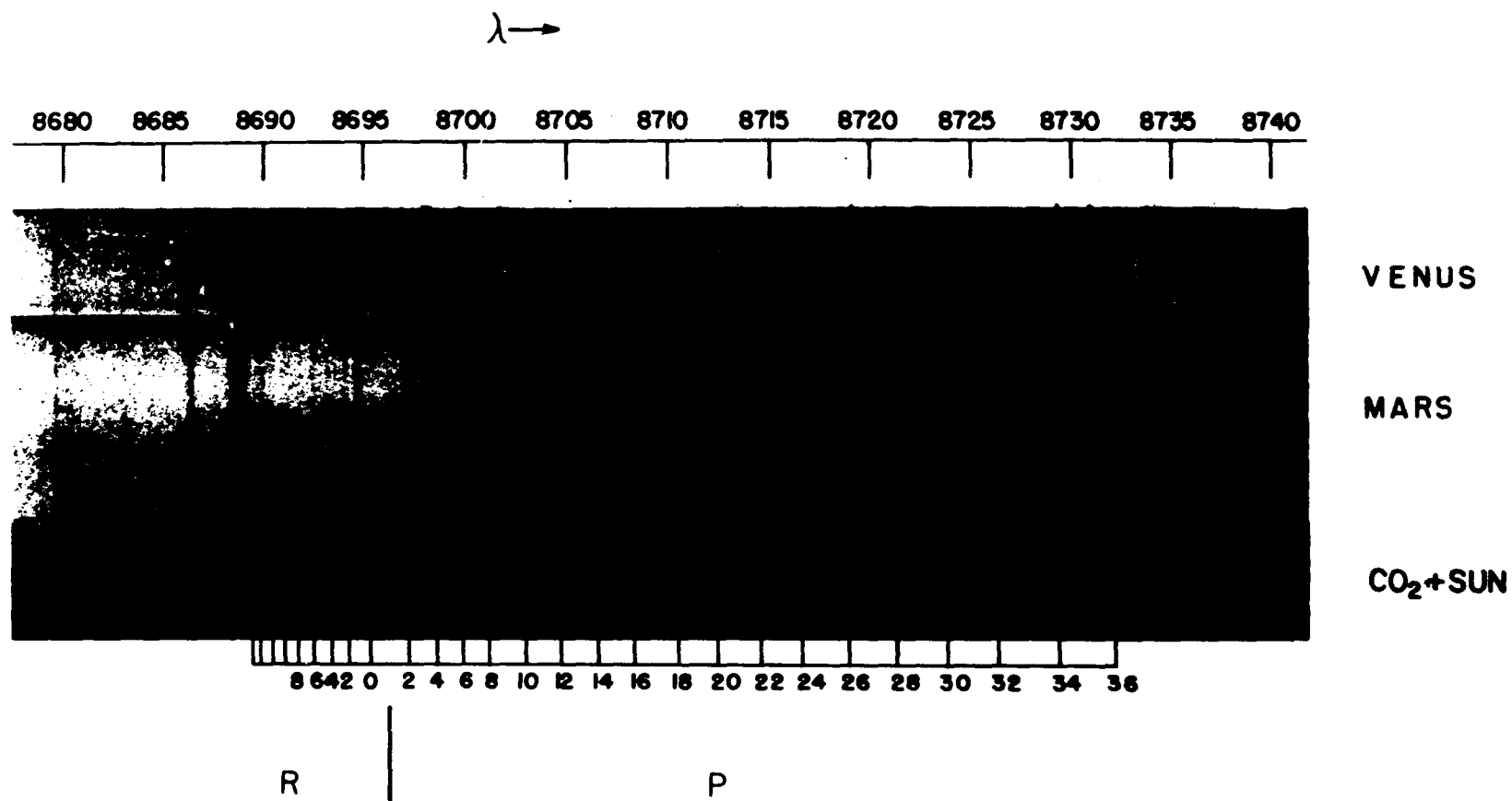
b) The Laboratory Calibration

Having a rough idea of the amount of gas needed to reproduce the Martian line intensities, a series of spectra was obtained in the laboratory with a range in equivalent path length from 85 to 350 m atm. Several combinations of pressure and optical path were used in order to test for pressure-broadening effects, which were found to be negligible within the accuracy of the determination. In an effort to avoid the uncertainty that KMS found to be associated with measurements of the equivalent widths of such weak lines as these, an initial attempt was made to compare the line intensities visually. For this purpose, four solar lines were chosen to serve as standards on each plate:  $\lambda 8667.37$  (Si,-1);  $\lambda 8668.46$  (o,-2d?);  $\lambda 8680.41$  (S,0); and  $\lambda 8728.60$  (Si,-2) (identifications and intensities from Babcock and Moore (1947)). On reproductions of the Mars spectrogram kindly made available by Dr. Spinrad, it is

evident that the Martian  $\text{CO}_2$  lines exhibit intensities intermediate between that of  $\lambda 8667.37$  and  $\lambda 8668.46$  or  $\lambda 8728.60$ . Of the latter two lines, the last one is barely indicated on the reproductions, the other line is not visible. This difference in intensity is also apparent on the laboratory plates. On this basis, it was found necessary for the laboratory path lengths to lie within the range  $241 \pm 44$  m atm in order to give intensities comparable with the Martian  $\text{CO}_2$  lines. The laboratory plate giving the closest match is reproduced with a copy of the Martian spectrogram in Figure 29. As a further check, densitometer tracings were made of the plates corresponding to the indicated range in path length and the relative intensities of the solar and  $\text{CO}_2$  lines were measured. The difficulties experienced in making these measurements corroborated the remarks of KMS, but the results served to confirm the visual estimate. The ratio of the mean intensity of the three  $\text{CO}_2$  lines to that of the solar line at  $8667.37 \text{ \AA}$  was .4, .6, and .9 for path lengths of 197, 241, and 289 m atm, respectively. KMS derive a mean equivalent width of  $3.8 \text{ m \AA}$  for the  $\text{CO}_2$  lines and give the corresponding value for the solar line as  $7 \text{ m \AA}$ . On this basis they conclude that an upper limit for the  $\text{CO}_2$  equivalent width lies between 5 and  $6 \text{ m \AA}$ . Taking ratios, this implies  $.4 \leq W_{\text{CO}_2}/W_{\odot} \leq .8$ , in good agreement with the result derived above. A smoothed

Fig. 29 Spectra of Venus, Mars, and a Laboratory Path Length of 223 m atm (NTP) of CO<sub>2</sub> with the Sun as Light Source. The J Numbers of R and P Branch Lines of the 5 $\nu_3$  Band are Shown at the Bottom.





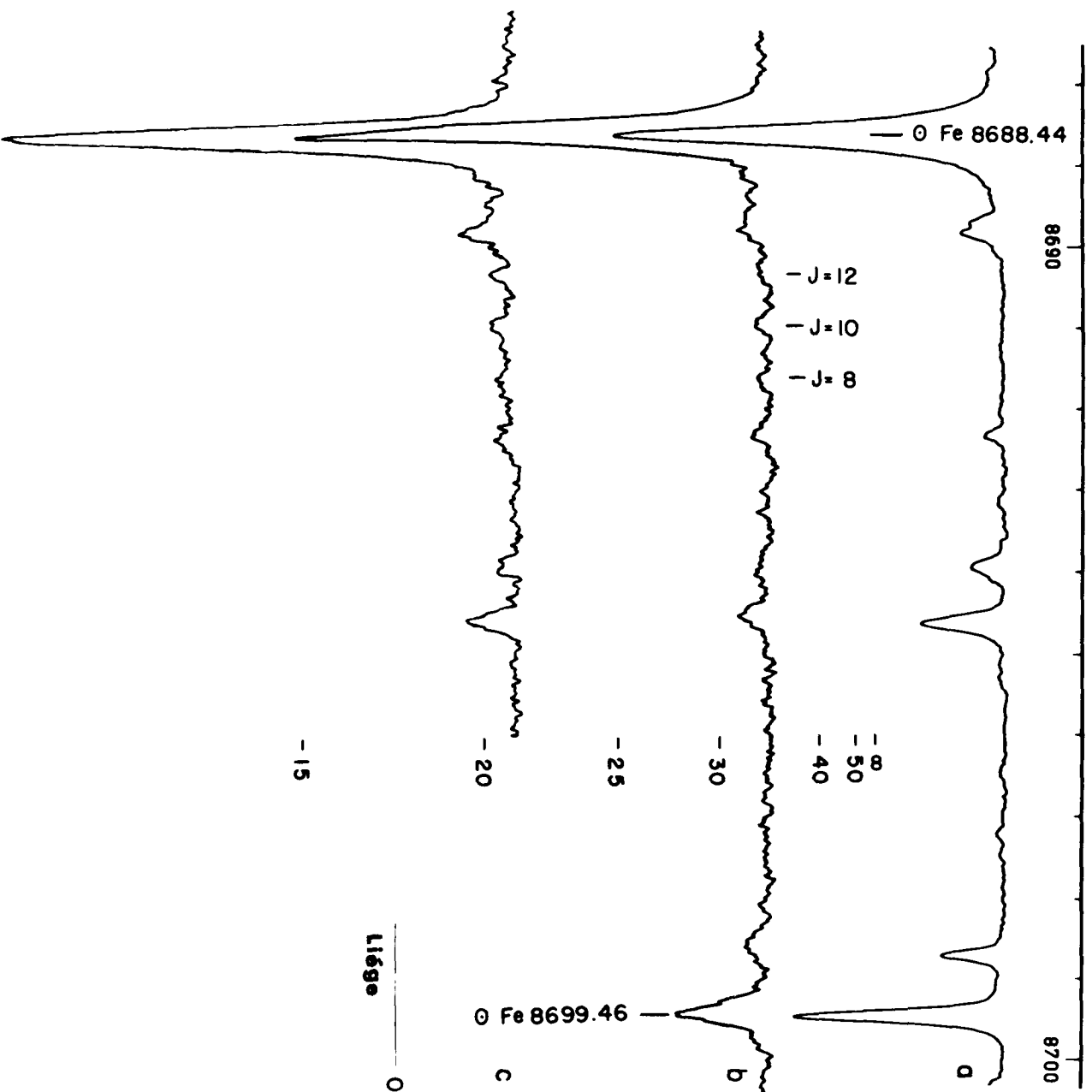
5  $\nu_3$  CO<sub>2</sub> LINES

densitometer tracing of the 241 m atm laboratory plate is presented for comparison with a similar tracing of the Martian spectrogram and a tracing of the direct solar spectrum in Figure 30.

In order to convert the equivalent path length derived above into an abundance of  $\text{CO}_2$  in the atmosphere of Mars, it is necessary to know the effective air mass and temperature at which the Martian spectrogram was obtained. KMS have calculated that for the geometry at which their observation was made, and with the smearing effects of seeing and guiding errors, the effective air mass is 3.6.

In computing this air mass, KMS restricted themselves to the southern one third of the planet. The present comparison was made using both the upper and lower thirds of the reproduced spectrum although the densitometer tracings were compared to the tracing of the southern one third prepared by KMS. As shown elsewhere (Owen and Kuiper 1964), the air mass corresponding to a slit placed pole to pole on the planet is 3.14 for weak lines. For a "polar" third of the disk this would be increased to 4.18. The reduction to the cited value of 3.6 presumably comes about as a result of the seeing and guiding errors the authors estimate to be present. These two effects will cause an apparent motion of the slit with respect to the disk of the planet and diminish the correspondence between a given position on the planet

Fig. 30 a) Solar Spectrum from the Liege Photometric Atlas, (b) Mt. Wilson Mars Spectrogram, (c) Laboratory Comparison (Sun + CO<sub>2</sub>).  
Note Presence of Three Rotational CO<sub>2</sub> Lines in (b) and (c).



and a given part of the spectrum. We assume a probable error of  $\pm 0.4$  in this value.

Use of an air mass of 3.6 leads to a value of  $67 \pm 15$  m atm. It remains to correct this figure for the difference in temperature between the laboratory and the Martian atmosphere. From a rough analysis of the relative intensities of the Martian  $\text{CO}_2$  lines, KMS conclude that "the apparent positions of the band maxima are consistent with an atmospheric temperature of about  $230^\circ\text{K}$ ." They note that the blending with solar lines and the uncertainty of their measures makes this an unreliable value. In view of the fact that the mean Martian surface temperature at aphelion is roughly  $240^\circ\text{K}$  (Pettit 1961), an atmospheric temperature of  $230^\circ\text{K}$  seems rather high. Perhaps with this in mind, KMS also use a value of  $200^\circ\text{K}$ , which would appear to be more reasonable. It would be highly desirable to obtain observations of an unblended  $\text{CO}_2$  band (e.g.,  $\nu_1 + 2\nu_2 + 3\nu_3$  at  $1.05\mu$ ), the rotational structure of which could be analyzed less ambiguously. For the present we will use the same two values for the temperature as KMS (cp. Appendices B and C to this section).

For a linear molecule such as  $\text{CO}_2$  the intensity of a rotational line in absorption is given by the expression (R branch lines)

$$1) \quad I_{\text{abs}} = \frac{C_{\text{abs}}}{Q_r} 2 (J + 1) \exp \left[ - BJ (J + 1) hc / kT \right] .$$

The intensity ratio of a line at temperatures  $T_1$  and  $T_2$  is then

$$2) \quad \frac{I_1}{I_2} = \frac{T_2}{T_1} \exp \left[ - BJ (J + 1) \frac{hc}{k} \left( \frac{1}{T_1} - \frac{1}{T_2} \right) \right] ,$$

in which the rotational state sum  $Q_r$  has been approximated by an integral:

$$3) \quad Q_r \approx \int_0^{\infty} (2J + 1) \exp \left[ - hc BJ (J + 1) / kT \right] dJ = \frac{kT}{hcB}$$

The latter should be a close approximation owing to the small value of  $B$  for  $\text{CO}_2$  (Herzberg 1950). For  $J = 10$ ,  $B = 0.3895$ ,  $T_1 = 297^\circ\text{K}$ , and  $T_2 = 230^\circ\text{K}$ ,  $200^\circ\text{K}$  we obtain

$$\frac{I_1}{I_2} = .82 \quad (T_2 = 230^\circ\text{K}), \quad .74 \quad (T_2 = 200^\circ\text{K}) .$$

Reducing the laboratory abundance to NTP we obtain  $62 \pm 15$  m atm. If this figure is now multiplied by the factors derived above, the Martian  $\text{CO}_2$  abundance is found to be  $51 \pm 15$  m atm ( $T = 230^\circ\text{K}$ ) or  $46 \pm 15$  m atm ( $T = 200^\circ\text{K}$ ). These figures represent the amount of gas at NTP which would give the intensities observed in the Martian spectrum if the gas were cooled to the assumed mean atmospheric temperature of Mars.

It is evident that the agreement with the results of KMS is quite good. Although the abundances reported here are somewhat lower than theirs, each set of figures falls well within the range of error corresponding to the other set. The agreement may even be better than it appears since it is not clear what temperature has been used by KMS to standardize their meter atmosphere. It has not been possible to reduce the probable error as much as had been hoped, but the accordance of the two sets of values strengthens the validity of each. It appears that additional observations of Mars are needed to increase the accuracy of the determination.

#### Note Added in Proof

After this paper was written, Dr. J. Chamberlain suggested to the writer that one might expect overlapping in the R branch of the  $8689\text{ \AA}$  band of  $\text{CO}_2$  due to doubling back of the rotational lines after formation of the band head. This will complicate the analysis because the temperature dependence of the lines with high J numbers will be different from that of the rotational lines considered here (mean  $J = 10$ ). The writer was unable to find accurate observed wavelengths of the higher rotational lines reported in the literature and could not resolve them on the plates discussed above. Therefore the rotational constants given by Herzberg and Herzberg (1953) were used to predict the

positions of these lines according to the approximate relation

$$4) \quad \nu_J = \nu_0 + 2B' + (3B' - B'') J + (B' - B'') J^2 .$$

The line  $J = 40$  was subsequently chosen as having a position close to that of  $J = 10$  and thus being representative of the problem. Using equation (1), we find the relative intensities of  $J = 40$  and  $J = 10$  are as follows:

$$T = 297^\circ\text{K}, \quad \frac{I_{10}}{I_{40}} = 4.85$$

$$T = 200^\circ\text{K}, \quad \frac{I_{10}}{I_{40}} = 20$$

If we now express the observed intensity as a simple sum of the intensities of  $J = 10$  and  $J = 40$  we have

$$\frac{I_{\text{lab}}}{I_0} = \frac{I_{10} (1 + \frac{1}{4.85})}{I_{10}' (1 + \frac{1}{20})} = 0.85$$

where  $\frac{I_{10}}{I_{10}'} = \frac{I_1}{I_2} = 0.74$  for  $T_1 = 297^\circ\text{K}$ ,  $T_2 = 200^\circ\text{K}$ .

In other words, the fact that we are dealing with a blend of two lines whose intensities change in opposite ways with a decrease in temperature implies that the amount of gas required in the Martian atmosphere to reproduce the observed intensities is somewhat greater than it would be otherwise.



Using the NTP laboratory value derived above, we find  $53 \pm 15$  m atm for the Martian  $\text{CO}_2$  abundance with an atmospheric temperature of  $200^\circ\text{K}$ .

This correction is obviously very rough and is intended primarily as an indication of another kind of uncertainty which is present in the abundance determination.

Brooks (private communication) has shown that the air mass corresponding to the KMS observation of Mars is better expressed as  $\eta = 3.9$ . His corrections include a more exact expression for the variation of air mass with zenith angle, a greater smearing effect due to seeing, and the use of the proper value for the angular separation of the Earth and Sun as seen from Mars. These corrections have been approved by Spinrad (private communication) and confirm the uncertainty assigned to the air mass in the present paper. Considering both the correction for doubling back and the new value for the air mass, the  $\text{CO}_2$  abundance becomes  $46 \pm 20$  m atm (NTP) for an assumed Martian atmospheric temperature of  $200^\circ\text{K}$ .

## 7. CONCLUSIONS

The investigations which have been reported in part 4 of this paper have not revealed any evidence for the presence of gases other than methane or ammonia in the spectrum of Jupiter. At the same time, it appears that the atmospheric temperature of that planet is considerably in excess of the value achieved by a simple black body equilibrium with the incident solar radiation. Neither methane nor ammonia has been regarded as an adequate absorber in the appropriate region of the spectrum to provide the necessary greenhouse effect with the result that attention has turned to the possible presence of other gases or an internal heat source. This unsatisfactory situation could be considerably modified through the use of additional observations of the  $3\nu_3$  band of methane, a calibration of the temperature dependence of bands at shorter wavelengths, and laboratory studies of the spectra of ammonia and methane in the 10-50 $\mu$  region. The observations of rotational line intensities in the spectrum of the planet would give additional direct evidence on the atmospheric temperature profile; the laboratory program would provide information on the wavelength dependence of the atmospheric absorption coefficient in the region of the spectrum of most importance to the planet's

radiative equilibrium. A study of ammonia in this region which has already been made (Walsh 1963) suggests that there is more absorption here than had previously been anticipated. In particular, a spectrum of 8.5 m atm of ammonia broadened by 150 m atm of  $N_2$  shows an average transmission of only 20% in the region 20-35 $\mu$  and there are no "windows".

In addition to the thermal balance problem, the presence of the observed colors in the cloud layers suggests the presence of additional substances in the atmosphere of the planet. Spectra obtained at higher resolution throughout the photographic and instrumental infrared region should permit considerably more sensitive tests for trace gases than those described here.

These observational studies must be supported by considerations of the mechanism of line formation at various wavelengths in order that accurate abundances can be determined. High resolution observations made over a long period of time at several locations on the disk of the planet can then be interpreted to give an idea of the local and secular variations of the cloud cover. When this information is combined with data on the atmospheric composition, the temperature profile described above, and the thermodynamic properties of ammonia, it should be possible to develop and test more accurate models of the Jovian atmosphere.

In the case of Mars, the requirements for additional information are less exacting. The most important data needed at the moment are additional values for the intensities of weak lines of  $\text{CO}_2$ . Since all but three of the rotational lines in the  $5\nu_3$  band (the only weak band which has been observed) are blended with solar lines, the best hope appears to be the three bands located further in the infrared near  $1.05\mu$ . Weak lines in these bands should provide a check on the abundance derived from the  $5\nu_3$  band and a consequent increase in the accuracy of the surface pressure.

The dissertation has been concerned primarily with studies of two planets, but the techniques described here have been applied to analyses of Venus, Saturn, and Uranus as well. This work is being continued and expanded to include the development of new equipment for the laboratory and the telescope. It is expected that a spectrograph currently in the design stage for use in observing the  $0.9\text{--}1.1\mu$  range of planetary spectra will also be employed in studies of the cooler stars.

## Appendix A

### THE TRANSFER OF RADIATION IN A SCATTERING ATMOSPHERE

The purpose of this appendix is to present a brief outline of the problems which arise in considering the formation of absorption lines in a planetary atmosphere containing scattering particles. The discussion is intended to be illustrative rather than rigorous and has particular relevance to Section 4.4. It is based on the work of van de Hulst (1952), Chamberlain and Kuiper (1956), and Chandrasekhar (1960).

The information which is desired is a relation between the equivalent width ( $W_J$ ) of a spectral line corresponding to absorption from a given rotational level  $J$ , and the number of absorbing molecules in that rotational level ( $N_J$ ). With this relationship established it is possible to deduce abundances of the absorbing species and meaningful rotational temperatures. The question to be resolved is how the relation between  $W_J$  and  $N_J$  differs in the two cases of an atmosphere containing scattering particles and a pure molecular atmosphere. The question is basic to laboratory interpretations of planetary spectra since the laboratory work is essentially limited to the pure molecular case.

We begin with a consideration of the simplest conditions: a plane parallel, homogeneous, pure molecular atmosphere. Let the gas composing this atmosphere have a mass absorption coefficient  $K_\nu$ . We assume throughout this discussion that Rayleigh scattering and thermal emission by the atmosphere are negligible (observations in the region  $0.6 - 1.1\mu$ ). The equation of transfer in this case is simply

$$1) \quad dI_\nu = - K_\nu \rho I_\nu \sec \theta dx$$

where  $\rho$  is the density of the gas,  $dx$  is a line element of the geometric path and  $\theta$  is the angle of the beam to the normal. Solving this equation we obtain

$$2) \quad I_\nu = I_{\nu_0} \exp \left[ - K_\nu \rho \sec \theta X \right].$$

For a double traversal of the planet's atmosphere (having scale height  $h$ ) this becomes

$$3) \quad I_\nu = I_{\nu_0} \exp \left[ - K_\nu \rho \sec \theta 2h \right].$$

Let us further assume that we are dealing with a weak line so  $K_\nu$  is small and Eq. (3) may be expanded:

$$4) \quad I_\nu = I_{\nu_0} (1 - K_\nu \rho \sec \theta 2h)$$

Now the equivalent width of a spectral line in frequency units is

$$5) \quad W_\nu = \int \frac{I_c - I_\nu}{I_c} d\nu = \int \left( 1 - \frac{I_\nu}{I_c} \right) d\nu$$

where  $I_c$  is the intensity of the continuum which in our case is simply  $I_{\nu_0}$ , the unattenuated intensity. Thus

substituting (4) into (5) we obtain

$$6) \quad W_{\nu} = \int K_{\nu} \rho \sec \theta \, 2h \, d\nu$$

Without writing down the absorption coefficient explicitly for a given case, we may state that in general it has the form  $K_{\nu} = N_J f(\nu)$ . Thus the result of the above integration is

$$7) \quad W_{\nu}(J) = \text{Const. } N_J$$

This is a simple confirmation of the well known fact that for a weak line the equivalent width is directly proportional to the number of absorbers.

Now we consider the case of a plane parallel atmosphere containing isotropically scattering particles with a grey mass scattering coefficient  $\sigma$ . As Chamberlain and Kuiper (op. cit.) have remarked, this includes the case of particles large with respect to the wavelength of the radiation since such particles will have a strong forward-scattering lobe which is indistinguishable from directly transmitted radiation in this problem. We again assume homogeneity, but now the atmosphere is considered to be semi-infinite so that no reflection occurs from the surface. We must therefore add two sources to the equation of transfer (1) to account for the diffusely reflected incident flux and light scattered into the beam. Let the incident flux be  $\pi F$  at an angle  $\theta_0$  to the zenith (we ignore the

azimuthal dependence because of the assumed isotropy).

Equation (1) is then

$$8) \quad dI_\nu = - (K_\nu + \sigma) \rho I_\nu \sec \theta \, dx + \frac{1}{4\pi} \int I_\nu \, d\omega (\sigma \rho \sec \theta \, dx) \\ - (K_\nu + \sigma) \rho \sec \theta_0 \, x \\ + \pi F e^{\left( \frac{\sigma}{4\pi} \rho \sec \theta \, dx \right)}.$$

Now let  $\tilde{\omega}_\nu = \frac{\sigma}{K_\nu + \sigma}$ ,  $d\tau_\nu = -(K_\nu + \sigma) \rho \, dx$ , and  $\mu = \cos \theta$ .

Making these substitutions and integrating over  $\varphi$ , we have

$$\int I_\nu \, d\omega = 2\pi \int_{-1}^{+1} I_\nu(\mu) \, d\mu,$$

and Eq. (8) may be written as

$$9) \quad \mu \frac{dI_\nu}{d\tau_\nu} = I_\nu - \frac{\tilde{\omega}}{2} \int_{-1}^{+1} I_\nu(\mu) \, d\mu - \frac{\tilde{\omega}}{4} F e^{-\tau_\nu/\mu_0}$$

This equation has been solved by Chandrasekhar (op. cit. p. 85) for the conditions we have specified in terms of his H-functions which he defines as

$$10) \quad H(\mu) = \frac{1}{\mu_1 \dots \mu_n} \frac{\prod_{i=1}^n (\mu + \mu_i)}{\prod_{\alpha=1}^{n-1} (1 + K_\alpha \mu)}$$

where the  $K_\alpha$  are roots of the characteristic equation he has set up to solve the case of a plane-parallel, semi-infinite isotropically scattering atmosphere with no incident flux. In terms of these H-functions then, the solution to Eq. (9) may be written down as



$$11) \quad I_{\nu}(\tau_{\nu} = 0, \mu) = \frac{\tilde{\omega}_{\nu}}{4} F \frac{\mu_0}{\mu + \mu_0} H(\mu) H(\mu_0).$$

In analogy to the preceding discussion of the pure molecular case, we need an expression for the quantity  $(I_c - I_{\nu})/I_c = (1 - I_{\nu}/I_c)$  in order to solve for the equivalent width. In the continuum,  $K_{\nu} = 0$  and thus  $\tilde{\omega} = 1$ . Referring to Eq. (11), we find

$$12) \quad (1 - I_{\nu}/I_c) = 1 - \frac{\tilde{\omega}_{\nu} H \tilde{\omega}(\mu) H \tilde{\omega}(\mu_0)}{H_1(\mu) H_1(\mu_0)}.$$

To obtain  $W_{\nu}(J)$ , it is necessary to simplify the expression in Eq. (12) so that it can be integrated over all frequencies. As in the pure molecular case, we consider only weak lines so  $K_{\nu} \ll 1$  and  $\tilde{\omega}_{\nu} \approx 1$ . To proceed further, Chamberlain and Kuiper (op. cit.) express  $H \tilde{\omega}(\mu)$  as

$$13) \quad H \tilde{\omega}(\mu) = \frac{H_1(\mu)}{1 + f \tilde{\omega}(\mu)} \approx H_1(\mu) \left[ 1 - f \tilde{\omega}(\mu) + f^2 \tilde{\omega}(\mu) \right]$$

where  $f \tilde{\omega} \ll 1$ . These authors then postulate that  $f \tilde{\omega} = A \mu^p$  where  $p > 0$ . Integral theorems derived by Chandrasekhar (op. cit. Chap. 5) are then used to derive conditions on  $f \tilde{\omega}$  which enable them to find  $p = 1$  and  $A = [3(1 - \tilde{\omega})]^{1/2}$  for the case  $\tilde{\omega} \approx 1$ . Substituting in Eq. (13) we find

$$14) \quad H \tilde{\omega}(\mu) = \frac{H_1(\mu)}{1 + \mu [3(1 - \tilde{\omega})]^{1/2}}$$

We can now substitute this in Eq. (12) to obtain our

desired expression for  $(1 - I_\nu / I_c)$ :

$$(1 - I_\nu / I_c) = 1 - \frac{\tilde{\omega}_\nu}{(1 + \mu [3(1 - \tilde{\omega}_\nu)]^{1/2})(1 + \mu_o [3(1 - \tilde{\omega}_\nu)]^{1/2})}$$

To simplify the calculation, we make the following substitutions:

a) Let  $\mu_o = \mu$  (observation at opposition; always a good approximation for Jupiter)

b) Since  $\tilde{\omega}_\nu \approx 1$ ,  $K_\nu \ll \sigma$  so  $1 - \omega_\nu \approx \frac{K_\nu}{\sigma}$ . Let  $\eta_\nu = \frac{K_\nu}{\sigma} \approx 1 - \tilde{\omega}_\nu$ .

We then multiply and combine terms to obtain

$$(1 - I_\nu / I_c) = \frac{\eta_\nu(1 + 3\mu^2) + (3\eta_\nu)^{1/2} 2\mu}{1 + (3\eta_\nu)^{1/2} 2\mu + 3\mu^2 \eta_\nu}.$$

Expanding the denominator the fraction on the right may be written as

$$\left[ \eta_\nu(1 + 3\mu^2) + (3\eta_\nu)^{1/2} 2\mu \right] \left[ 1 - (3\eta_\nu)^{1/2} 2\mu + 9\mu^2 \eta_\nu \right].$$

Carrying through this multiplication but rejecting terms of  $\eta_\nu^n$  where  $n > 1$ , we obtain

$$\eta_\nu(1 + 3\mu^2) + (3\eta_\nu)^{1/2} 2\mu - 3\eta_\nu 4\mu^2.$$

Combining terms and substituting for  $\eta_\nu$  this yields

$$1 - \frac{I_\nu}{I_c} \approx \frac{K_\nu}{\sigma} (1 - 9\mu^2) + 2\mu 3^{1/2} \left( \frac{K_\nu}{\sigma} \right)^{1/2}.$$

Since we are concerned with observations of Jupiter,  $\mu \approx 1$  at all times and since  $\eta_\nu \ll 1$ , the above expression reduces to

$$15) \quad 1 - \frac{I_\nu}{I_c} \approx 2\mu 3^{1/2} \left( \frac{K_\nu}{\sigma} \right)^{1/2}.$$

The equivalent width is thus

$$16) \quad W_{\nu} = \int_{2\mu} 3^{1/2} \left( \frac{K_{\nu}}{\sigma} \right)^{1/2} d\nu = \text{Const. } N_J^{1/2}$$

Comparison with Eq. (7) indicates that the presence of isotropically scattering particles indeed affects the relation between the equivalent width and the number of absorbers. The relation defined by Eq. (16) is familiar as the so-called strong-line approximation in the pure molecular case. The presence of scattering particles requires the use of this (square root) relation for weak lines.

In terms of laboratory comparisons, Eq. (16) signifies that the amount of gas used in the laboratory to match the intensity of a weak planetary absorption line will not yield the correct abundance of this gas in the atmosphere of the planet (if the atmosphere is of the type considered here). The abundances will be greatly overestimated. As was indicated in Section 4.4, it seems unnecessary to use this expression in the case of Jupiter near  $1\mu$  but such considerations may be important at shorter wavelengths. If so, more gas should be required to match the intensities of weak lines at (say)  $6450 \text{ \AA}$  than at  $1\mu$ , provided the temperature dependence of the two sets of lines are the same. At present there are insufficient data to carry out this test. However, the importance of these

considerations for problems such as the determination of the hydrogen abundance is obvious and suggests that the importance of particle scattering at a given wavelength must be assessed before accurate abundances can be derived.

## Appendix B

### ATMOSPHERIC TEMPERATURE AND THE $1.05\mu$ $\text{CO}_2$ BANDS

As a first approximation, we can assume that the atmosphere is adiabatic to the height above the surface corresponding to the mean level at which the  $\text{CO}_2$  absorption occurs. At this level, the pressure is approximately equal to one-half that at the surface. If we adopt the atmospheric mixture derived previously (Owen and Kuiper 1964), the adiabatic lapse rate for the Martian atmosphere is  $3.7^\circ\text{C}/\text{km}$ . (The circularity of this argument is not as bad as it may seem in that a fair range in the proportions of  $\text{CO}_2$  and  $\text{N}_2$  results in roughly the same lapse rate.) The adiabatic assumption then leads to the relation  $T_{1/2} = 0.833T_S$  where  $T_{1/2}$  is the temperature at the mean absorbing level and  $T_S$  is the surface temperature. Using Pettit's value for  $T_S = 240^\circ\text{K}$ , one finds  $T_{1/2} = 200^\circ\text{K}$ . It should be pointed out that since the abundance determination is essentially restricted to the polar thirds of the planet, an even lower mean surface temperature than that assumed here is probably appropriate so  $200^\circ\text{K}$  may be an upper limit.

Ideally, of course, one would like to determine the atmospheric temperature from the same bands used for the abundance analysis. This is not possible in the case of the 8689 Å band since only three rotational lines are unblended and these are very weak. One is thus led to an investigation of the stronger bands near 1.05μ. These bands are described in Table 13 which is based on a similar table prepared by Herzberg and Herzberg (1953). On the intensity scale in this table, the 5ν<sub>3</sub> band at 8689 Å has the value unity. Figure 31 shows the appearance of the bands at 1.036μ and 1.049μ at three path lengths which bracket the equivalent optical path for absorption in the Martian atmosphere as deduced in Section 6. All three spectra were obtained at atmospheric pressure (~700 mm Hg). The Sun is again used as a light source so these spectra are very similar to what one would actually observe when obtaining spectra of Mars. It is apparent that even at the smallest observed path lengths, the 1.048μ band is much stronger than 5ν<sub>3</sub> and both P and R branch lines are easily visible. The strongest of these lines may be slightly saturated at the low pressure of the Martian atmosphere but the presence of the weaker band at 1.036μ allows an empirical evaluation of this possibility. There is a still weaker band at 1.063μ (not shown) which is barely visible at the intermediate path length and relatively easy to discern at the

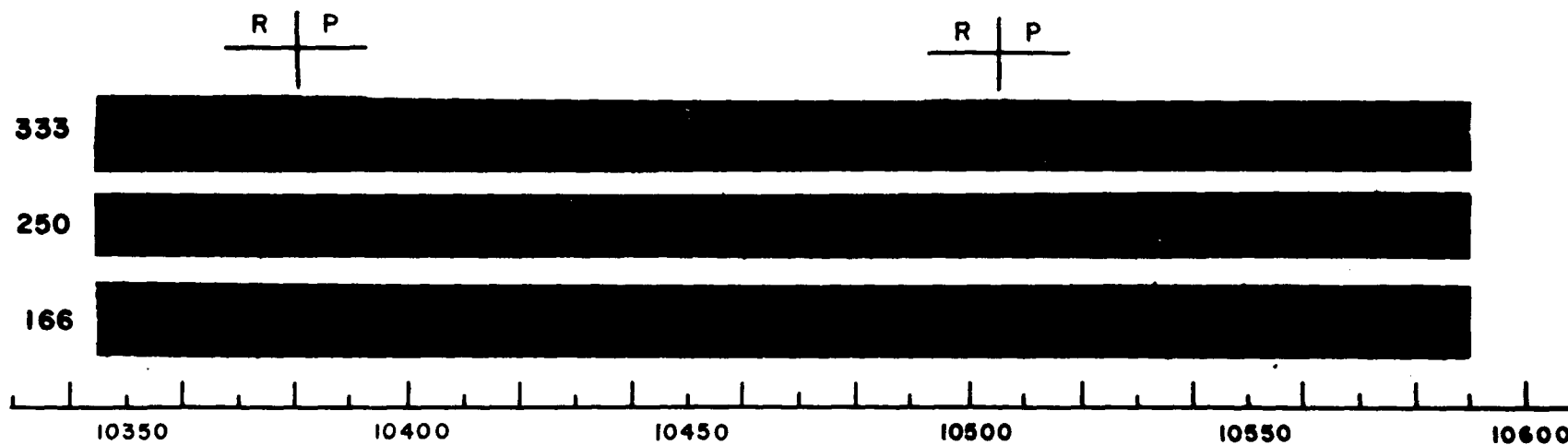
Table 13

CO<sub>2</sub> BANDS NEAR 1.05 $\mu$ 

$\lambda_h$ (air)	$\nu_h$ (vac)	Intensity	$\nu_o$ (vac)	Ass.	$\lambda_o$ (air)
10626.7	9407.7	4	9389.0	$4\nu_2+3\nu_3$	10647.8
10487.6	9532.3	20	9517.0	$\nu_1+2\nu_2$ $+3\nu_3$	10504.6
10361.8	9648.2	8	9631.4	$2\nu_1+3\nu_3$	10381.0

Fig. 31 Laboratory Spectra of  $2\nu_1 + 3\nu_3$  and  $\nu_1 + 2\nu_2 + 3\nu_3$  of  $\text{CO}_2$  at Three Path Lengths (NTP). The Sun was Again Used as Light Source.





maximum path length. Thus the three bands taken together should provide a valuable independent check on both the  $\text{CO}_2$  abundance and the mean atmospheric temperature.

Such a study would not be free of observational difficulties, however. This region of the spectrum requires the use of the I-Z emulsion which is notoriously slow and grainy. It is doubtful that the resolution illustrated in Figure 31 could be achieved on Martian spectrograms but a considerable sacrifice can be afforded. As an illustration, we can consider the lines in the P branch of the  $1.049\mu$  band. The original dispersion of the laboratory plate was  $5 \text{ \AA/mm}$  and the spacing of these lines is roughly  $2.4 \text{ \AA}$ . Thus a dispersion of  $15 \text{ \AA/mm}$  would leave the lines separated by  $.16 \text{ mm}$ . This is slightly greater than the separation of the last resolvable lines of the R branch on the present plates and would therefore be acceptable if the projected slit width remains the same. This is not a prohibitive assignment for a suitably designed spectrograph.

The remaining difficulty is the problem of blending with solar features. Inspection of Figure 31 indicates that several such blends occur, but there are a sufficient number of unblended lines to give reliable results, particularly if all three bands are used.

## Appendix C

### A CONSIDERATION OF SATURATION EFFECTS IN THE MARTIAN CO<sub>2</sub> LINES

In Section 6 when the abundance of CO<sub>2</sub> in the Martian atmosphere was derived it was assumed that the Martian and laboratory lines were not saturated, i.e., the intensities were assumed to be directly proportional to the number of absorbing molecules. While this is likely to be correct for the laboratory work (minimum pressure ~350 mb), it is possible that on Mars the effective pressure is so low that the lines would be very sharp and there would be some saturation. Kaplan, Münch and Spinrad (1964) (KMS) have tested this possibility and found that a slight saturation indeed exists. The intent of this appendix is to verify their result for the conditions of temperature and pressure assumed in Section 6 and to consider the implications for the 1.05 $\mu$  bands as well.

If we make the assumption that the lines are on the linear part of the curve of growth, then we can use the conventional expansion

$$1) \quad I_{\nu} = I_{\nu_0} (1 - hN\alpha_{\nu})$$

and find

$$2) \quad W_\nu = \int \left(1 - \frac{I_\nu}{I_{\nu_0}}\right) d\nu = \int hN \alpha_\nu d\nu = hN \frac{\pi \epsilon^2}{mc} f.$$

Converting to wave numbers, we have

$$W_{1/\lambda} = \frac{1}{c} W_\nu = \frac{1}{c} (hN \frac{\pi \epsilon^2}{mc} f) = hNS.$$

Here  $h$  is the length of the absorbing path,  $N$  is the number of molecules/cm<sup>3</sup> and  $S$  is the line intensity in cm<sup>-1</sup>/unit optical density. For consideration of the Mars problem we set  $hN = \eta w = u$  where  $\eta$  is the effective Martian air mass and  $w$  is the optical density (in km atm or molecules/cm<sup>2</sup>). From the laboratory work of Rank quoted by KMS (and essentially confirmed by the results of Section 6) we have an average value of  $S = 0.030$  cm<sup>-1</sup>/km atm for one of the  $J = 8, 10, \text{ or } 12$  lines of the R-branch of  $5\nu_3$  at 200°K. Thus if there were no saturation, the CO<sub>2</sub> abundance would simply be

$$w = \frac{W}{S\eta} = 43 \text{ m atm}$$

in reasonable agreement with the result of Section 6.

To test for the presence of saturation, we would now like to use the complete expression for the equivalent width to find that value of  $u$  ( $=\eta w$ ) which satisfies the observed values of  $S$  and  $W$ . We have

$$3) \quad W_\nu = \int \left(1 - \frac{I_\nu}{I_{\nu_0}}\right) d\nu = \int \left(1 - e^{-\alpha_\nu u}\right) d\nu.$$

To determine the proper form of the absorption coefficient ( $\alpha_\nu$ ) to use for this problem, we compare the half-widths of a Doppler- and a collision-broadened line under the anticipated conditions. The Doppler width is

$$4) \quad \gamma_D = \frac{\nu_0}{c} \left( \frac{2kT}{M} \right)^{1/2}.$$

For a temperature of 200°K, this is  $\gamma_D = 3.1 \times 10^8 \text{ sec}^{-1}$ .

The collision width is

$$5) \quad \gamma_c = \frac{1}{2\pi\tau},$$

where  $\tau$  is the mean time between collisions. Calculating  $\frac{1}{2\pi\tau}$  for  $T = 200^\circ\text{C}$  and  $P = 20 \text{ mb}$  (half the maximum anticipated surface pressure) we find  $\gamma_c = 1.9 \times 10^7 \text{ sec}^{-1}$ . It thus appears safe to restrict the discussion to Doppler broadening. In this case, we have

$$6) \quad \alpha_\nu = \frac{S}{\gamma_D \sqrt{\pi}} \exp \left[ - \left( \frac{\nu}{\gamma_D} \right)^2 \right].$$

Substituting in Eq. (3) there results

$$W_\nu = \int 1 - \exp \left[ - \frac{Su}{\gamma_D \sqrt{\pi}} \exp - \left( \frac{\nu}{\gamma_D} \right)^2 \right] d\nu.$$

Letting  $x = \frac{\nu}{\gamma_D}$  and  $y = \frac{Su}{\gamma_D \sqrt{\pi}}$ , this becomes

$$7) \quad W_\nu = \gamma_D \int 1 - \exp \left[ - y \exp - x^2 \right] dx.$$

This expression may be expanded and integrated term by term,

leading to the following series:

$$\begin{aligned} \frac{W_y}{\gamma_D} &= \sqrt{\pi} \left( y - \frac{y^2}{2! \sqrt{2}} + \frac{y^3}{3! \sqrt{3}} - \frac{y^4}{4! \sqrt{4}} + \dots \right) \\ &= \sqrt{\pi} y \left[ \sum_{n=2}^{\infty} \frac{y^{n-1} (-1)^{n-1}}{n! \sqrt{n}} + 1 \right]. \\ 8) \quad W_y &= Su \left[ \sum_{n=2}^{\infty} \frac{\left( \frac{Su}{\gamma_D \sqrt{\pi}} \right)^{n-1} (-1)^{n-1}}{n! \sqrt{n}} + 1 \right]. \end{aligned}$$

Knowing  $W$ ,  $S$ , and  $\gamma_D$ , we can now find that value of  $u$  for which Eq. (8) is satisfied. To facilitate this calculation, we re-write (8) in the following way:

$$9) \quad \frac{W_y}{\sqrt{\pi} \gamma_D} = y \left[ \sum_{n=2}^{\infty} \frac{y^{n-1} (-1)^{n-1}}{n! \sqrt{n}} + 1 \right] = yQ.$$

Using the same numbers as in the unsaturated case, we have the condition  $yQ = 0.273$ . A table of  $y$  and  $Q$  has been compiled by Ladenburg (1930), which shows that this condition is satisfied for  $y = 0.31$ . Solving for  $u$ , one obtains  $u = w\eta = 0.189$  km atm or

$$w = 48.5 \text{ m atm.}$$

Comparing this with the result obtained on the assumption that the lines were on the linear part of the curve of growth, we see that the new value of the abundance is slightly larger. This means that for the measured value of

S, more gas is needed to produce the observed value of  $W$  than is implied by the linear assumption, i.e., the lines are slightly saturated.

This effect will lead to an underestimate of the Martian  $\text{CO}_2$  abundance by about 10% and suggests an increase of the value given in Section 6 to 50 m atm. In view of the present uncertainty of  $\pm 45\%$  in the abundance, this refinement may seem somewhat premature but should be borne in mind for future work. As an example, this consideration certainly applies to the observations of the  $1.05\mu$  bands proposed in Appendix B since these bands are considerably stronger than  $5\nu_3$ . Thus the strongest rotational lines will be saturated and a discussion similar to that presented here will be necessary to derive an abundance if only the strong lines or the integrated band intensities are observed.

## REFERENCES

- Adel, A., and Slipher, V. M. 1934, Phys. Rev., 46, 902.
- Allen, C. 1963, Astrophysical Quantities, 2nd ed. (London: Athlone Press).
- Alsop, L., and Giordmaine, J. A. 1961, Columbia Radiation Laboratory, Special Technical Report AD 263 565.
- Babcock, H. D., and Moore, C. E. 1947, The Solar Spectrum,  $\lambda 6600$  to  $\lambda 13495$ , (Washington, D. C.: Carnegie Institution of Washington).
- Badger, R. M. 1930, Phys. Rev., 35, 1038.
- Bardwell, J., and Herzberg, G. 1953, Ap. J., 117, 462.
- Bernstein, H. J., and Herzberg, G. 1948, J. Chem. Phys., 16, 30.
- Baum, W. A., and Code, A. D. 1953, A. J., 58, 108.
- Bibinova, V. P., Kuzmin, A. D., Salomonovich, A. E., and Shavlovskii, I. V. 1962, Astr. Zhur., 39, 1083.
- Binder, A., Cruikshank, D., and Kuiper, G. P. 1964, Comm. L.P.L., Vol. II, (in press).
- Cadle, R. 1962, J. Atm. Sci., 19, 281.
- Campbell, W. W. 1895, Ap. J., 2, 127.
- Chamberlain, J., and Kuiper, G. P. 1956, Ap. J., 124, 399.
- Chandrasekhar, S. 1960, Radiative Transfer (New York: Dover Publications), Chap. 1 and 3.
- Chao, S.-H. 1936, Phys. Rev., 50, 37.
- Childs, W. H. J. 1936, Proc. Roy. Soc. Lon. A., 153, 555.
- Childs, W. H. J., and Jahn, H. A. 1936, Nature, 138, 285.



## REFERENCES (Continued)

- . 1939, Proc. Roy. Soc. Lon. A., 169, 428, 451.
- Cleeton, C. E., and Williams, N. H. 1934, Phys. Rev., 45, 234.
- Czerny, M., and Turner, A. F. 1930, Zs. f. Physik, 61, 792.
- Delbouille, L., and Roland, G. 1963, Photometric Atlas of the Solar Spectrum from  $\lambda 7498$  to  $\lambda 12016$ , from Mem. Soc. R. Sci. Liege, Special Volume No. 4.
- Dennison, D. M., and Ingram, S. B. 1931, Phys. Rev., 36, 1455.
- Dollfus, A. 1951, Comptes Rendus, 232, 1066.
- . 1955, Thesis (Paris: University of Paris), NASA Tech. Trans. NASA TT F-188.
- . 1961, Planets and Satellites, ed. G. P. Kuiper and B. M. Middlehurst (Chicago: University of Chicago Press), Chap. 9.
- Drake, F. D., and Ewen, H. I. 1958, Proc. I.R.E., 46, 53.
- Dunham, T. 1933, Pub. A.S.P., 45, 200.
- . 1952, The Atmospheres of the Earth and Planets, ed. G. P. Kuiper (Chicago: University of Chicago Press), Chap. 11.
- Durie, R. A., and Herzberg, G. 1960, Canadian J. Phys., 38, 806.
- Ebert, H. 1889, Ann. der Physik und Chem., ed. G. Wiedemann (Neue Folge), 38, 490.
- Fastie, W. G. 1952a, J.O.S.A., 47, 641.
- . 1952b, ibid., 647.
- Fehrenbach, C. and Guerin, P. 1964, Comptes Rendus, 258, 1403.
- Field, G. 1963, quoted by Lasker, B. 1963, q.v.

## REFERENCES (Continued)

- Foltz, J. V., and Rank, D. H. 1963, Ap. J., 138, 1319.
- Fraunhofer, J. 1828, Edinburgh J. Sci., 8, 7.
- Fredrick, L. W. 1963, Pub. A.S.P., 75, 414.
- Gallet, R. 1963, in "The Planet Jupiter", ed. R. Wildt, H. J. Smith, E. E. Salpeter, and A. G. W. Cameron, Phys. Today, 16, No. 5, 19.
- Giordmaine, J. A., Alsop, L. E., Townes, C. H., and Mayer, C. H. 1959, A. J., 64, 332.
- Giver, L. 1964, Ap. J., 139, 727.
- Grandjean, R., and Goody, R. M. 1955, Ap. J., 121, 548.
- Herzberg, G. 1938, Ap. J., 87, 428.
- . 1945, Infrared and Raman Spectra of Polyatomic Molecules (Princeton, Toronto, London, and New York: van Nostrand Co., Inc.).
- . 1945a, ibid., p. 294.
- . 1945b, ibid., p. 297.
- . 1950, Spectra of Diatomic Molecules (Princeton, Toronto, London, and New York: van Nostrand Co., Inc.).
- . 1952, The Atmospheres of the Earth and Planets, ed. G. P. Kuiper (Chicago: University of Chicago Press), Chap. 13.
- Herzberg, G., and Herzberg, L. 1953, J.O.S.A., 43, 1037.
- Herzberg, G., and Spinks, J. W. T. 1934, Proc. Roy. Soc. Lon. A, 147, 434.
- Hess, S. 1953, Ap. J., 118, 151.
- Huggins, W. 1864, Phil. Trans. Roy. Soc., 154, 413.
- . 1871, Proc. Roy. Soc., 19, 488.

## REFERENCES (Continued)

- Hulst, H. C. van de 1952, The Atmospheres of the Earth and Planets, ed. G. P. Kuiper (Chicago: University of Chicago Press), Chap. 3.
- Humason, M. 1961, Planets and Satellites, ed. G. P. Kuiper and B. M. Middlehurst (Chicago: University of Chicago Press), Chap. 16.
- Jahn, H. A. 1938, Proc. Roy. Soc. Lon. A., 168, 469, 495.
- James, H., and Coolidge, A. 1938, Ap. J., 87, 438.
- Kaplan, L., Münch, G., and Spinrad, H. 1964, Ap. J., 139, 1.
- Keeler, J. 1895, M. N., 55, 475.
- Kiess, C. C., Corliss, C. H., and Kiess, H. K. 1960, Ap. J., 132, 221.
- Kuiper, G. P. 1950, Reports on Progress in Physics, 13, 247.
- . 1952, The Atmospheres of the Earth and Planets, ed. G. P. Kuiper (Chicago: University of Chicago Press), Chap. 12.
- . 1952a, ibid., p. 374.
- . 1952b, ibid., pp. 349-50.
- . 1952c, ibid., p. 348.
- . 1963, Mem. Soc. R. Sci. Liege, 5th ser., 9, 365.
- . 1964, Comm. L.P.L., Vol. II, No. 31 (in press).
- . 1964, Tables prepared for Landolt-Bernstein (in press).
- Ladenburg, R. 1930, Zs. f. Physik, 65, 200.
- Lasker, B. 1963, Ap. J., 138, 709.

## REFERENCES (Continued)

- Lorenz, E. 1951, Project for the Study of Planetary Atmospheres, Rept. No. 9, p. 21.
- Mayer, C. H. 1961, Planets and Satellites, ed. G. P. Kuiper and B. M. Middlehurst (Chicago: University of Chicago Press), Chap. 12.
- Mayer, C. H., McCullough, T. P., and Sloanaker, R. M. 1958a, Ap. J., 127, 11.
- . 1958b, Proc. I.R.E., 46, 260.
- McMath, R. R., and Mohler, O. C. 1962, Hdb. d. Phys., ed. S. Flüge (Berlin: Springer Verlag), 53, 1.
- Menzel, D. H., Coblentz, W. W., and Lampland, C. O. 1926, Ap. J., 63, 177.
- Munch, G., and Spinrad, H. 1963, 1964 (private communications).
- Munch, G., and YOUNKIN, R. L. 1964, paper presented at 116th meeting of A.A.S., Flagstaff, Arizona, June 24-27, 1964.
- Murray, B. C., and Wildey, R. L. 1963, Ap. J., 137, 692.
- Murray, B. C., Wildey, R. L., and Westphal, J. A. 1964, Ap. J., 139, 986.
- Nishida, M., and Jugaku, J. 1964, J. Atm. Sci., 21, 568.
- Opik, E. 1962, Icarus, 1, 200.
- Owen, T. C. 1963, Pub. A.S.P., 75, 314.
- Owen, T. C., and Kuiper, G. P. 1964, Comm. L.P.L., Vol. II, No. 32 (in press).
- Owen, T., Richardson, E. H., and Spinrad, H. 1964, Ap. J., 139, 1374.
- Owen, T. C., and Staley, D. O. 1963, J. Atm. Sci., 20, 347.
- Pettit, E. 1961, Planets and Satellites, ed. G. P. Kuiper and B. M. Middlehurst (Chicago: University of Chicago Press), Chap. 10.

## REFERENCES (Continued)

- Rea, D. G. 1962, Space Sci. Rev., 1, 159.
- Rutherford, L. M. 1863, Am. J. Sci., 85, 71.
- Sagan, C. 1960, A. J., 65, 499.
- Sagan, C., and Miller, S. 1960, A. J., 65, 499.
- Secchi, A. 1863, A. N., No. 1405, 13.
- . 1869, Comptes Rendus, 158, 761.
- Sinton, W., and Strong, J. 1960, Ap. J., 131, 470.
- Slipher, V. M. 1933, M. N., 93, 44.
- Spinrad, H. 1962, Pub. A. S. P., 74, 156.
- . 1962, Ap. J., 136, 311.
- . 1964, App. Optics, 3, 181.
- Spinrad, H., Münch, G., and Kaplan, L. 1963, Ap. J., 137, 1319.
- Spinrad, H., and Trafton, L. 1963, Icarus, 2, 19.
- Squires, P. 1957, Ap. J., 126, 185.
- Thornton, D. D., and Welch, W. J. 1963, Icarus, 2, 228.
- Urey, H. C. 1952, The Planets (New Haven: Yale University Press), Chap. 4.
- . 1959, Hdb. d. Phys., ed. S. Flügge (Berlin: Springer Verlag), 52, 400.
- Vaucouleurs, G. de 1954, Physics of the Planet Mars (London: Faber and Faber), Chap. 4.
- Vedder, H., and Mecke, R. 1933, Zs. f. Phys., 86, 137.
- Vogel, H. 1895, Ap. J., 1, 196, 273.

## REFERENCES (Continued)

- Walsh, T. E. 1963, Prog. Rep., ONR Contract NONr 2481 (58), Johns Hopkins University.
- White, J. 1942, J.O.S.A., 32, 285.
- Wildt, R. 1932, Veröff U. Sternw. Göttingen, 2, Heft 22, 171.
- . 1937, Ap. J., 86, 321.
- Wilson, E. B., Jr. 1935, J. Chem. Phys., 3, 276.
- Wu, T.-Y. 1946, Vibrational Spectra and Structure of Polyatomic Molecules (Ann Arbor: J. W. Edwards), p. 196.
- Zabriskie, F. 1962, A. J., 67, 168.